

Robustness of steel structures further to a column loss: influence of the yielding of the indirectly affected part on the global response of the structure

Auteur : Dewez, Jérôme

Promoteur(s) : Demonceau, Jean-Francois; Jaspard, Jean-Pierre

Faculté : Faculté des Sciences appliquées

Diplôme : Master en ingénieur civil des constructions, à finalité spécialisée en "civil engineering"

Année académique : 2017-2018

URI/URL : <http://hdl.handle.net/2268.2/4637>

Avertissement à l'attention des usagers :

Tous les documents placés en accès ouvert sur le site le site MatheO sont protégés par le droit d'auteur. Conformément aux principes énoncés par la "Budapest Open Access Initiative"(BOAI, 2002), l'utilisateur du site peut lire, télécharger, copier, transmettre, imprimer, chercher ou faire un lien vers le texte intégral de ces documents, les disséquer pour les indexer, s'en servir de données pour un logiciel, ou s'en servir à toute autre fin légale (ou prévue par la réglementation relative au droit d'auteur). Toute utilisation du document à des fins commerciales est strictement interdite.

Par ailleurs, l'utilisateur s'engage à respecter les droits moraux de l'auteur, principalement le droit à l'intégrité de l'oeuvre et le droit de paternité et ce dans toute utilisation que l'utilisateur entreprend. Ainsi, à titre d'exemple, lorsqu'il reproduira un document par extrait ou dans son intégralité, l'utilisateur citera de manière complète les sources telles que mentionnées ci-dessus. Toute utilisation non explicitement autorisée ci-avant (telle que par exemple, la modification du document ou son résumé) nécessite l'autorisation préalable et expresse des auteurs ou de leurs ayants droit.



Université de Liège
Faculté des sciences appliquées

**Robustness of steel structures further to a column loss:
influence of the yielding of the indirectly affected part on the
global response of the structure**

Travail de fin d'études réalisé par

DEWEZ Jérôme

en vue de l'obtention du grade de master Ingénieur Civil des Constructions

Membres du jury

Jaspart J.-P. (promoteur)
Demonceau J.-F. (promoteur)
Denoël V.
Huvelle C.

Année académique 2017-2018

Acknowledgements

I would like to deeply thank my thesis promoters Associate Professor Demonceau Jean-François and Professor Jaspert Jean-Pierre for the time they spent to advise and to support me all along the accomplishment of the present work.

I thank D'Antimo Marina for the interesting advices she gave me.

Finally, I would like to thank my family for their continuous encouragements and supports.

Jérôme Dewez

Summary

From several decades, the concept of robustness took its place in most building engineering institutions worldwide. Indeed, a growing interest for the subject was caused by a series of disasters involving the loss of many lives such as the Ronan Point collapse in 1968, the Murrah building collapse in 1995 and the 11th September 2001 World Trade Center disaster among others. Recommendations given in modern codes, allowing robustness checks to be performed when exceptional events occur, such as the loss of a column, are continually improving. Nevertheless, no tool is proposed to evaluate quickly and in an easily applicable way whether a given building is able to attain a stable deformed state after such exceptional events, i.e. if the structure is robust enough to sustain the loss of one of its bearing members for instance.

This is the scope within which several works on the topic of robustness were initiated at the University of Liège. Two PhD theses were written for that purpose. The current professor Demonceau J.-F. and Hai L.N.N have jointly developed an analytical method to predict the response of 2D frames under the exceptional "loss of a column" event. The previous method showed several weaknesses that were highlighted through the Master thesis of Huvelle C. and through her research subsequently conducted over several years. Finally, thanks to these years of research, a complete analytical procedure to assess the response of a frame submitted to a column loss was available at the University of Liège. The latter method makes it possible to derive the states of a frame losing a column when the directly affected part of the structure (the part above the lost element) by the event considered as exceptional may yield and when the indirectly affected part of the structure (the rest of the structure) remains elastic. In other words, this method considers that the lateral restraint brought about by the elements located elsewhere than just above the lost element is constant. Therefore, the predicted displacements in the structure are underestimating the displacements occurring in reality. Moreover, the predicted redistribution of loads in the structure is associated with fictive states of the latter as the indirectly affected part is considered fully elastic.

This is the scope of the present work. The first goal consists of analysing the effect of the progressive yielding of the indirectly affected part on the global response of a 2D steel frame losing one column. More particularly, the study is aiming to evaluate how far the analytical predicted behaviour is from the realistic behaviour of a frame losing a column reflected by an indirectly affected part that may progressively yield. This is achieved by performing numerical simulations on three structures with a differing number of spans. The second goal of the present work is to determine analytically the moment of collapse of the structure and the associated state of the latter (i.e. the internal forces and the deformations). Indeed, on the basis of the latter, everything will thus be gathered to perform robustness checks, i.e. to verify if a structure is able to find a stable deformed state after the loss of one of its bearing elements.

It is shown that the first yielding of the indirectly affected part leads to a chain formation of plastic hinges in the structure inducing a rather quick collapse of the latter. Moreover, a series of identified failure modes are presented thanks to the analysis of the redistribution of loads following the loss of the column. Therefore, a series of verification recommendations are exposed for the investigated structures.

Finally, a breakpoint estimating the collapse of a structure losing one of its bearing elements is analytically determined on the basis of an easy to apply approach exploiting the results given by the existing complete analytical procedure. The developed method shows fairly good results but has still some weaknesses such as the significant underestimating value of the displacements of the elements located above the lost element.

Contents

Glossary	1
I General introduction on the topic of robustness	3
I.1 Introduction	4
I.2 Design situations and further definitions	6
I.3 Norms and standards	7
I.3.1 Indirect methods	8
I.3.2 Direct Methods	8
I.3.2.1 Alternative load path method	8
I.3.2.2 Key element method	9
I.3.3 Applied strategy	9
I.4 Recent developments on robustness at the University of Liège	9
I.4.1 General behaviour of a 2D frame that loses one column	10
I.4.2 Study of Phase 2 (Huvelle [1])	13
I.4.3 Study of Phase 3	14
I.4.3.1 Complete analytical model	15
I.4.3.2 Evolution of internal stresses in the IAP during Phase 3	17
I.4.4 Conclusion	20
I.5 Subject and aim of the present thesis	21
II Design of the reference structure under SLS and ULS	23
II.1 Introduction	24
II.2 Design	25
III Modelling of the reference structure	27
III.1 Implementation of the structure in the software FINELG	28
III.1.1 Discretization of the elements	28
III.1.2 Discretization of the elements' cross-sections	30
III.1.3 Material laws	30
III.1.4 Summary of choices made in FINELG	31
III.2 Combination of actions for accidental design situations	31
III.3 Methodology followed in FINELG to simulate the loss of the column	32
III.4 Conclusion	35
IV Global response and failure modes of the reference structure (numerical analysis)	37
IV.1 Introduction	38
IV.2 Analysis of the reference structure under the loss of its central column	39
IV.2.1 DAP elastic-perfectly plastic - IAP elastic	39
IV.2.1.1 Identification of successive phases in the behaviour of the structure	39
IV.2.1.2 Analysis of the internal forces' distribution in the elements of the structure	41

IV.2.2	DAP elastic-perfectly plastic - IAP elastic-perfectly plastic	49
IV.2.2.1	Identification of successive phases in the behaviour of the structure	50
IV.2.2.2	Analysis of the internal forces' distribution in the elements of the structure	50
IV.2.3	Identified failure modes	57
IV.3	Analysis of the reference structure under the loss of an intermediate column	60
IV.3.1	DAP elastic-perfectly plastic - IAP elastic	60
IV.3.1.1	Identification of successive phases in the behaviour of the structure	60
IV.3.1.2	Analysis of the internal forces' distribution in the elements of the structure	61
IV.3.2	DAP elastic-perfectly plastic - IAP elastic-perfectly plastic	64
IV.3.2.1	Identification of successive phases in the behaviour of the structure	64
IV.3.2.2	Analysis of the internal forces' distribution in the elements of the structure	65
IV.3.3	Identified failure modes	67
IV.4	Analysis of the reference structure under the loss of an exterior column	68
IV.4.1	DAP elastic-perfectly plastic - IAP elastic & elastic-perfectly plastic	68
IV.4.1.1	Identification of successive phases in the behaviour of the structure	68
IV.4.1.2	Analysis of the internal forces' distribution in the elements of the structure	69
IV.4.2	Identified failure modes	70
IV.5	Conclusion	71
V	Parametric study (numerical analysis)	73
V.1	Introduction	74
V.2	Increase in the number of spans from 4 to 6	75
V.2.1	Loss of the central column	75
V.2.2	Loss of the intermediate column 1	78
V.2.3	Loss of the intermediate column 2	80
V.2.4	Loss of the exterior column	80
V.3	Increase in the number of spans from 6 to 8	81
V.3.1	Loss of the central column	81
V.3.2	Loss of the intermediate column 1	82
V.3.3	Loss of the intermediate column 2	82
V.3.4	Loss of the intermediate column 3	83
V.3.5	Loss of the exterior column	83
V.4	Comparison between the numerical results for 4, 6 and 8 spans	84
V.4.1	Loss of a central column	84
V.4.2	Loss of an intermediate column	86
V.4.3	Redistribution of loads during the loss of a column	87
V.4.4	Failure modes	87
V.5	Conclusion	90
VI	Analytical study	91
VI.1	Introduction	92
VI.2	General method for the calculation of the plastic mechanism in the IAP	93
VI.3	Combination of the previous general method with the complete analytical procedure	95
VI.4	Method to predict the different failure modes on the basis of the available analytical model results	103
VI.5	Conclusion	104

VII General conclusions and perspectives	105
VII.1 Conclusions	106
VII.2 Perspectives	109
Annex A	111
Bibliography	121
List of Figures	123
List of Tables	126

Glossary

E Young's modulus.

M Bending moment.

M_{pl} Cross-section plastic moment when the normal force in the latter is null.

N Normal force.

$N_{AB,normal}$ Compressive force in the column before its removal.

N_{AB} Varying compressive force in the lost column.

N_{lost} Applied downwards load at the top of the lost column (simulating the progressive loss of the column).

T Shear force.

λ Load factor.

ν Poisson's ratio.

θ Angle at the extremities of the beams of the DAP.

f_y Yield strength.

p_{floor} Accidental combination of actions applied on the floors.

p_{roof} Accidental combination of actions applied on the roof.

u Vertical displacement at the top of the lost column.

DAP Directly affected part.

dof degrees of freedom.

H Horizontal load applied on the panel plastic mechanism.

IAP Indirectly affected part.

SLS Serviceability limit state.

ULS Ultimate limit state.

V Vertical load applied on the panel plastic mechanism.

Chapter I

General introduction on the topic of robustness

I.1 Introduction

From several decades, the concept of robustness took its place in most building engineering institutions worldwide. The interest around this subject is getting more and more intense in the field of civil engineering. But for what reasons that notion is getting important to the point that control offices in buildings engineering start to impose its consideration into the design of a structure?

First, let's begin with the source of the development of the so-called robustness of structures. In 1968, a disaster happened in the United Kingdom, the Ronan Point failure, see figure I.1. This residential building was a 24 storeys built with precast concrete.



Figure I.1: The Ronan Point failure in 1968 [2]

A partial progressive collapse suddenly appeared and was initiated by a gas explosion at the 18th storey in a kitchen which was located at the corner of the building. The explosion blew out a concrete wall. As a consequence, the upper floor lost its support, see figure I.2. As the connections were not strong enough to maintain all the elements in place, the upper floors fell down on the 18th one. Considering that the floor wasn't designed to withstand those loads, it led to a progressive collapse of the apartments located at the corner of the building [3].

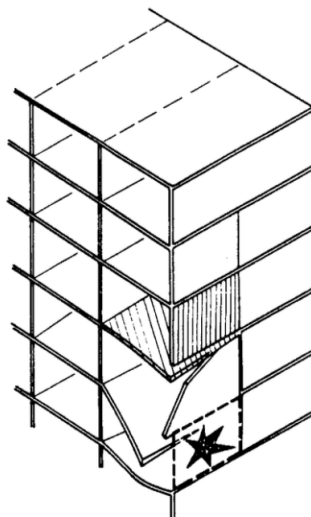


Figure I.2: Failure mode of the Ronan Point in 1968 [2]

From that event, authorities and governments reacted and first recommendations about robustness appeared in the UK codes known as British Standards. That event was the first well-known example of a localized failure, induced by a localized action (explosion), which led to the damage of a larger part of the structure. Thus, the basic principle of making a structure robust is to prevent it from presenting, one day, a disproportionate collapse which could be a partial progressive collapse as it was the case for the Ronan Point building.

In the Eurocode 1 part 1-7, the robustness is defined as *"the ability of a structure to withstand events like fire, explosions, impact or the consequences of human error, without being damaged to an extent disproportionate to the original cause"* [4].

After the Ronan Point disaster, the subject lost a bit of its interest and people started to give up its development gradually. Until a second huge disaster happened, the Murrah building in Oklahoma in 1995. A bomb exploded at the ground level next to the structure, see figure I.4 for its location. That localized action induced the collapse of a huge part of the building, see figures I.3 and I.4.



Figure I.3: The Murrah building failure in 1995 [2]

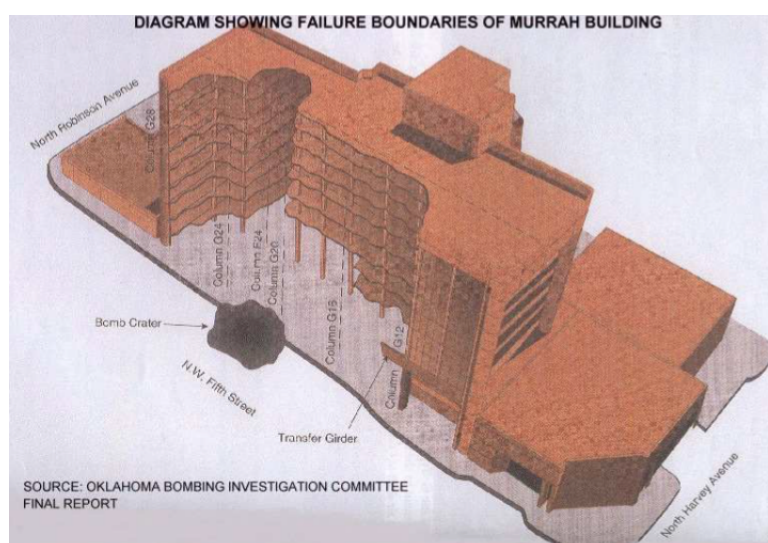


Figure I.4: The Murrah building failure in 1995 [2]

Few years after the previous event, the disaster of the World Trade Center happened 11th September 2001. Two planes hit respectively each of the two towers. The structures remained stable during a few hours. Those localized actions led to the entire collapse of the twin towers. As a consequence,

all of these catastrophes led to a growing interest and a gradual development of the robustness notion. The main aim is to save the maximum amount of lives by maintaining the integrity of the structure after such an event.

I.2 Design situations and further definitions

A structure is designed under loads called design loads. Among them, variable loads, permanent loads and accidental loads may be found. Those loads are defined as design loads because of their probability of occurrence which is rather high. Indeed, the probability of occurrence of a strong wind against a building is rather high. In this design situation, the structure will be checked for Serviceability limit state (SLS) and for Ultimate limit state (ULS). The first verification is achieved considering the deflections of the elements in a structure which cannot exceed limits defined theoretically in codes. The second is done considering the resistance of the elements' cross-sections and the global stability of the structure is checked as well as the local stability of each elements. Thus, in a design situation, the structure will be checked for SLS and for ULS.

When the concept of robustness is introduced, an additional event has to be considered, the exceptional event. Thus, under an exceptional event, the loads induced are called exceptional loads. The distinction between these latter loads and the design loads is made by the probability of occurrence that characterizes them. In the course of M. Demonceau and M. Dewals [2], the example of an earthquake of 0.4g of magnitude is taken. In Turkey, the probability of occurrence of such an event is rather high. Thus, the loads induced by this event will be considered as design loads (and more particularly in an accidental design situation). On the other hand, an earthquake of that magnitude in Belgium is rather rare. Thus, in Belgium, this event is then considered as exceptional. An exceptional load has a too low probability of occurrence to be taken into account in the design [2].

Under exceptional events, where the Eurocode defines the robustness, the aim is no longer to check deflections or resistances of single elements directly but to ensure the integrity of the structure.

The exceptional event treated in the present thesis is the loss of a column in steel structures. The latter may be induced by a terrorist attack which leads to the explosion of a bomb next to a column of the structure for instance. In this case, the elements in the structure will have to withstand loads for which they weren't designed for. Thus, the Eurocode recommends to design the structure in a way that allows the integrity of the last to be kept under such an event. After the loss of one of its column, the structure will present increasing displacements. The goal of keeping the integrity of the structure is not to avoid those displacements to happen but rather to find a way to keep it stable under such second order effects. In other words, the aim is to reach a stable deformed state [2].

To summarize, a structure is designed under SLS and ULS considering design loads including permanent loads, variable loads and accidental loads. When an exceptional event happens such as the loss of a column, it induces disorders in the structure. In such situation, requirements on robustness are given within Eurocodes aiming to prevent the building from suffering disproportionate damages. The aim is to keep the integrity of the structure and by that mean to avoid partial or complete progressive collapses of the latter. In this situation, services as fire brigades will be able to intervene on site to save a maximum amount of lives.

I.3 Norms and standards

The recommendations prescribed in codes such as the Eurocodes distinguish two types of strategies in the case of accidental design situations, see figure I.5. "*STRATEGIES BASED ON IDENTIFIED ACCIDENTAL ACTIONS*" in which accidental actions are clearly identified. Recommendations are given to prevent the structure against these accidental actions. For instance, an impact of a car against a column of a structure could be the accidental action. And a way to prevent this action to affect the column is to build a protection around the considered column for instance (protective measure). Other strategies may be to design the structure to have sufficient robustness or to design the structure to sustain the action.

The second type of strategies is "*STRATEGIES BASED ON LIMITING THE EXTENT OF LOCALISED FAILURE*". This category is related to strategies based on unidentified accidental actions. An example of a situation that is covered by this type of strategies is the loss of a column in a structure for which no information is given about the accidental actions that led to the loss of this column. A strategy given to treat the latter situation may be to apply the alternative load paths method. The latter will be described in the following of the section.

The Eurocode 1 part 1-7 specifies several classes of consequences which qualify the consequences of a collapse of a building mainly regarding the loss of lives. For instance, robustness recommendations are not the same for an hospital than for a storage warehouse in terms of lives saving. Thus, first of all, it is necessary to identify the classes of consequences divided into three main categories: CC1, low consequences of failure; CC2, medium consequences of failure; CC3, high consequences of failure.

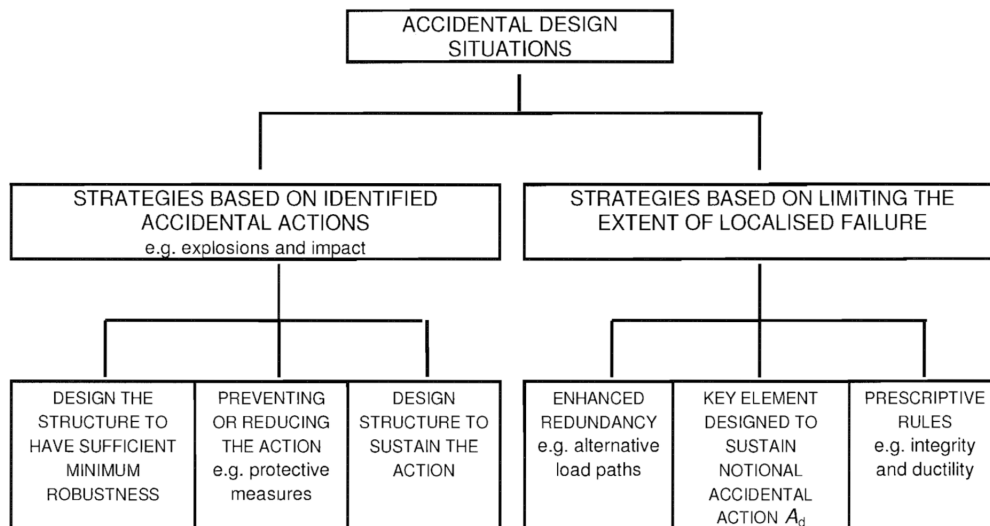


Figure I.5: Strategies for Accidental Design Situations [4]

First recommendations were given in the British Standards. These British Standards do not exist anymore today. In these latter British Standards, two types of methods were given. The first type is about indirect methods for which no scenario is identified and recommendations are given regarding design rules. These latter design rules do not need a structural analysis. Among them, the tying method is found and will be detailed further. The second type is about direct methods for which a scenario is identified and recommendations are given to counteract the consequences of that scenario on the structure. This second type of methods requires a structural analysis [5].

I.3.1 Indirect methods

Through the indirect methods, no scenario is identified but only design rules/requirements are prescribed. Among these methods, the tying method is found.

This method provides requirements regarding the addition of ties and the design of these latter. For instance, in the case of horizontal ties for framed structures, it is said in the EN 1991-1-7 [4]: "*Horizontal ties should be provided around the perimeter of each floor and roof level and internally in two right angle directions to tie the column and wall elements securely to the structure of the building*", page 36. Moreover, "*Horizontal ties may comprise rolled steel sections, steel bar reinforcement in concrete slabs, or steel mesh reinforcement and profiled steel sheeting in composite steel/concrete floors (if directly connected to the steel beams with shear connectors). The ties may consist of a combination of the above types*".

The latter codes provide requirements regarding the tensile load that the latter ties should be capable of sustaining. The recommendations regarding the internal ties are given on the basis of the evaluation of a design tensile load T_i and for the perimeter ties, they are given on the basis of the evaluation of a design tensile load T_p , see the two following expressions.

$T_i = 0,8(g_k + \psi q_k)sL$ or 75 kN, whichever is the greater.

$T_p = 0,4(g_k + \psi q_k)sL$ or 75 kN, whichever is the greater.

where s is the spacings of ties, L is the span of the tie and ψ is the relevant factor in the expression for combination of action effects for the accidental design situation (i.e. ψ_1 or ψ_2 in accordance with expression (6.11 b) of EN 1990), see EN 1991-1-7 [4] page 36.

Further informations on the latter horizontal ties and on vertical ties may be found in the EN 1991-1-7 [4].

I.3.2 Direct Methods

For these methods, a scenario is clearly identified. A discussion between the builder and the landlord of the building should be taken to target the risks against which the landlord wants to be protected. The safer the building the bigger the bill will be for the future owner. Scenarios of events are identified and during the discussion, the landlord specifies against which of the latter he wants to be protected as an impact of a car for instance.

Among the direct methods, the alternative load path method and the key element method are found. As previously explained, the direct methods need the accomplishment of a structural analysis.

I.3.2.1 Alternative load path method

The alternative load path method is not about giving recommendations on how to design an element to sustain an action but rather to analyse the behaviour of the structure after the loss of an element. When a frame loses one of its columns, there will be a redistribution of the loads that the lost column was sustaining. The redistribution will logically depend on the location of the lost column. Thus, the goal is not to prescribe design recommendations through the alternative load path method but rather to determine if the structure is able to make the redistribution of loads and finally reach a stable deformed state.

The method consists in identifying the damages associated to scenarios, then to identify the load paths in the damaged structure and finally to check the structural integrity of the building under investigation [2].

The alternative load path method is done through a non linear analysis in which geometrical and material non linearities, second order effects and elasto-plastic behaviour are taken into account in order to reach the most realistic behaviour of the considered building.

I.3.2.2 Key element method

A key element is defined in EN 1991-1-7 [4] as "*a structural member upon which the stability of the remainder of the structure depends*" (a column for instance). In the method, the goal is to identify these key elements and to design them to make them resistant enough to sustain the effects of a model of accidental action A_d according to EN 1991-1-7 [4]. In the latter codes, it is said: "*The recommended model for buildings is a uniformly distributed notional load applicable in any direction to the key element and any attached components (e.g. claddings, etc). The recommended value for the uniformly distributed load is 34 kN/m² for building structures*".

The Eurocode defines a key element as an element for which if it is removed, it leads to the collapse of more than 100 m² or 15 % of the floor area (the minimum of the two has to be taken) on two adjacent floors caused by the removal of the key element (which could be a column, pier or wall) (EN 1991-1-7 page 17 [4]).

The main disadvantage of this method is the cost of making a key element resistant enough to sustain the event considered.

I.3.3 Applied strategy

In the present thesis, the structures under investigation are office buildings. The latter type of structure is classified in the second class of consequences (CC2) and especially in the class 2b (upper risk group) according to Table A.1 page 34 in Eurocode 1 part 1-7 [4]. Among other recommendations for the latter class of consequences (2b), it is recommended in EN 1991-1-7 page 35 [4]: "*the building should be checked to ensure that upon the notional removal of each supporting column and each beam supporting a column, or any nominal section of load-bearing wall as defined in A. 7 (one at a time in each storey of the building) the building remains stable and that any local damage does not exceed a certain limit*".

The identified scenario considered in the present thesis is the loss of a column (exceptional event) in the case of an unidentified action, i.e. there is no information about how the column is lost (impact of a car, explosion, etc.). The strategy applied takes place into the category of "*STRATEGIES BASED ON LIMITING THE EXTENT OF LOCALISED FAILURE*" and especially through the application of the alternative load paths method.

I.4 Recent developments on robustness at the University of Liège

At the University of Liège, many research has been made on the robustness topic and especially on the study of the behaviour of steel and composite frames under the exceptional event "loss of a column".

The global aim of the previous studies in Liège was to determine through analytical methods the state of the structure by analysing the redistribution of internal forces during the loss of a column. This redistribution is done through the activation of alternative load paths. Finally, if the evolution of internal forces in the structure is known, it is possible to give practical guidelines through recommendations on how to design a structure to withstand the exceptional event "loss of a column".

Research on that topic at the University of Liège was initiated by two PhD theses. The current professor Demonceau J.-F. and Hai L.N.N have developed an analytical method to predict the response of 2D frames under the exceptional event "loss of a column" (Demonceau [6] and Hai [7]). The latter analytical method has shown several weaknesses that were highlighted through the Master thesis of Huvelle C. [1] and through scientific articles made by Huvelle C., professor Jaspard J.-P., professor Demonceau J.-F. and Hoang V.-L. ([8] and [9]). It led to the development of a complete analytical procedure to assess the response of a frame submitted to a column loss [9].

Demonceau J.-F., Hai L.N.N and Huvelle C.'s research has been made by considering a static behaviour of the frame, i.e. the loss of the column is assumed to be progressive and slow enough to consider it static. The dynamic effects (bomb explosion for instance) were studied in the Master thesis of Comeliau L. [10].

Hjeir Farah has studied the structural requirements through parametrical studies and gives recommendations on the design of the structure in order to make the latter robust enough to withstand the exceptional event "loss of a column" in 2D steel frames [11].

All the above mentioned research was made on 2D frames. But, the behaviour of the structure is influenced by 3D effects as the presence of secondary beams and two-ways concrete slabs for instance. The study of the 3D behaviour of a structure under the exceptional event "loss of a column" was made by Florence Lemaire through her Master thesis [12]. A Few years later, Abhishek Ghimire studied the structural requirements through parametrical studies of 3D steel structures further to a column loss in his Master thesis [13].

In the following of the present chapter, the general behaviour of a 2D frame that loses one column will be presented with the last developed analytical tools.

I.4.1 General behaviour of a 2D frame that loses one column

Basic knowledge on the general behaviour of a 2D frame that loses one column will be explained through definitions and theoretical basis defined in accordance with University of Liège past research on robustness notion.

In the context of the exceptional event "loss of a column", the structure is divided into two parts, the Directly affected part (DAP) and the Indirectly affected part (IAP).

The DAP (surrounded in red on figure I.6) is made up of all the beams and columns situated above the damaged column. It includes as well all the joints that connect the DAP to the rest of the structure, i.e. the IAP.

The IAP is made up of the rest of the structure.

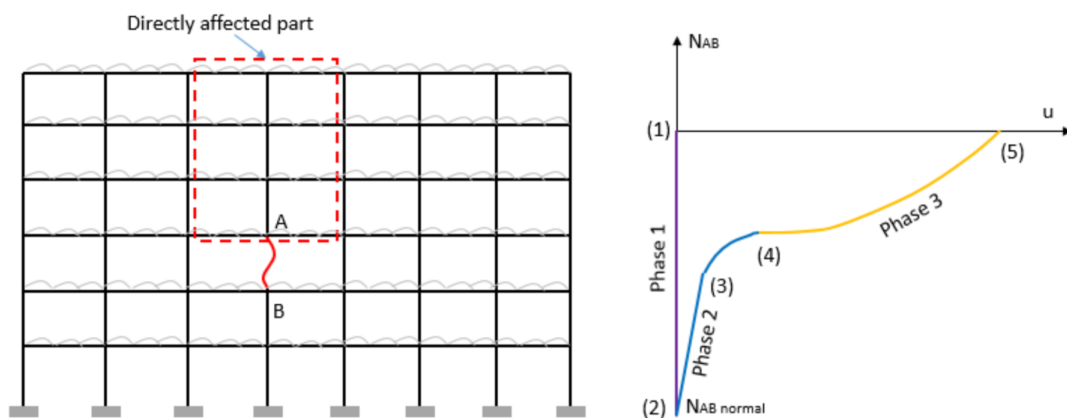


Figure I.6: Behaviour of a frame submitted to a column loss [9]

During the progressive loss of column AB on figure I.6, the behaviour of the structure is divided into three phases expressing the evolution of the internal compression force N_{AB} in the column AB in function of the evolution of the vertical displacement u of the top of the damaged column (i.e. point A).

Phase 1 consists in the loading of the structure and is characterized by the path from point (1) to point (2) on the graph of figure I.6. The internal force N_{AB} in the column AB grows from 0 to the value of $N_{AB,normal}$ corresponding to the compression force in the column when the frame is fully loaded. In practise, this situation is simulated by removing one column in the frame and by adding the corresponding internal forces at the top of the removed column. It is well illustrated on figure I.7 in the case of the loss of the frame's central column. Thus, at the end of Phase 1, i.e. when the frame is fully loaded, the central column is simulated by adding the internal compression force vertically and upwards to the frame. The two situations on figure I.7 are equivalent.

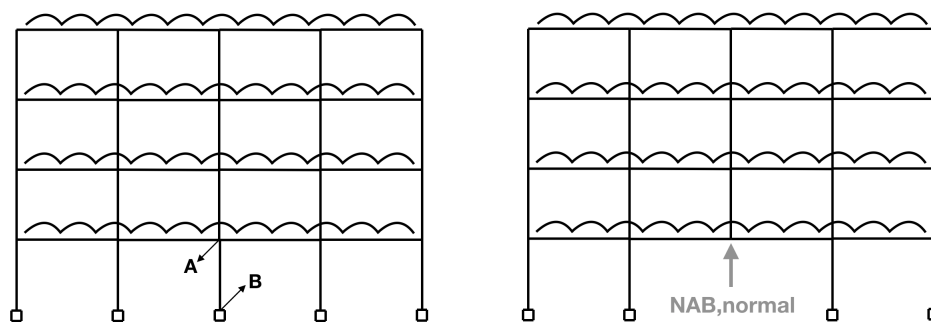


Figure I.7: Phase 1

Phase 2 (from point (2) to point (4)) marks the beginning of the progressive removal of the column. Point (3) marks the formation of the first plastic hinge in the DAP. From point (3) to point (4), each change of the slope of the curve corresponds to the formation of one plastic hinge in the DAP. Thus, each formation of hinge in the DAP is associated to a loss of stiffness translated by a change of the slope of the curve. At point (4), a complete plastic mechanism is formed in the DAP, the mechanism is illustrated on the schema on the right on figure I.8. In practise, the progressive removal of the column, in the case of the loss of a central column, is simulated by adding a vertical force called N_{lost} in the opposite direction of $N_{AB,normal}$, see the schema on the left of figure I.8. Thus, N_{lost} will progressively increase from value 0 at point (2) to simulate the progressive loss of the column. The evolution of the effort N_{AB} is given by the following expression:

$$N_{AB} = N_{AB,normal} - N_{lost} \quad (I.1)$$

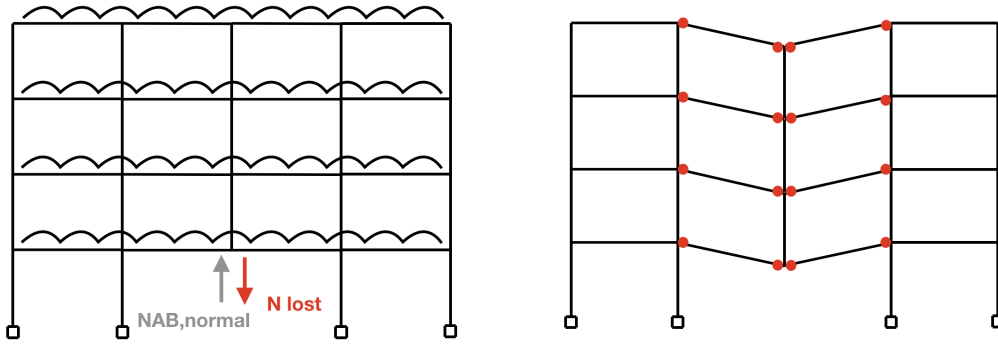


Figure I.8: Phase 2

Phase 3 (from point (4) to point (5)) begins when the plastic mechanism in the DAP is reached. At point (4), the slope of the curve is equal to zero meaning that there is no more stiffness coming from the DAP since a plastic mechanism is reached. Starting from point (4), the value of N_{lost} continues to increase and significant vertical displacements of point A occurs as there is no more first order stiffness in the DAP. During the latter increase of the vertical displacement of point A, the beams in the DAP tend to be put in tension. This effect is called the catenary action, see the blue arrows on figure I.9. It is characterized by an increase of the slope of the $(u;N_{AB})$ curve during Phase 3. The activation of these catenary actions is permitted by the second order stiffness brought by the IAP.

As it is well explained in [9], "*the role of the indirectly affected part during phase 3 is to provide a lateral anchorage to these catenary actions: the stiffer the indirectly affected part is, the higher the catenary actions will be in the directly affected part*". Thus, the development of the catenary actions is possible if the IAP is stiff enough to provide a lateral anchorage to allow the development of tensile forces in the beams. Finally, at point (5) (i.e. the end of phase 3), the force N_{AB} is equal to zero meaning the column is fully lost, i.e. N_{lost} is equal to $N_{AB,normal}$. Thus, the principal of making a structure robust consists in making it reaching point (5). In his master thesis [11], Hjeir F. gives the design requirements to make a structure robust enough to withstand the exceptional event "loss of a column" in case of 2D steel frames.

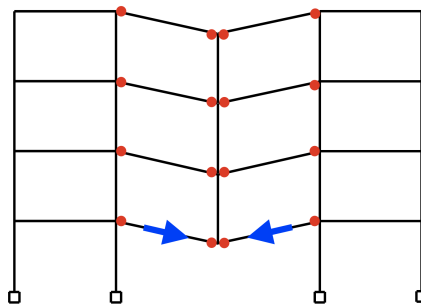


Figure I.9: Catenary actions (Phase 3)

According to [8], it is possible to reach the complete loss of the column, i.e. to reach point (5), only if two conditions are respected. The first condition says the loads reported in the IAP from the DAP during the progressive loss of the column should not induce a failure (buckling of an element or formation of a plastic mechanism in the IAP). The second condition says that all the elements in the structure need to have sufficient ductility to develop the corresponding vertical displacement of the top of the column (point A) to reach point (5).

Today, the response of a 2D frame under the loss of a column, i.e. from point (2) to point (5), can be analytically predicted. Therefore, the analytical tools developed to predict the response of the frame during Phase 2 will be firstly presented and explained. Secondly, the complete analytical procedure

to assess the response of a frame submitted to a column loss during phase 3 will be presented and explained.

I.4.2 Study of Phase 2 (Huvelle [1])

The study of Phase 2 was well summarized in the Master thesis of Huvelle C. [1] (from page 15 to page 17). As it is important to understand what is mastered during Phase 2 before going into the study of Phase 3, the summarize of Huvelle C. will be recalled in the present thesis. The aim is to understand what is known at the end of Phase 2.

The behaviour of the structure during Phase 2 has been studied by Hai through his Phd thesis [7]. In the latter, he has developed an analytical model allowing the study of the DAP during Phase 2 by establishing a substructure of the DAP shown on figure I.10.

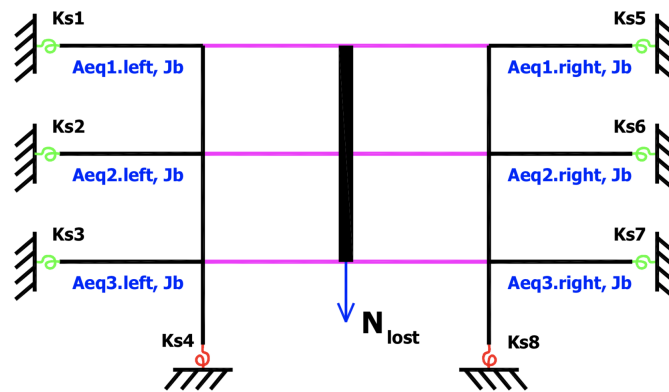


Figure I.10: Substructure of Hai [7]

The elements that need to be determined in order to know all the elements of the substructure are:

- The rotational springs k_{si} ;
- The equivalent area $A_{eq,i}$.

In the Phd thesis of Hai [7], he has described the methodology to determine those elements. The methodology was verified in the master thesis of Muller F. [14]. Moreover, Muller has described an analytical procedure to determine the development of each hinge in the DAP translated by successive changes of the slope of the curve between point (3) and point (4) on the $(u; N_{AB})$ curve, see figure I.6.

Finally, Muller has identified the key elements that need to be verified during Phase 2. These are the followings:

- The upper beam (poutre équivalente supérieure);
- The bottom beam (poutre équivalente inférieure);
- The beside columns (colonnes adjacentes).

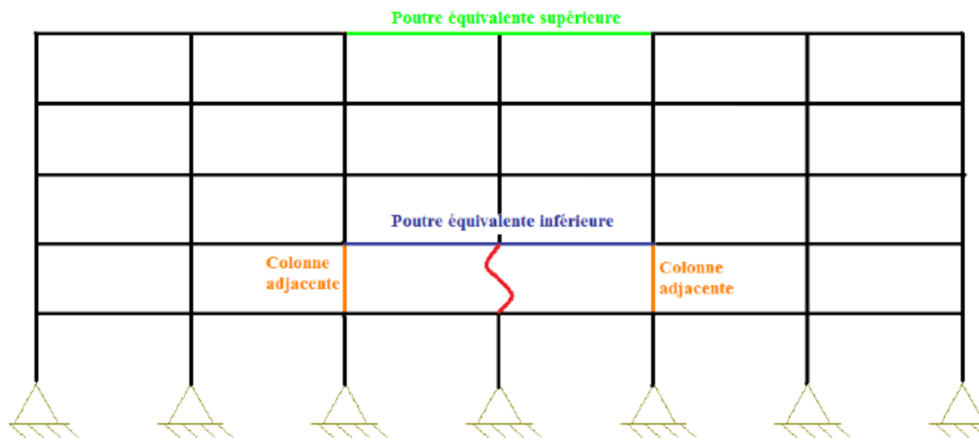


Figure I.11: Key elements to be verified during Phase 2, Muller [14]

The rest of the structure is assumed not to be affected during Phase 2.

- The upper beam needs to be verified because it is put in compression during Phase 2. Indeed, the horizontal displacements of the IAP imply an arch effect inducing compression forces in the upper beam;
- The bottom beam has to be verified because it is put in tension during Phase 2;
- Finally, beside columns need to be verified because their internal compressive forces are increasing during the progressive loss of the column. Moreover, the internal moments of these columns are significantly increasing.

As a consequence, failure modes that need to be verified are:

- Lack of rotational capacity: If the hinges are developing in the beams, the cross-sections of the beams need to be of class 1 to have sufficient rotational capacity in order to perform a plastic analysis, see course "Calcul d'éléments métalliques" page 3-1 (Jaspart J.-P. [15]). If the hinges are developing in the joints, these latter need to be properly designed in order to have sufficient rotational capacity and sufficient resistance to withstand the applied forces;
- The buckling of the upper beam under compression needs to be verified;
- The resistance of the bottom beam and its joints needs to be sufficient to sustain the tensile force;
- The buckling of the beside columns needs to be checked. Indeed, these latter are submitted to both an increase of their internal compressive forces and their internal moments.

As well in the master thesis of Huvelle C. as in the present master thesis, it will be assumed that the state of the structure is known at the end of Phase 2, i.e. all the displacements and internal forces (M,N,T) have been correctly analytically established.

I.4.3 Study of Phase 3

Phase 3 begins when the plastic mechanism is fully developed in the DAP. As it was presented in section I.4.1 page 12, Phase 3 is characterized by the development of the catenary actions. The behaviour of the structure during Phase 3 was first investigated through the PhD thesis of Demonceau J-F [6] in which he had developed a substructure and an associated analytical model. These latter will not be detailed in the present thesis. Indeed, Huvelle C. has highlighted some weaknesses of the model through her Master thesis. Her work allowed the definition of a complete analytical procedure

to assess the response of a frame submitted to a column loss presented in the articles [8] and [9].

In the present section, the final analytical model will be presented and explained. Then, the evolution of the internal forces in the elements of the IAP explained by Hai through his PhD thesis [7] will be explained.

I.4.3.1 Complete analytical model

Again, the general purpose followed is to be able to establish the redistribution of internal forces in the whole structure on the basis of analytical results predictions. By knowing the latter redistribution of forces in the structure, the practitioner will have all the tools needed to determine if the structure is robust enough to withstand the exceptional event "loss of a column". It is through that general purpose that the complete analytical procedure was established.

More particularly, the complete analytical model determines the global response of a structure loosing a column during Phase 3. It derives the part of the $(u; N_{AB})$ curve corresponding to Phase 3, i.e. from point (4) to point (5) on figure I.6. It is determined and is valid only for structures with a DAP that may yield and an IAP remaining fully elastic.

The model was established on the basis of the definition of a generalized substructure representing the DAP and taking into account of the presence of the IAP through horizontal springs, see figure I.12.

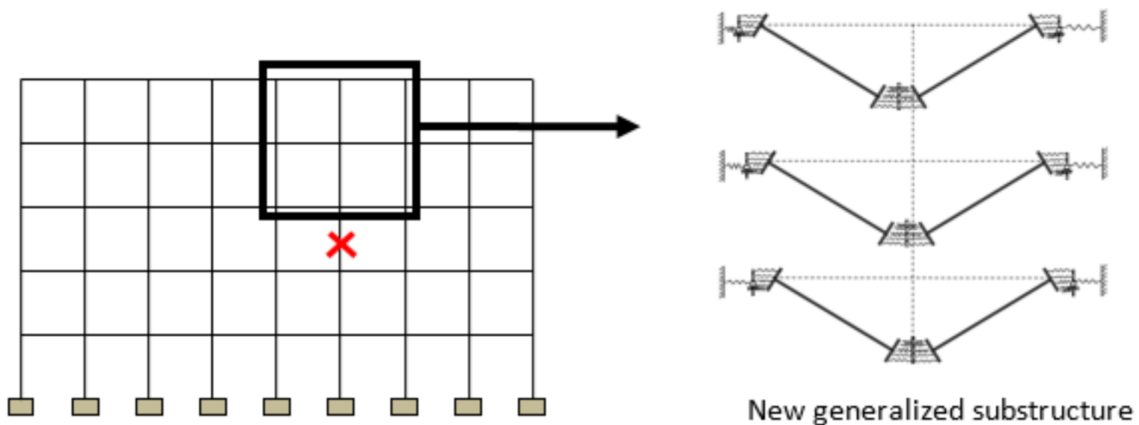


Figure I.12: Generalized substructure model [9]

The generalized substructure shown on figure I.12 incorporates a series of localized substructures of beams of the DAP, see figure I.13.

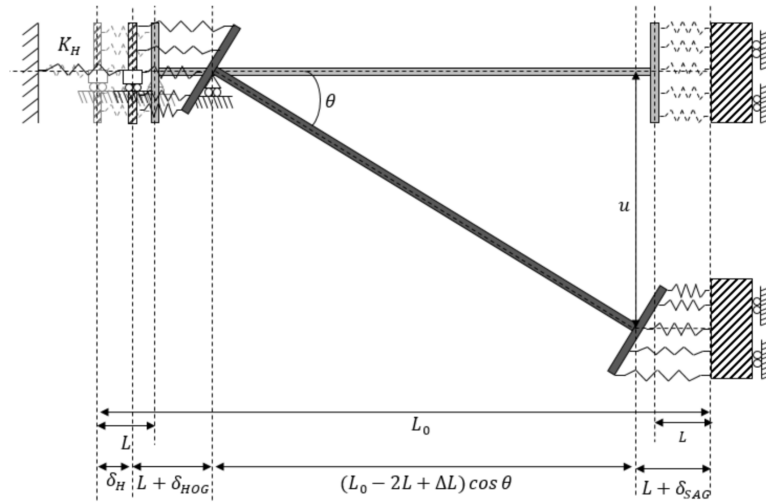


Figure I.13: Substructure model [9]

The substructure shown on figure I.13 characterizes one beam of the DAP. The two extremities of the beam, i.e. where the hinges will form during Phase 2, are modelled by several springs in parallel with each a length equal to L in the initial state of the beam, i.e. when there is no deflection ($u = 0$). Those springs follow an elastic-perfectly plastic force-displacement law. When the joints are fully resistant, the hinges will form in the beam cross-sections and the length of these hinges is called L as previously stated. If the beam to column joints are partially resistant, the hinges will form in the joints. In that case, the length of the hinges L is taken equal to 0 because the length of the joints is assumed to be much shorter than the length of the beam.

The IAP is taken into account in the model through the definition of horizontal springs with each their own stiffness K_H at the connections to the IAP of the beams from the DAP. As the IAP is considered fully elastic in the analytical model, the lateral restraints brought by the IAP stay constant, i.e. the stiffness of the springs remain constant.

In the example of the frame on figure I.12, there are three floors above the lost column in the DAP. All the floors have the same vertical displacement since it is assumed that the columns elongations between each floor are neglected in the model, see [8] section 2.3. Thus, the generalized substructure includes all those 3 floors connected vertically between each other through their columns. An horizontal spring is placed at each extremity of the generalized substructure, i.e. there are 6 horizontal springs simulating the lateral restraints of the IAP.

The calculation of the lateral restraints brought by the IAP is made through the definition of the horizontal displacement δ_{Hi} at the storey i given as $\delta_{Hi} = \sum s_{ij} F_{Hj}$. The coefficients s_{ij} form the flexibility matrix of the IAP. They can be easily determined through a first order elastic analysis considering that the IAP remains elastic [8]. These coefficients are equal to the horizontal displacements at storey i when a unitary force is acting at storey j . When the lost column is not the central column of the frame, as for instance the situation exposed on figure I.14, the displacements of the extremities from the left of the DAP will not be equal to the displacements of the extremities from the right of the DAP. Thus, the total horizontal displacement of the storey i of the DAP when a unitary force is acting at the storey j is defined as $s_{ij} = s_{l,ij} + s_{r,ij}$ where $s_{l,ij}$ is the displacement of the left extremity of the storey i and $s_{r,ij}$ is the displacement of the right extremity of the storey i . F_{Hj} is the horizontal load applied at storey j . These previous definitions are the same than the ones defined in the paper [9]. The calculation of the flexibility matrix of the IAP is illustrated on figure I.14. An horizontal unitary force is successively applied at each storey above the lost column in the DAP to determine respectively each term of the flexibility matrix.

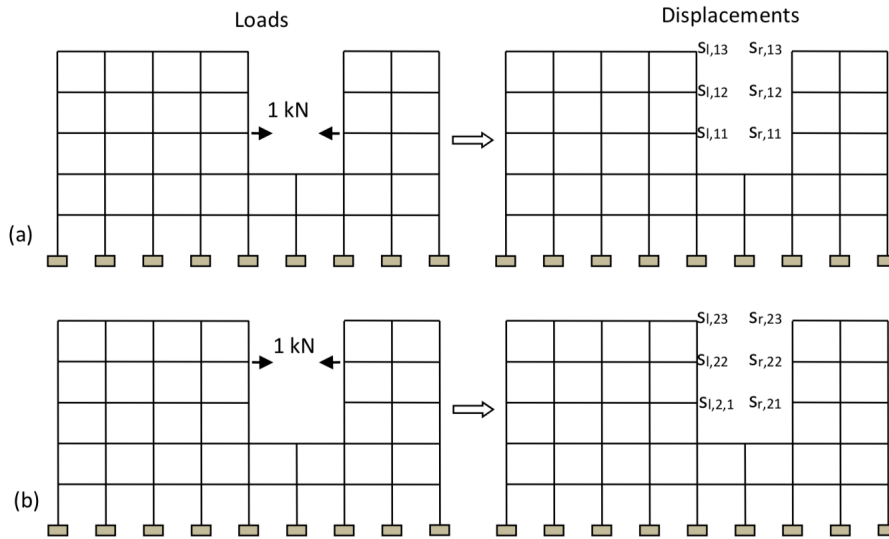


Figure I.14: Calculation of the coefficients s_{ij} [9]

Then, a load N_{lost} (or equivalently P as defined in the papers) applied at the top of the lost column (and thus applied on the generalized substructure) is progressively increased to simulate the progressive loss of the column. Thanks to this complete analytical procedure, all the internal forces are known in the DAP, i.e. the normal forces, the bending moments and the shear forces are known in each element of the DAP.

The input data to this analytical model are gathered in table 5 page 19 of the paper [9]. The set of equations and unknowns are gathered in table 6 page 21 of the paper [9]. These latter can be implemented in a solver as Matlab for instance.

This final analytical model was validated through comparisons between analytical results given by the latter with numerical results for different frames, see [9] figure 18 page 20. The numerical results were obtained through non linear analysis made on Finelg (finite element software that will be detailed in the following of the present thesis).

In short, a complete analytical model exists to simulate the behaviour of a 2D frame that loses one column in the situation where the DAP may yield and where the IAP remains fully elastic. Thus, in this model, the horizontal restraints coming from the IAP remain constant during the loss of the column and especially during the phase under investigation in this section, i.e. Phase 3 [9].

I.4.3.2 Evolution of internal stresses in the IAP during Phase 3

Huvelle C. has already summarized the evolution of internal forces in the IAP during Phase 3 through her Master thesis [1] based on the PhD thesis of Hai [7]. However, it will be recalled in the present thesis as it represents an important background knowledge that has to be mastered in this work.

Through the PhD thesis of Hai [7], it is said that during Phase 3, it is the damaged level that sustains the increase of horizontal forces coming from the increase of the tensile forces in the bottom beams of the DAP (catenary actions). It includes all the columns at the same level than the lost column and the beams just above and below these latter columns, see figure I.15.

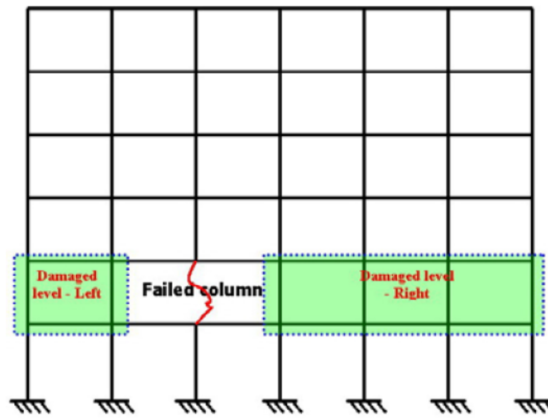


Figure I.15: Damaged level (Hai [7])

The elements of the damaged level are shown on figure I.16. These are called:

- The "beside column", i.e. the nearest column from the IAP to the DAP;
- The "inter column";
- The "side column", i.e. the furthest column.

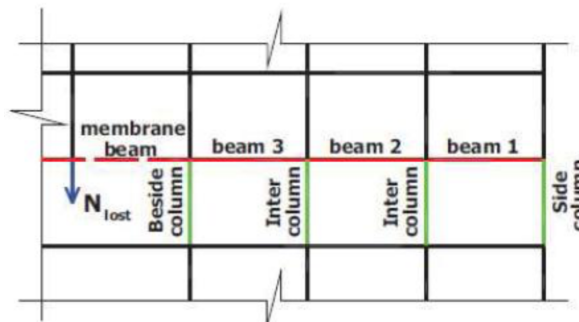


Figure I.16: Elements of the damaged level (Hai [7])

The evolutions of the internal forces in the columns of the damaged level in the IAP were determined by Hai through his PhD thesis and are exposed on figure I.17. It shows the bending moments $M_{columns}$ in the columns in function of the value of N_{lost} on the one hand and on the other hand it shows the normal forces $N_{columns}$ in the columns in function of N_{lost} .

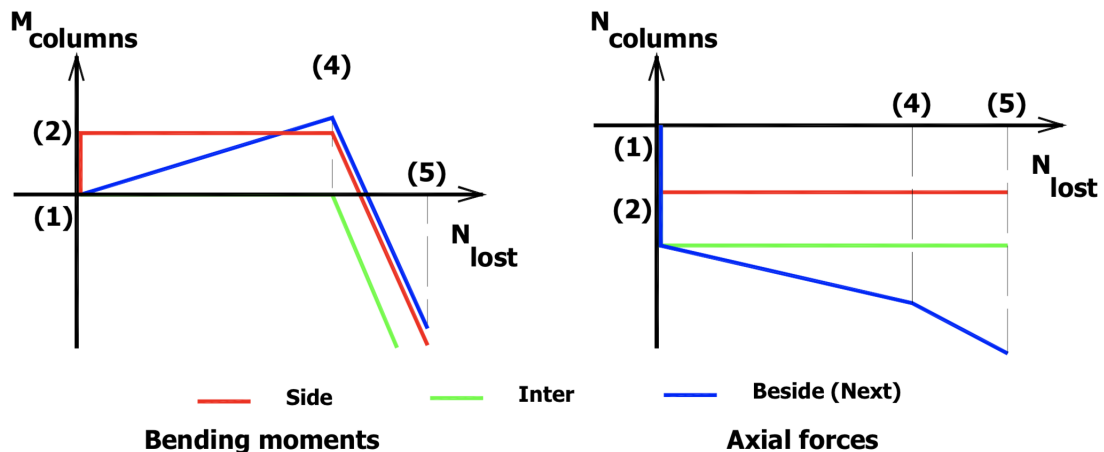


Figure I.17: Evolution of the internal forces in the columns of the damaged level in the IAP during all the three phases (Hai [7])

On the figure I.17, the points (1) to (5) are the exact same points defined on figure I.6 and characterize the successive three phases defining the behaviour of a frame under the event "loss of a column". Thus, the point (2) marks the end of Phase 1, the point (4) marks the end of Phase 2 and the point (5) marks the end of Phase 3.

During Phase 1, i.e. during the loading of the frame, the moment increases in the side column while it remains equal to zero in the other columns. In parallel, the axial loads $N_{columns}$ are increasing in all the columns.

During Phase 2, i.e. during the increase of N_{lost} , only the beside columns see an increase of their internal moment while it remains constant for the other columns. In parallel, only the beside columns see an increase of their axial loads $N_{columns}$ while it remains constant for the other columns. It means that during Phase 2, only the beside columns are feeling the removal of the column. It means that all the loads previously sustained by the lost column are entirely redistributed in the beside columns.

At the beginning of Phase 3 (point (4)), i.e. when the plastic mechanism is fully formed in the DAP, the bending moments in the columns start to decrease and then their signs change, i.e. they become negative. It is well understandable because during Phase 3, the catenary actions develop in the bottom beams and thus horizontal forces are acting at the top of the columns inducing a change of the sign of the moment. Through her Master thesis [1], Huvelle C. has well explained that effect through figure I.18 and figure I.19.

Under uniformly distributed loads, the deflection of the columns is the one exposed on figure I.18.

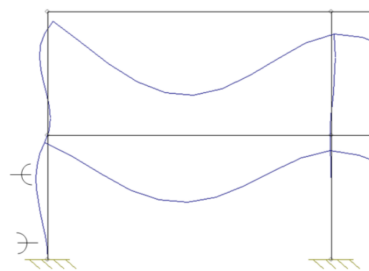


Figure I.18: Deflection of the columns under uniformly distributed loads [1]

When a horizontal load is acting at the top of the columns, the deflection is the one on figure I.19.

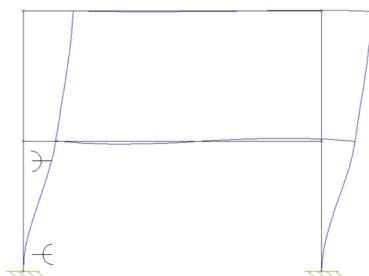


Figure I.19: Deflection of the columns under an horizontal applied load [1]

Thus, it is understandable that the sign of the moments in the columns will change during Phase 3. Indeed, during Phase 2, the deflection of the columns will be as the one shown on figure I.18 and during Phase 3, it will be as the one shown on figure I.19. Indeed, the activation of the catenary actions during Phase 3 is characterized by significant increase of the tension in bottom beams of the DAP that then pulls on the IAP.

In parallel, as shown on figure I.17, the normal loads in the beside columns continue to increase while it remains constant in the other columns. But, why is there a change of the slope in the evolution of $N_{columns}$ in the beside columns in function of N_{lost} from Phase 2 to Phase 3? As shown on figure I.6 and as previously explained in the section I.4.1 page 12, during Phase 3 the vertical displacement of the top of the lost column (i.e. point A) is quickly increasing as there is no more first order stiffness in the DAP. As shown on figure I.20, the tensile load in the bottom beams (F_{memb}) brings an horizontal load (H_{memb}) and a vertical load (N_{memb}) since the top of the lost column (i.e. point A) presents a vertical displacement. Thus, as the vertical displacement of the top of the lost column is quickly increasing during Phase 3, the vertical load (N_{memb}) is thus increasing faster during Phase 3 than during Phase 2. This is why the axial loads $N_{columns}$ in the beside columns are increasing faster during Phase 3 than during Phase 2. Finally, it explains why a change of the slope is observed for the ($N_{lost}; N_{columns}$) graph on figure I.17.

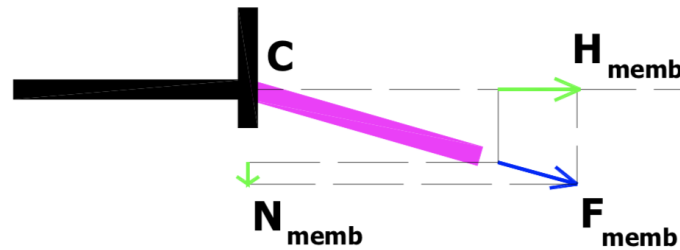


Figure I.20: Supplement compressive forces in the beside columns (Hai [7])

I.4.4 Conclusion

From all the points exposed in the present section, it is concluded that the evolution of the internal forces in the DAP is known during all the three Phases for a DAP that may yield and an IAP remaining fully elastic for a 2D frame.

This will be kept in mind during the whole present thesis.

I.5 Subject and aim of the present thesis

The aim of my work is globally to analyse the behaviour of 2D steel frames under the exceptional event "loss of a column" and to analyse the influence of the yielding of the IAP on the latter behaviour. Indeed, today, it is possible to predict the response of a frame submitted to a column loss (covering all the 3 Phases) in the case where the IAP remains fully elastic. Thus, my work consists in studying the influence of the yielding of the IAP on the global response of a 2D steel frame submitted to a column loss and to compare it with what is predicted today.

In chapter II, the design of the reference structure, on which this study will be based, is detailed.

In chapter III, the modelling of the latter on a finite element software is exposed.

In chapter IV, the general behaviour of the reference structure (detailed further) will be analysed in the case of an IAP remaining elastic and in the case of an IAP which may yield through numerical simulations of the "loss of a column" event. It will be compared to the predicted behaviour detailed earlier in section I.4. In the case of an IAP that may yield, the aim will be to identify the order of formation of plastic hinges in the IAP. The goal is to be able to identify the moment of appearance of the first plastic hinges in the IAP and the moment of the collapse of the structure in order to qualify the influence of the yielding of the IAP on the global response of the structure. The types of collapses will be investigated through several simulations of the event "loss of a column". It could be imagined that the collapse of the structure shown on I.21 may happened through the formation of a panel plastic mechanism in the IAP for instance.

The analysis of the yielding of the IAP will allow to identify if the formation of the first hinges in the IAP will induce a quick reach of the collapse of the structure. In other words, it will permit to conclude if the value of N_{lost} needed to form the first hinges in the IAP is significantly smaller than the one needed to induce the collapse of the structure. Thus, the differences between these latter values of N_{lost} will be determined to quantify the effect of the yielding of the IAP on the global response of the frame.

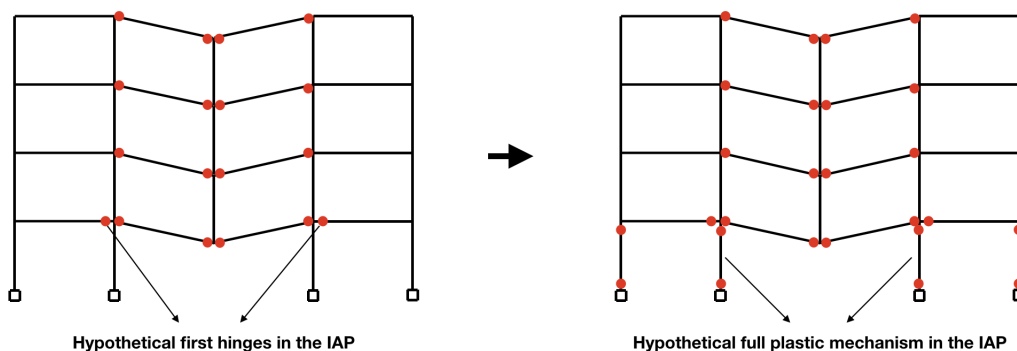


Figure I.21: From the hypothetical first hinges in the IAP to the hypothetical full plastic mechanism in the IAP

In this context, the redistribution in the structure of the loads previously withstood by the lost column will be analysed. The goal is to identify what elements need additional verifications than the ones already made for the SLS and ULS. Muller F. has already highlighted the elements that need additional verifications until the end of Phase 2. Thus, based on these latter, the goal will be to generalize the elements that need additional verifications until the end of Phase 3. This will lead to design recommendations as for instance the prescription of a cross-section of class 1 for the beams' cross-sections where the hinges are developing in the DAP during Phase 2 (presented in section I.4.2). These inves-

tigations will bring to the identification of several possible failure modes of the structure during the "loss of a column" scenarios.

In chapter V, the influence of the increase of the number of spans on the behaviour of the structure will be analysed for several simulations of the loss of a column. The goal is to identify if the yielding of the IAP affects similarly the structures with more spans than the reference structure. Thus, the locations of formation of hinges will be identified as well as their order of development. An analysis of the redistribution in the structure of the loads previously supported by the lost column will also be investigated. Then, a comparison between the behaviour of the different structures will be achieved. Based on these previous investigations, it will be possible to generalize the identified failure modes on the investigated cases.

In chapter VI, the principal goal is to find an easily applicable method to predict the internal forces in the structure until its collapse. It will then be possible to know what loads the elements have to sustain in order to avoid the collapse of the structure under the loss of a column.

As previously explained, a complete analytical model describes well the behaviour of a 2D frame that loses one column in the situation where the DAP may yield and where the IAP remains fully elastic. From this model, all the internal forces in the DAP are known. Thus, the aim is to be able to predict as accurately as possible the point of collapse of the structure in the case where the IAP may yield on the basis of the results from the analytical model which considers the IAP as fully elastic. In other words, the goal is to determine the internal forces in the structure on the basis of the analytical model results to fit as well as possible the real internal forces in the structure at the moment of its collapse. The real internal forces in the structure are determined through numerical simulations considering that the DAP and the IAP may yield. It is thus to these latter numerical results that the analytical results will be compared.

As a consequence, this method will allow the practitioners to do robustness checks and to predict failure modes of the structure in an easy and in a low time consuming way instead of using a finite element software which then requires heavy calculations and which is time consuming.

Chapter II

Design of the reference structure under SLS and ULS

II.1 Introduction

The configuration of the reference structure adopted is taken identical to the one adopted by Farah Hjeir [11], see figure II.1.

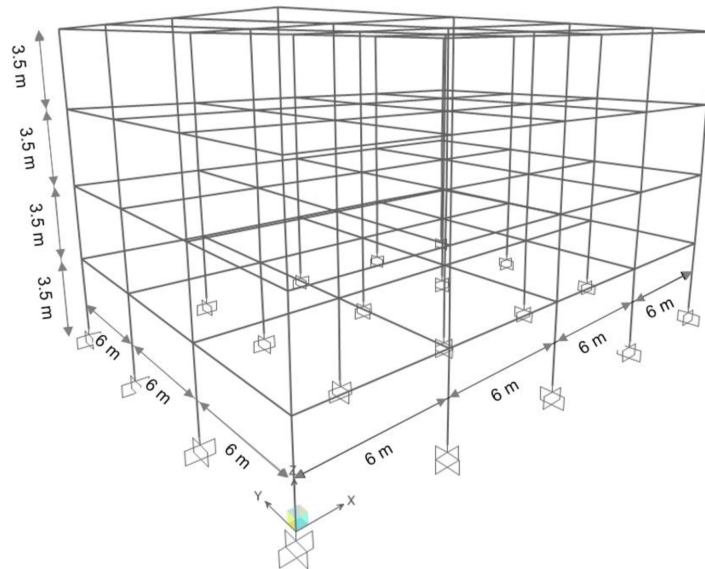


Figure II.1: 3D reference structure [11]

In the plane XZ, the building is made up of 4 spans of 6 meters each and in the plane YZ, there are 3 spans of 6 meters each. Every storey has a height of 3,5 meters. The primary beams lay in the X direction while the secondary beams lay in the Y direction. The elements are made of steel. On each floor and on the roof, the structure withstands two ways concrete slabs of 25 centimetres of thickness. The category B for office areas, defined in the EN 1991-1-1 [16], was chosen for the building. These data are chosen in accordance with those of Farah Hjeir.

Assumptions on the configuration of the 3D reference structure:

- The joints between columns and beams are assumed to be fully rigid. They are assumed to be fully resistant in order to make happen the yielding in the element and not in the joint;
- The supports are embedded in the ground (see figure II.2 for the illustration of embedded supports);
- The secondary beams are assumed to be simply supported by the primary beams in order not to transfer moment and make the design easier;
- There is no connection and therefore no composite actions between the concrete slabs and the steel beams.

Knowing that the study consists of the analysis of the behaviour of a 2D frame, only the design of the internal frames along the XZ plane will be checked without any consideration of the 3D effects in the behaviour of the 2D frame. Few assumptions may be made on the 2D model of the frame:

- No out-of-plane instability is considered;
- The buckling of the elements occurs around their strong axis in the plane.

The configuration of the 2D reference frame is exposed on figure II.2.

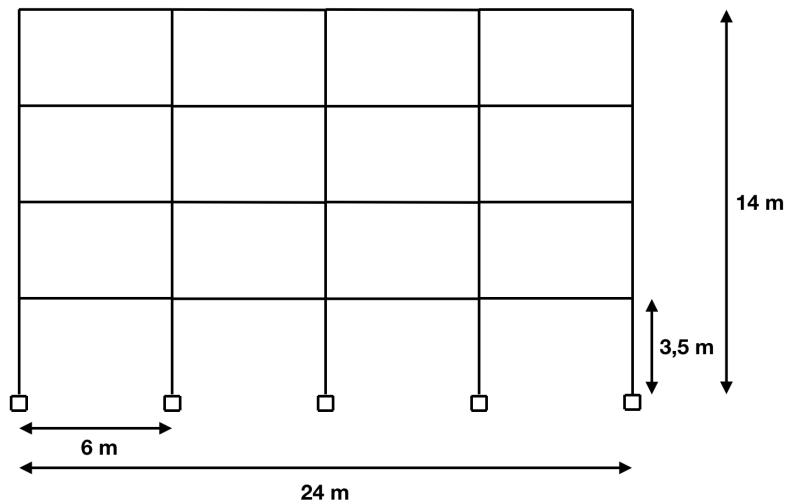


Figure II.2: 2D reference frame

II.2 Design

The structure of interest was designed according to a conventional design situation, i.e. following the SLS and ULS verifications.

The SLS was verified based on a list of characteristic combinations established according to the formula (6.14b) from the Eurocode EN 1990 [17]:

$$E_d = \sum_{j \geq 1} G_{k,j} + Q_{k,1} + \sum_{i > 1} \psi_{0,i} Q_{k,i} \quad (\text{II.1})$$

The maximum transverse displacement for one storey (visual comfort) allowed is $\frac{h}{250}$ where h is the height of one storey. The maximum transverse displacement for the entire structure allowed is $\frac{H}{500}$ where H is the height of the structure. The maximum deflection for floor beams (visual comfort) allowed is $\frac{L}{300}$ where L is the length of one beam. The maximum deflection for roof beams (visual comfort) allowed is $\frac{L}{300}$.

The ULS was verified based on a list of combinations established according to the formula (6.10) from the Eurocode EN 1990 [17]:

$$E_d = \sum_{j \geq 1} \gamma_{G,j} G_{k,j} + \gamma_{Q,1} Q_{k,1} + \sum_{i > 1} \gamma_{Q,i} \psi_{0,i} Q_{k,i} \quad (\text{II.2})$$

where $\gamma_{G,j} = 1,35$, $\gamma_{Q,i} = 1,5$ and values of $\psi_{0,i}$ may be found in the Table A1.1 page 49 of EN 1990 [17] depending on the action considered (wind, snow, etc.).

All the loads considered are listed in the Annex A. The verification of the design of the reference frame is detailed through the Annex A. The initial design taken by Farah Hjeir ([11]) is thus verified and shown on figure 3 in the Annex A.

Chapter III

Modelling of the reference structure

III.1 Implementation of the structure in the software FINELG

In order to make possible the analysis of the realistic behaviour of the reference structure, the use of a numerical tool is essential and in particular a finite element software. The software used is FINELG, a finite element software developed at the University of Liège in 1974 in association with Greisch design office.

The software allows us to make a 2D full non linear analysis including material non linearities and geometrical non linearities. Material non linearities include the yielding of the elements while the geometrical non linearities include the second order effects coming from the deformed shape of the frame.

All the following informations were found in the FINELG user's manual [18].

III.1.1 Discretization of the elements

The aim is to model the behaviour of a 2D frame. Thus, the elements chosen in the finite element model are plane beams with two nodes, i.e. one at each extremity of the element, see figure III.1.

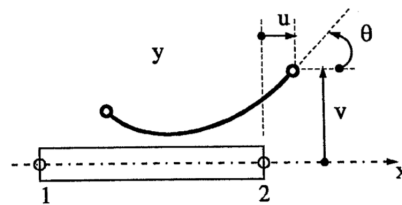


Figure III.1: Classical 2D element [18]

As the behaviour is in two dimensions, at each node, there are three degrees of freedom (dof), u the displacement along the x axis, v the displacement along the y axis and θ the rotation around the axis perpendicular to the plane (the z axis). As it was said in section II.1 page 24, out-of-plane instability is not considered. Indeed, these 2D beam elements do not allow to take into account any local buckling phenomenon. The lateral-torsional buckling is not taken into account neither. These considerations are the same than the ones adopted in the 2D composite frame computation in the PhD thesis of Demonceau J.-F. [6]. The M-V interaction is not taken into account by these elements.

The whole structure was first implemented on Ossa2D. The latter is a linear elastic computation software for 2D structures and was developed at the University of Liège [19]. Then, the file ".OD2" was extracted to the extension ".DAT" adapted to be treated on the software FINELG.

On FINELG, each element (beams and columns) is divided into a number of sections of integration. In our case, the choice is to divide each element in four sections of integration, see figure III.2 (the parameter defining the number of sections of integration is called NUIT on FINELG).



Figure III.2: Discretization of the elements

Then, one element is characterized by two nodes (figure III.1) and by four sections of integration (figure III.2). The software will deliver the displacements at the nodes and the internal forces (moment, shear force, normal force) at each section of integration. It should be noticed that internal forces are also done at each node of the elements but these latter are not the true internal forces in the elements but rather an interpolation of the values given at each sections of integration. Thus, it is understandable that the bigger the distance between the sections of integration (black dots on figure III.2) and the nodes (blue dots) the less precise the model will be.

Thus, as a consequence, in order to get an accurate model, the wish would be to increase the number of sections of integration. But, considering there cannot be more than four sections of integration by element, it is needed to divide the beams and the columns into several elements. The wish would then be to put the maximum amount of elements per beam and per column but the more elements in the structure the longer time of calculation. So, a compromise must be made between the time of calculation and the accuracy of the model.

The level of accuracy was determined based on the variation of the values of internal forces between the sections of integration near the extremities of the beams or columns and the values of internal forces at the extreme nodes of the beams or columns. As a picture is worth a thousand words, the image on the right of figure III.2 illustrates these latter locations in the place surrounded in red on the figure. The level of accuracy was also determined by analysing the values of the plastic moment at the location of plastic hinges at sections of integration and these latter were compared to their analytical values. Moreover, as the analytical prediction of the mechanism in the DAP is possible, the value of N_{lost} that causes the formation of the full plastic mechanism in the DAP determined analytically was compared to the one obtained numerically through FINELG. The analytical developments made to calculate the N_{lost} are not recalled in the present thesis (see Muller [14] and Huvelle [1]).

After having tested several configurations and analysed the precision of the results, it was concluded that the configuration obtained by dividing each beam and column into fifteen elements meets a good accuracy and not a too long calculation time. As an example, the figure III.3 illustrates the final discretization of a beam into fifteen elements. As shown, the elements are shorter near the extremities of the beam. Indeed, these are the critical locations where plastic hinges will develop and thus where the discretization needs to be more refined. Thus, the wish is to put more elements near the extremities for the sake of accuracy.

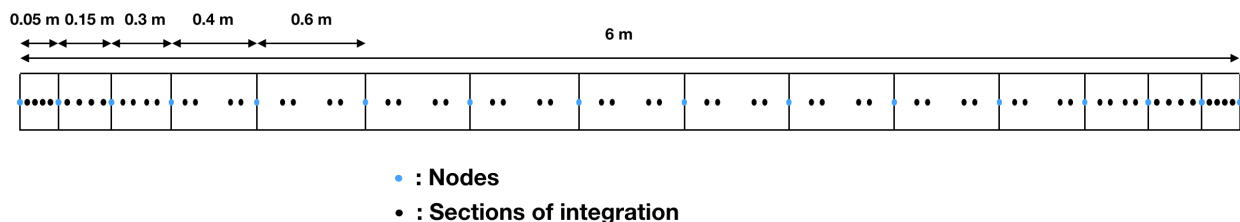


Figure III.3: Illustration of the beams' discretization

Moreover, the total sum of all the loads applied on the structure was compared to the total sum of the reactions at the supports. It is found that these latter are equal.

Seen the difficulty in performing tests for validating the model, several checks were done to establish the reliability of the results. After all these checks, the finite element model is considered as valid.

III.1.2 Discretization of the elements' cross-sections

Each cross-section of integration is discretized into several integration points. As illustrated on figure III.4, the flanges are made up of three rows of seven integration points respectively (in black color). The fillets are made up of one integration point each (in blue color). Finally, the flange is made up of nine integration points (in gray color). The latter configuration of the cross-sections' discretization was the default configuration defined by OSSA2D when exporting the file to the FINELG extension (".DAT").

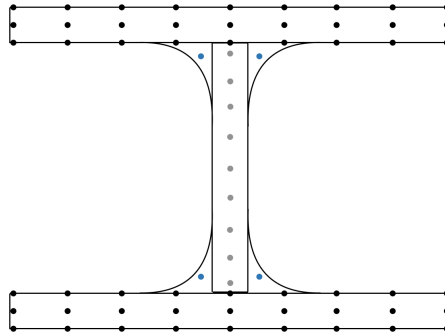


Figure III.4: Illustration of the cross-sections' discretization

III.1.3 Material laws

The material law for the steel is either the linear law from Hooke when the wish is to model an elastic behaviour of the frame and a bilinear law (elastic-perfectly plastic) when the wish is to model the yielding of the frame. The figure III.5 illustrates the linear law for a material infinitely elastic and the figure III.6 illustrates the bilinear law with an infinite ductility. An infinite ductility is chosen to maximise the deformation of the structure in order to analyse the behaviour of the latter as far as it is possible in terms of deformations. Indeed, as stated in chapter I, in robustness consideration, large displacements happen especially during Phase 3 to activate the catenary actions.

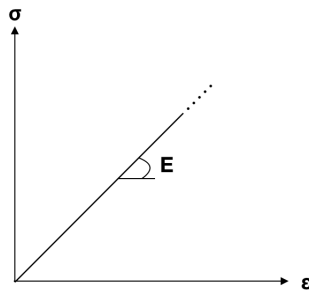


Figure III.5: Linear elastic law (infinite elastic behaviour)

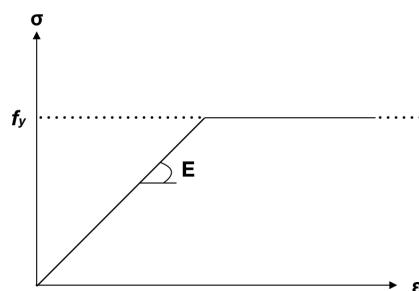


Figure III.6: Bilinear law - elastic perfectly plastic law (with infinite ductility)

For the linear law, the Young's modulus (E) has to be given as an input data to the software. For the bilinear law, see figure III.6, the Yield strength (f_y) and E have to be given as input data to the software. Moreover, the Poisson's ratio (ν) is also given for both laws. The table III.1 exposed the values of these latter.

E [Mpa]	205000
f_y [Mpa]	355
ν [-]	0.3

Table III.1: Input data for material laws

Characteristic values are taken for the resistance in the model, i.e. a security factor equals to 1. Indeed, the goal is not to accomplish a design of the frame but rather to analyse the behaviour of the latter.

III.1.4 Summary of choices made in FINELG

All the choices previously made on the model through the use of FINELG are the following:

- 2D full non linear analysis including material non linearities and geometrical non linearities;
- Out-of-plane instabilities are not considered as it is a 2D behaviour under investigation;
- Fifteen elements per beam and per column;
- When the material is wanted to be indefinitely elastic, it follows the Hooke's law, see figure III.5. When the material is wanted to yield, the bilinear law is followed, see figure III.6. An infinite ductility is considered in order to go as far as possible in terms of deformations.

III.2 Combination of actions for accidental design situations

The Eurocode prescribes that the study of the behaviour of a frame that loses one column (exceptional event) has to be made under a loading defined in accordance with the combination of actions of an accidental design situation. Thus, the loading of the reference structure will be established based on an accidental combination of actions.

The combination of actions for accidental design situations considered in the following analysis is established in accordance with the formula (6.11b) given in the EN1990:2002 page 45 [17] as follows:

$$E_d = \sum_{j \geq 1} G_{k,j} + A_d + \psi_{1,1} Q_{k,1} + \sum_{i > 1} \psi_{2,i} Q_{k,i} \quad (\text{III.1})$$

The term A_d is considered equal to 0 because neither impact nor fire and no other accidental actions are considered during the loss of the column.

The accidental combination considered includes only gravity loads (vertical loads), i.e. no horizontal actions are considered as for instance the wind, etc. This choice is made to keep a simple loading of the structure in order to simplify the further analysis of its behaviour including the analysis of the evolution of the internal forces in the elements following the loss of the column. The combination of actions considered is the following:

$$E_d = G_k + \psi_{1,1} Q_{k,1} + \psi_{2,2} Q_{k,2} \quad (\text{III.2})$$

where G_k includes the weight of the concrete slab and the topping layer, $Q_{k,1}$ is the live loads either for the roof ($6kN/m$) either for the floors ($18kN/m$), $Q_{k,2}$ is the snow load acting on the roof ($2,4kN/m$),

$\psi_{1,1}$ is equal to 0,5 for live loads in buildings of category B (office areas) and $\psi_{2,2}$ is equal to 0 for snow loads acting on buildings situated at an altitude lower than 1000 meters above sea level according to the Table A1.1 page 49 of the EN1990:2002 [17]. Note that the self weight is included in the study (for steel elements, it is taken equal to 7850 kg/m^3). The loads are detailed in Annex A.

The accidental combination of actions applied on the roof is:

$$p_{roof} = 46,5 + 0,5 * 6 = 49,5 \text{ kN/m}$$

The accidental combination of actions applied on the floors is:

$$p_{floor} = 46,5 + 0,5 * 18 = 55,5 \text{ kN/m}$$

See figure III.7 to see the repartition of these latter loads.

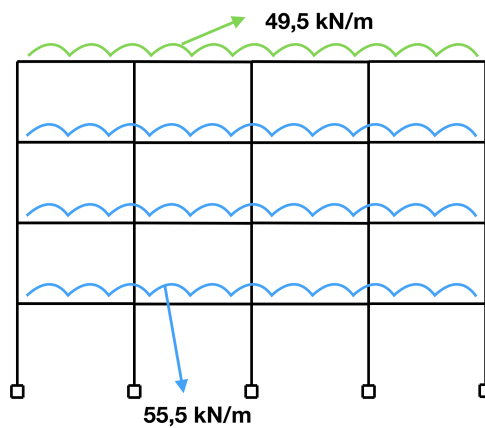


Figure III.7: Loading of the reference structure

III.3 Methodology followed in FINELG to simulate the loss of the column

As illustrated on figure III.8, the column AB is modeled in FINELG through the application of its internal forces to the frame ($N_o; V_o; M_o$). Thus ($N_o; V_o; M_o$) corresponds to the internal forces in the central column at ground level when the frame is loaded.

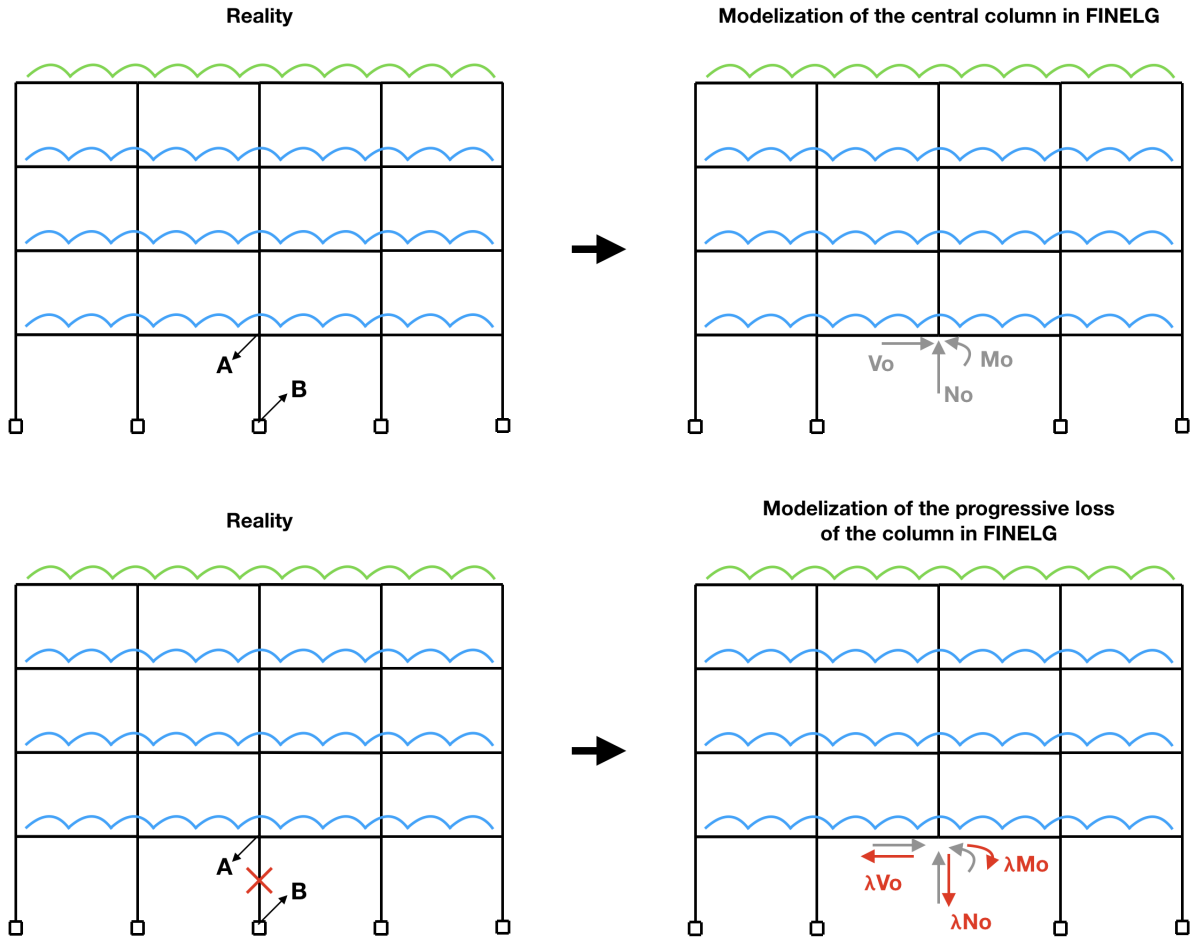


Figure III.8: Modelization of the central column of the frame at ground level

To model the progressive loss of the column, the task consists in applying progressively the same forces than $(N_o; V_o; M_o)$ but in the opposite direction, i.e. applying forces $(\lambda N_o; \lambda V_o; \lambda M_o)$ where λ is a coefficient varying from 0 to 1. When λ is equal to 0, it means that the column is undamaged and when λ is equal to 1, it means that the column is completely lost. And the values of the coefficient λ between 0 and 1 characterize the progressive loss of the column.

The schema showing the modelization of the progressive loss of the column, see figure III.8, may be divided into two sequences in FINELG. The figure III.9 illustrates these two sequences. The first sequence consists in removing the central column at ground level and replacing it by applying its internal forces $(N_o; V_o; M_o)$ to the frame which then simulates a fictive presence of the column. As it is the central column which is removed, the behaviour of the structure is symmetrical. Thus, V_o and M_o are both null, only the vertical forces remain¹. The internal normal force into the column is chosen to be named $N_{AB,normal}$ and is equal to N_o while λN_o is chosen to be named N_{lost} to stay in accordance with the formalisms defined in chapter I.

As already stated in chapter I, the general behaviour of the 2D frame under the loss of its central column will be analysed based on the evolution of the varying force in the column during its destruction, i.e. $N_{AB} = N_{AB,normal} - N_{lost}$, see figure III.9, in function of the displacement of the top of the lost column, i.e. the point A on III.8.

¹In the case of the loss of an other column than a central column, it is necessary to take into account the V_o and M_o .

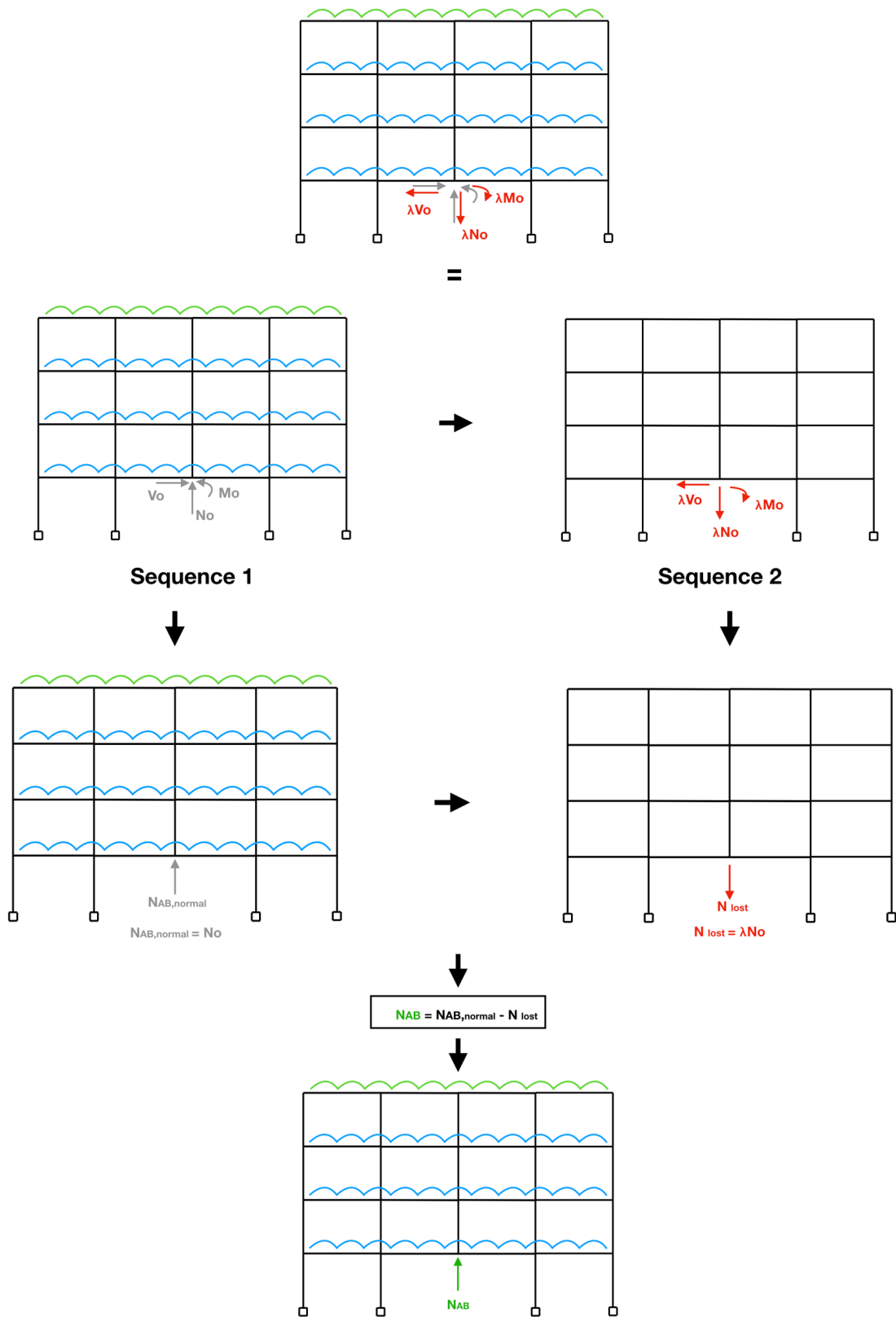


Figure III.9: Modelization of the sequences followed in FINELG to model the progressive loss of the column

III.4 Conclusion

All the choices and assumptions made on the model in the finite element software FINELG were exposed in the present chapter.

The considered loading was detailed.

Finally, the methodology followed to simulate the loss of the column in FINELG was exposed.

Everything is now ready to start several investigations on the influence of the yielding of the IAP on the global response of frames losing one column through simulations in next chapters.

Chapter IV

Global response and failure modes of the reference structure (numerical analysis)

IV.1 Introduction

Within the present chapter, the task will be to analyse the global response of the reference structure both for the case where the IAP remains fully elastic and for the case where the IAP may yield and to compare these latter. The successive phases in the behaviour of the structure identified in Chapter I will be highlighted and explained for both previous situations. As already mentioned in section I.5, the aim is to evaluate the successive developments of plastic hinges in the IAP. Indeed, the goal is to determine if the first hinges in the IAP induce a chain development of additional plastic hinges bringing to a quick collapse of the structure. In other words, the goal is to know if the N_{lost} inducing the collapse of the structure is significantly bigger than the N_{lost} inducing the formation of the first hinges in the IAP.

Then, an analysis of the redistribution of internal forces in the structure during the loss of a column will be performed. The aim is to be able to identify which elements in the structure are seeing their internal forces changing during the scenarios bringing to identified failure modes. Thus, it will be possible to prescribe verification recommendations.

The latter tasks will be done through three scenarios, the loss of a central column firstly, the loss of an intermediate column secondly and the loss of an exterior column thirdly, see figure IV.1. The aim is to analyse the influence of the location of the lost column on the global response of the frame. For the three scenarios, the associated identified failure modes will be presented. These are the goals followed through section IV.2 and through section IV.3.

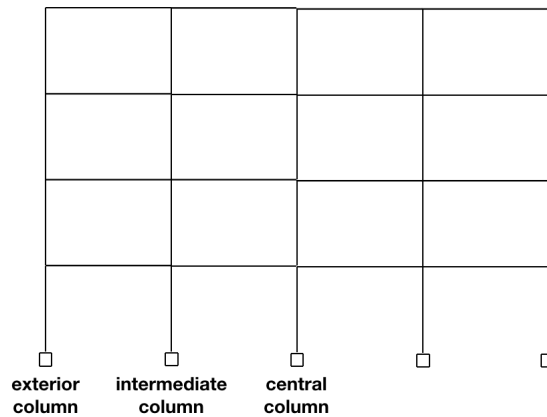


Figure IV.1: Scenarios considered regarding the analysis of the global response of the reference structure

IV.2 Analysis of the reference structure under the loss of its central column

In the present section, the global response of the frame will be detailed in both cases where the IAP remains elastic and where the IAP may yield in the situation of the loss of a central column. On figure IV.2, the DAP is drawn in red while the IAP is drawn in blue.

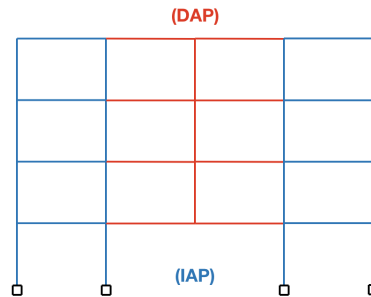


Figure IV.2: DAP and IAP of the reference structure under the loss of its central column

IV.2.1 DAP elastic-perfectly plastic - IAP elastic

The $(u; N_{AB})$ curve for an IAP remaining fully elastic and a DAP elastic-perfectly plastic is given on figure IV.3.

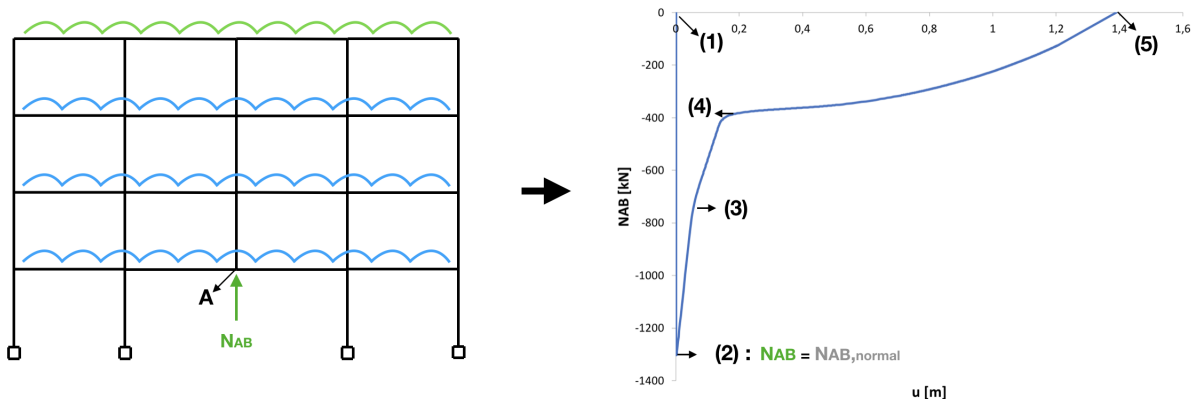


Figure IV.3: DAP elastic-perfectly plastic - IAP elastic

IV.2.1.1 Identification of successive phases in the behaviour of the structure

The successive phases in the behaviour of the structure will be compared to the ones presented in section I.4.1 based on the $(u; N_{AB})$ curve shown on figure IV.3.

Phase 1 : Loading of the structure (1) -> (2)

During this phase, the frame is progressively loaded and the internal normal force in the column AB is growing from 0 (point (1)) to the value of $N_{AB,normal}$ (point (2)). In the present situation, $N_{AB,normal}$ is equal to $1302,5kN$. At point (2), the vertical displacement of the point A (u) is very small.

Phase 2 : Progressive removal of the column (2) -> (4)

Point (2) marks the start of the progressive removal of the column. At point (2), N_{lost} (λN_o) is equal to zero, indeed λ is equal to zero (as previously explained in section III.3). From point (2) to point (3), λ is gradually increasing leading to an increase of the value of N_{lost} . Thus, the absolute value of N_{AB} is decreasing as shown on figure IV.3 in accordance with the equation I.1 in Chapter I. From point (2) to point (3), the DAP remains elastic. At point (3), the first plastic hinge is formed in the DAP.

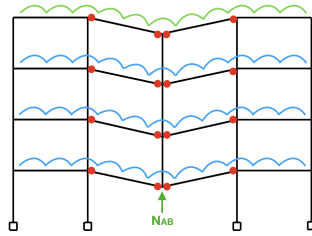


Figure IV.4: Beam plastic mechanism in the DAP

From point (3) to point (4), the slope of the curve is progressively decreasing, see figure IV.3. It corresponds to the progressive formation of plastic hinges in the DAP. At point (4), a beam plastic mechanism is fully developed in the DAP as shown on figure IV.4. During Phase 2, the vertical displacement of point A (u) is governed by the first order stiffness coming from the DAP. When the beam plastic mechanism is formed (point (4)), there is no more first order stiffness. Indeed, as shown on the chart of figure IV.3, a plateau is reached when the plastic mechanism is developed.

Phase 3 : Progressive removal of the column (4) -> (5)

From point (4) to point (5), the slope of the curve is progressively increasing. Indeed, the IAP brings a second order stiffness allowing an increase of N_{lost} through the development of catenary actions translated by an increase of the tension in the bottom beams of the DAP. As shown on the graph of figure IV.3, the value of u is significantly increasing during Phase 3 as there is no more first order stiffness in the DAP since a complete plastic mechanism is formed. While these large displacements happen, tensile forces are developing in the bottom beams. These latter are pulling on the IAP which then acts as a lateral anchorage. These pulling forces acting on the IAP are inducing lateral displacement of the latter. As a consequence, the upper beams of the DAP are put into compression. The latter behaviour may be called the arch effect, see figure IV.5. This will be explained in detail in section IV.2.1.2. Finally, at point (5), the column is fully lost and N_{lost} is thus equal to $N_{AB,normal}$ leading to $N_{AB} = 0kN$.

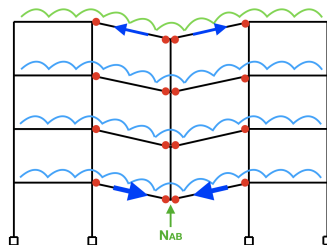


Figure IV.5: Catenary actions and arch effect

The global response of the frame with an IAP remaining elastic and a DAP elastic-perfectly plastic which was analysed previously based on a numerical simulation made on the software FINELG has shown a complete accordance with the behaviour presented in Chapter I.

IV.2.1.2 Analysis of the internal forces' distribution in the elements of the structure

As already mentioned in section III.2 page 31, the accidental combination of actions includes only vertical loads. Thus, the evolution of internal forces in the frame is symmetrical since it is the central column that is lost. As a consequence, the evolution of internal forces will be analysed only for half of the structure as shown on the right of figure IV.6. The cross-sections under investigation in the following points are the critical cross-sections, i.e. where the hinges will develop in the DAP for instance and thus the critical locations that may break and induce a failure.

Evolution of the normal forces into the beams of the DAP:

The figure IV.6 shows the evolution of the normal forces N into the beams 1, 2, 3 and 4 of the DAP (and especially of the beams' cross-sections shown on the right of the latter figure) in function of the value of N_{lost} .

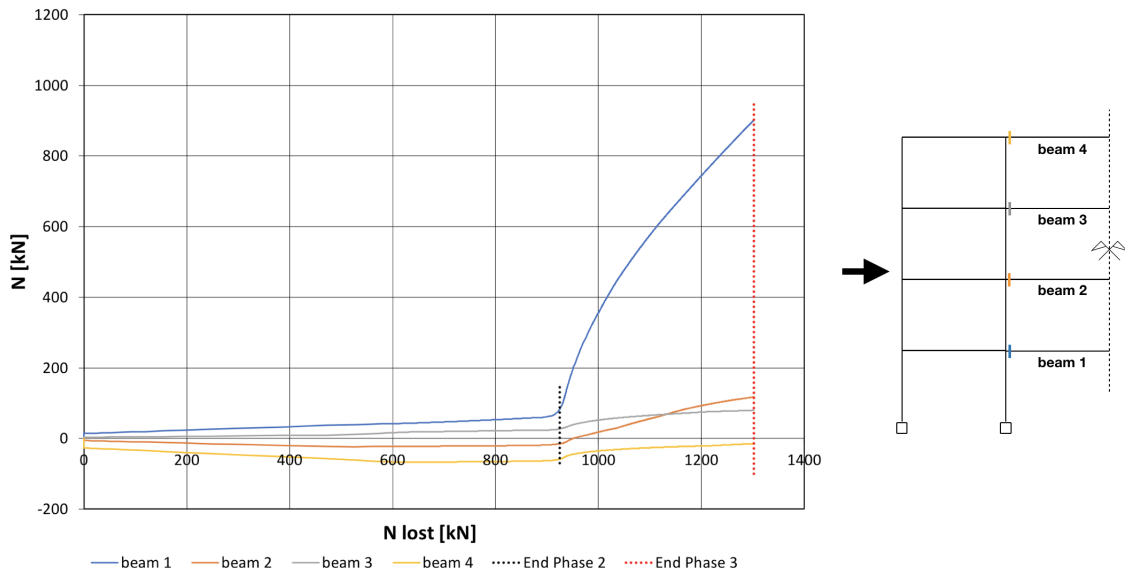


Figure IV.6: Evolution of the normal forces into beams' cross-sections of the DAP

From the end of Phase 1 (i.e. for $N_{lost} = 0kN$) to the end of Phase 2 (marked by a vertical black dotted line on the graph of figure IV.6), as known the displacement of the top of the central column (u) is increasing with an increase of N_{lost} . The increase of N_{lost} implies a progressive appearance of tensile forces into the beams 1 and 3 (since N is positive) that start to pull slightly on the IAP. These small pulling forces acting on the IAP induce small lateral displacements of the IAP as it is schematically illustrated on figure IV.7. These lateral displacements induce the appearance of compressive forces into beams 2 and 4 (since N is negative), see figure IV.6. The tension forces into beams 1 and 3 that are likely to lead the IAP towards the center of the structure are thus countered by the compression in beams 2 and 4 during Phase 2. This effect may be called the arch effect. Finally, during Phase 2, beam 1 presents the maximum tensile force while beam 4 presents the maximum compression force.

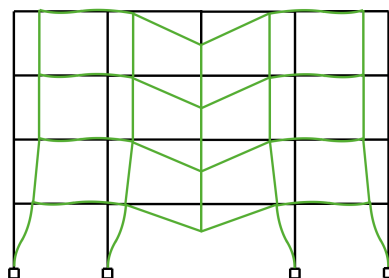


Figure IV.7: Schema of the frame's deformation (End Phase 2)

When the beam plastic mechanism is fully formed in the DAP, i.e. at the end of Phase 2, tensile forces are significantly increasing in beam 1. This increase of the tensile forces in the beam 1 illustrates the catenary actions. In parallel, beam 3 sees an increase of its tensile forces. Beam 2, previously in compression, is put into tension and the tensile forces increase until the end of Phase 3. Finally, beam 4 sees a decrease of its compression during Phase 3 but is not put into tension. As a result, the large vertical displacements (u) occurring during Phase 3 tend to put all the beams of the DAP into tension. In the case of the present structure, only beams 1, 2 and 3 are put into tension during Phase 3. The normal forces acting in the beams of the DAP at the end of Phase 3 are illustrated on figure IV.8.

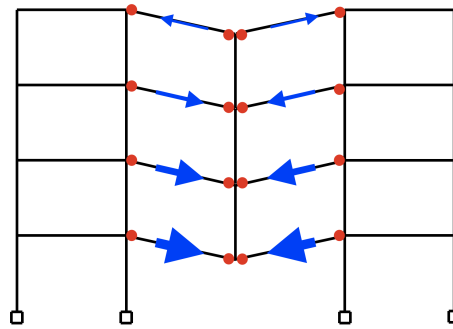


Figure IV.8: Illustration of the normal forces into the beams of the DAP (End Phase 3)

Evolution of the bending moments into beams of the DAP:

The evolution of the bending moments into beams of the DAP will be shown for the cross-sections where hinges are developing in the DAP and especially for the beams' cross-sections near the IAP, see figure IV.9.

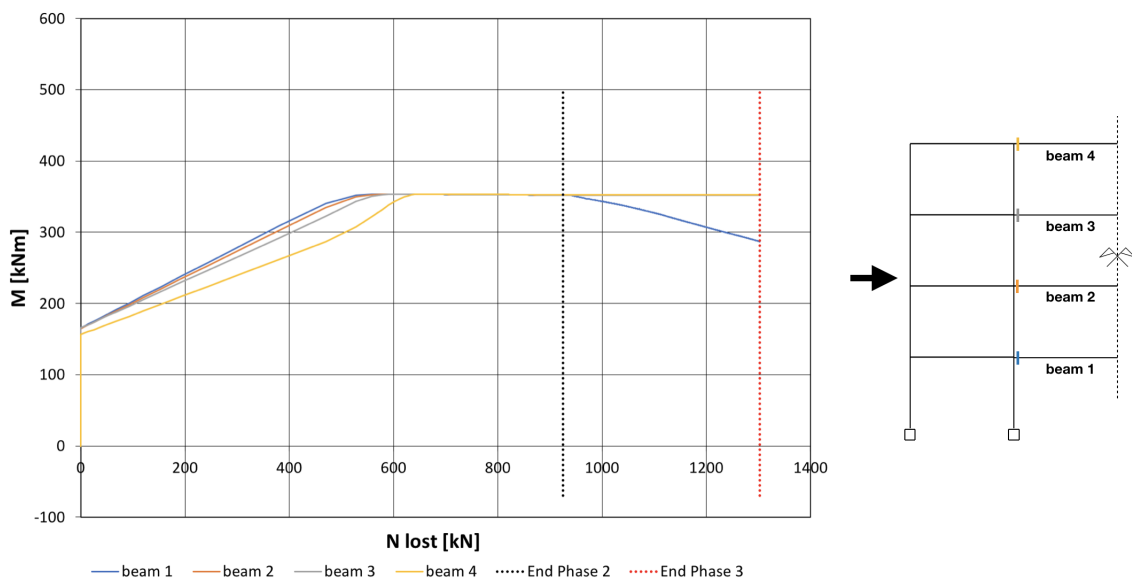


Figure IV.9: Evolution of the bending moments into beams' cross-sections of the DAP

For N_{lost} equals to 0, the bending moment is increasing in each of the four beams' cross-sections, see figure IV.9. This corresponds to Phase 1, i.e. when the frame is loaded ($N_{lost} = 0kN$). The bending moment distribution into the structure at the end of Phase 1 is shown on figure IV.10.

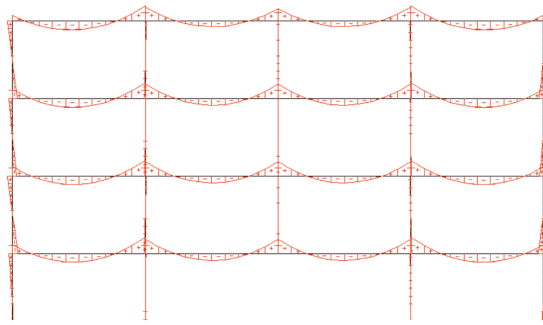


Figure IV.10: Bending moment diagram at the end of Phase 1

The beginning of Phase 2 is marked by an increase of N_{lost} which leads to an increase of the bending moments of the beams' cross-sections as shown on figure IV.9. The bending moments are increasing until they reach the plastic moment M_{pl} which then marks the beginning of their yielding. The yielding is characterized by the plateau on the graph. The bending moment distribution into the structure at the end of Phase 2 is shown on figure IV.10.

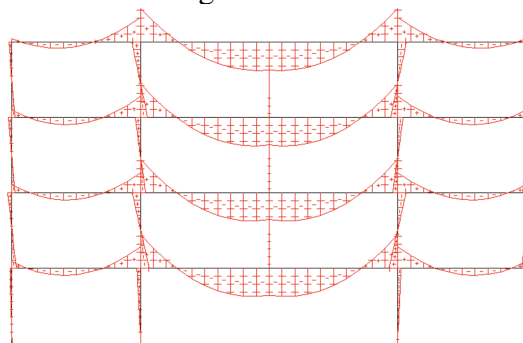


Figure IV.11: Bending moment diagram at the end of Phase 2

The transition in the shape of the bending moment diagram from figure IV.10 to figure IV.11 occurs as a result of the application of the vertical and downwards load N_{lost} . If only the load N_{lost} was acting on the frame, the shape of the bending moment in the structure would have been the one shown on figure IV.12. Thus, knowing the shape of the bending moment in the structure when the frame is loaded under the accidental combination of actions considered (figure IV.10) and knowing the shape of the bending moment in the structure under the only action of N_{lost} on the frame (figure IV.12), it is understandable that the shape of the bending moment in the structure obtained by considering these two latter loadings will be the one shown on figure IV.11.

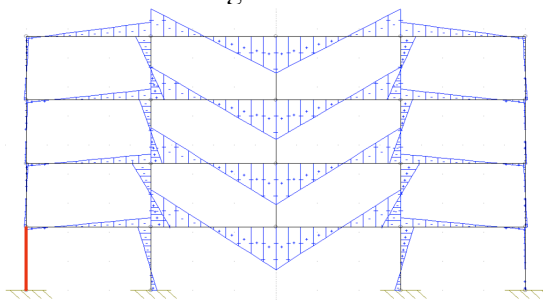


Figure IV.12: Bending moment diagram under a downwards vertical load applied at the top of the lost column

During Phase 3, i.e. for the range between the two vertical dotted lines on figure IV.9, all the bending moments remain on the plateau except the one for the section of beam 1. Indeed, as previously explained and as shown on figure IV.6, the tension into beam 1 is significantly increasing during Phase 3. As a consequence, the decrease of the bending moment for the cross-section of beam 1 shows simply the M-N interaction as the N became significant enough to have an impact on the evolution of the M . The bending moment diagram in the structure at the end of Phase 3 is the one

shown on figure IV.13. As shown, the moments into the columns at ground level in the IAP have significantly increased in comparison with the end of Phase 2. Moreover, the moments in the bottom beams of the IAP have significantly increased as well. These latter considerations will be analysed through the next points.

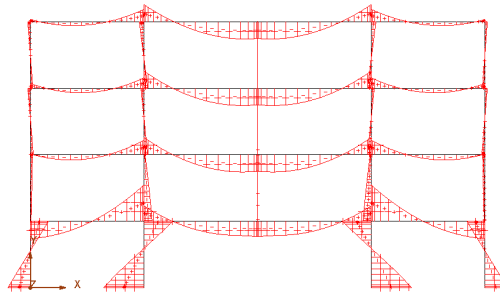


Figure IV.13: Bending moment diagram at the end of Phase 3

Evolution of the normal forces into columns of the IAP:

Within these paragraphs, the designations of the columns of the IAP will follow the same designations defined by Hai through his PhD thesis and summarized in the section I.4.3.2 in Chapter I.

As shown on figure IV.14, when N_{lost} is equal to 0, i.e. during Phase 1, the normal forces into the columns are increasing since the frame is loaded. When N_{lost} starts to increase, it marks the beginning of Phase 2. Until the end of Phase 2, the compressive force in column 1 (side column) remains almost constant, the compression decreases a bit. In parallel, the compressive force in column 2 (beside column) is increasing almost linearly from the end of Phase 1 until the end of Phase 2. The increase of the compressive force in column 2 comes from the redistribution of the normal load previously supported by the central column and the redistribution of the normal load coming from the slight decompression of column 1.

Since the decompression of column 1 is very small, the compression force in column 1 remains almost constant during Phase 2. As a result, the increase of the compression in column 2 during Phase 2 is mainly induced by the redistribution of the normal load previously supported by the central column. A linear curve is drawn on the figure (gray dashed line called "N lin") showing the evolution of N in column 2 if only N_{lost} was redistributed into the beside columns, i.e. $\frac{N_{lost}}{2}$ in the beside column from the left (column 2) and $\frac{N_{lost}}{2}$ in the other beside column (not shown on the figure). The difference between the value of N in column 2 and the one of "N lin" at the end of Phase 2 is about 2,7%.

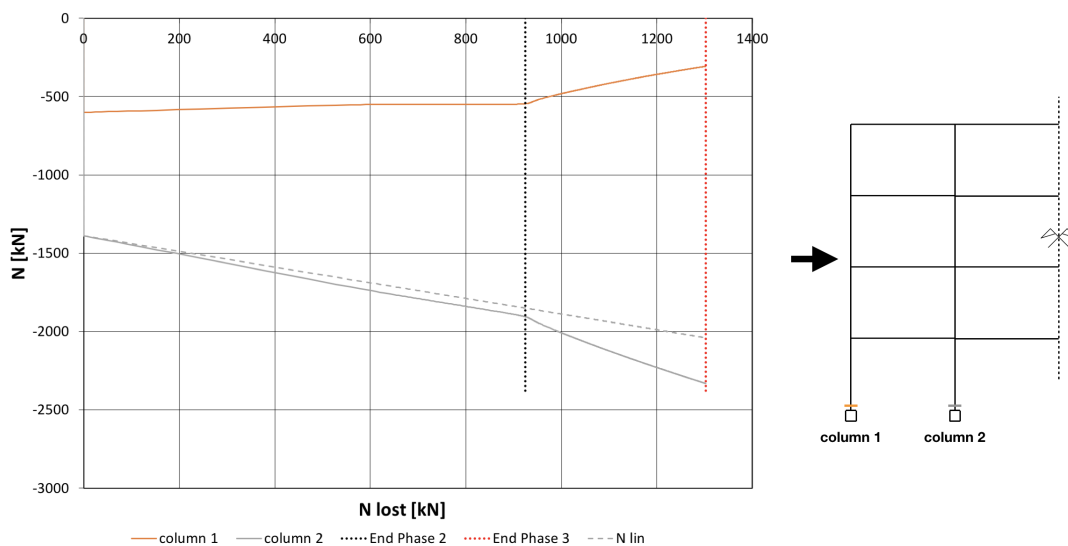


Figure IV.14: Evolution of the normal forces into columns' cross-sections of the IAP

During Phase 3, a change in the slope is shown both for the curves corresponding to column 1 and to column 2. As previously explained in section I.4.3.2, the change of the slope of the curve of the normal forces in beside column comes from the increase of N_{memb} coming both from the increase of F_{memb} and from the increase of the vertical displacement of the top of the lost column (u) increasing the inclination of F_{memb} and thus increasing the value of its vertical component N_{memb} , see figure I.20 in chapter I.

But, Hai in his PhD thesis shows a graph on which the compression in the side column (column 1 in the present situation) remains constant both during Phase 2 and Phase 3, see figure I.17 in section I.4.3.2. It is obviously not the case in the present situation, see figure IV.14.

During Phase 3, as previously stated, the tension in the beam 1 is significantly increasing. Thus, the horizontal component of the latter tensile force is significantly increasing as well. The latter horizontal load is acting on the IAP in the same way than the horizontal load illustrated on figure IV.15. The latter implies vertical reactions at the bottom of the two columns as shown on the figure. Thus, the horizontal load implies a downwards vertical reaction for the left column and an upwards vertical reaction for the right column. That is why a decompression appears for column 1. That also explains the increase of the compression appearing in column 2 in addition to the increase of the compression induced by the redistribution of N_{lost} .

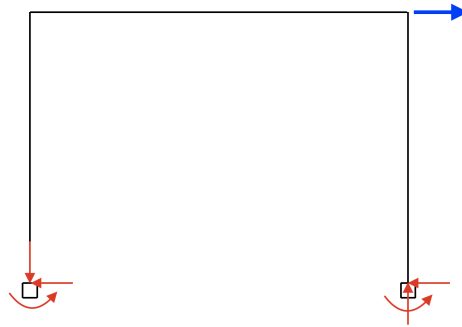


Figure IV.15: Effect of an horizontal load

To summarize, the change of the slope of the $(N_{lost};N)$ curve for the column 2 during Phase 3 is mainly due to both the increase of N_{memb} and the action of H_{memb} coming from the increase of the tensile force F_{memb} in beam 1, see figure I.20 in section I.4.3.2. The change of the slope of the $(N_{lost};N)$ curve for the column 1 during Phase 3 is mainly due to the action of H_{memb} coming from the increase of the tensile force F_{memb} in beam 1 and thus the effect shown on figure IV.15.

The difference between the N in the column 2 and the N of the "N lin" curve at the end of Phase 3 is about 15%.

Evolution of the bending moments into columns of the IAP :

As shown on figure IV.16, the evolution of the bending moments in column 1 and 2 until the end of Phase 2 is similar to the one detailed by Hai in his Phd thesis and summarized in the section I.4.3.2 and will not be repeated here to avoid redundancy.

The evolution of the bending moments in both columns during Phase 3 follows the same trend as the evolution of the normal forces in the beams of the DAP shown on figure IV.6 as the bending moments in columns 1 and 2 are mainly induced by the normal forces in the beams of the DAP.

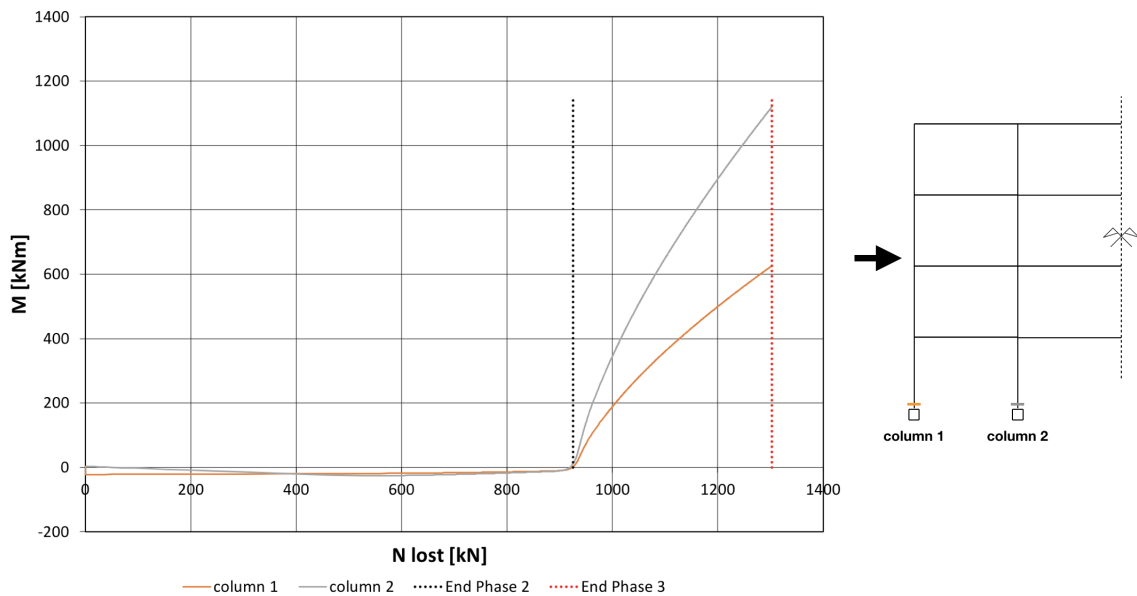


Figure IV.16: Evolution of the bending moments into columns' cross-sections of the IAP

Evolution of the normal force into the bottom beam of the IAP:

As shown on figure IV.17, the evolution of the normal force into the bottom beam of the IAP is chosen to be presented for the nearest cross-section to the DAP. Indeed, it is the latter cross-section of the beam that will present the biggest bending moment and thus represents the most critical section.

For N_{lost} equals to 0, i.e. during Phase 1, the normal force in the bottom beam of the IAP is positive and thus corresponds to tension. During Phase 2, i.e. when N_{lost} is increasing, the tensile force remains almost constant. Indeed, the normal force into beam 1, is only slightly increasing during Phase 2 and thus it cannot affect that much the shape of the normal force into the bottom beam of the IAP.

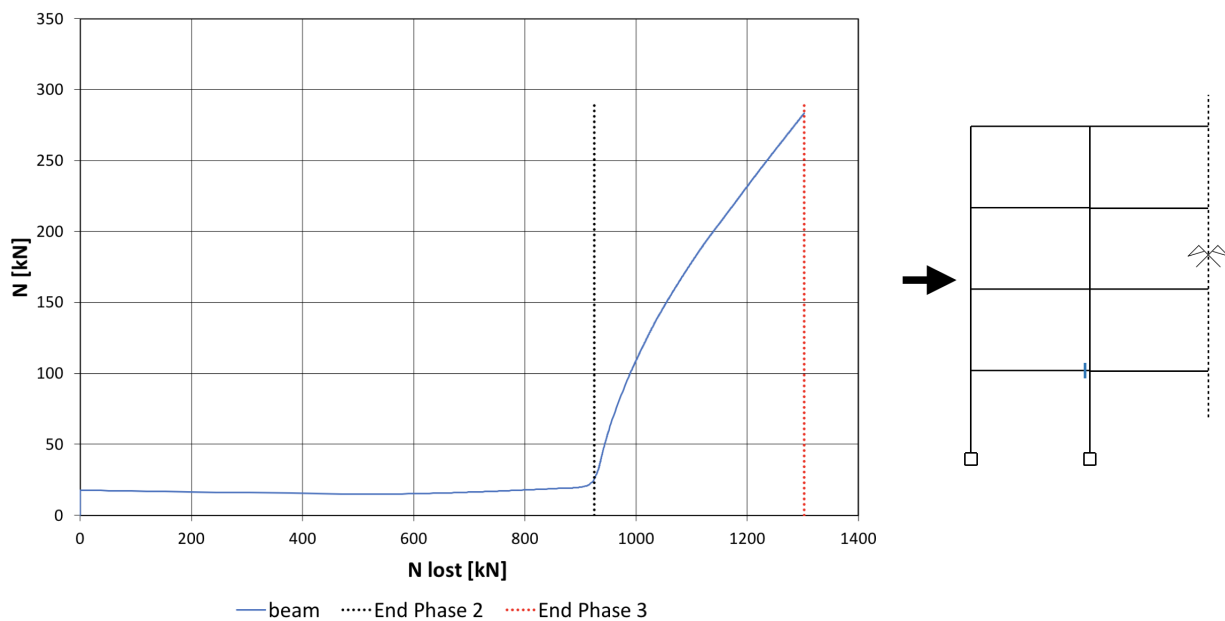


Figure IV.17: Evolution of the normal force into bottom beam's cross-section of the IAP

From the end of Phase 2 to the end of Phase 3, N is significantly increasing, see figure IV.17. It is logical since the tension in the beam 1 of the DAP is significantly increasing during Phase 3 as shown on figure IV.6.

Evolution of the bending moment into the bottom beam of the IAP:

As shown on figure IV.18, the bending moment is increasing for N_{lost} equal to 0, i.e. during Phase 1. It corresponds to the loading of the structure where uniformly distributed loads are acting on each beam and thus create a bending moment into the beams.

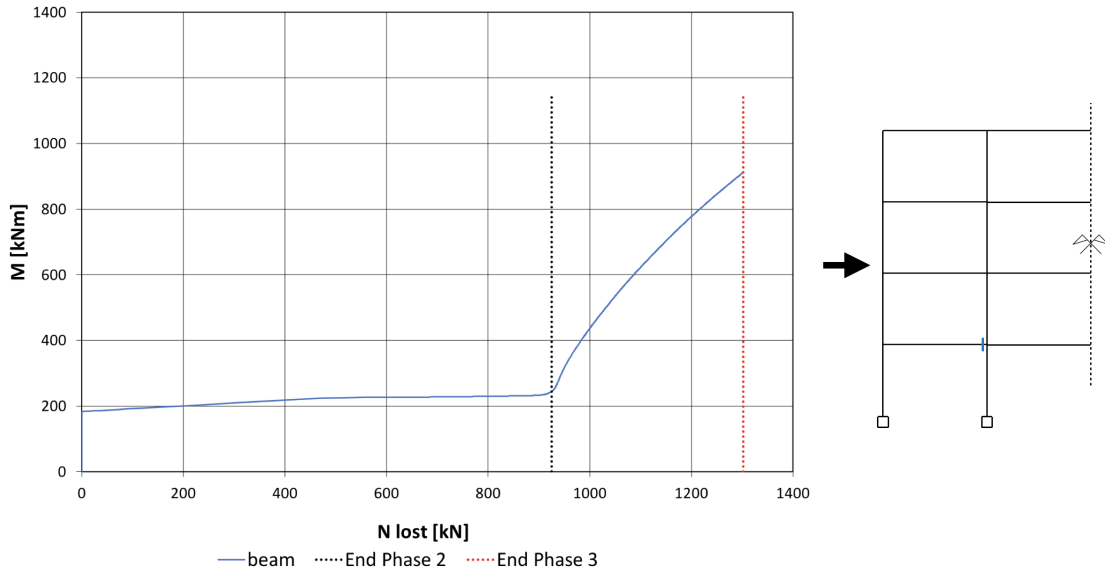


Figure IV.18: Evolution of the bending moment into bottom beam's cross-section of the IAP

The bending moment is slightly increasing during Phase 2 and significantly increasing during Phase 3 as shown on figure IV.18. To understand why the bending moment is increasing, it is necessary to analyse what loads are acting on the beam and what effects they imply.

The application of a downwards uniformly distributed load on the beam of the simple frame presented at the top of figure IV.19 implies the shown bending moment diagram (top left of the figure). At the end of Phase 1, when the frame is fully loaded and thus when the bottom beam of the IAP is submitted to a downwards uniformly distributed load (p_{floor} defined in section III.2), the shape of the bending moment diagram in the beam is similar, see figure IV.10.

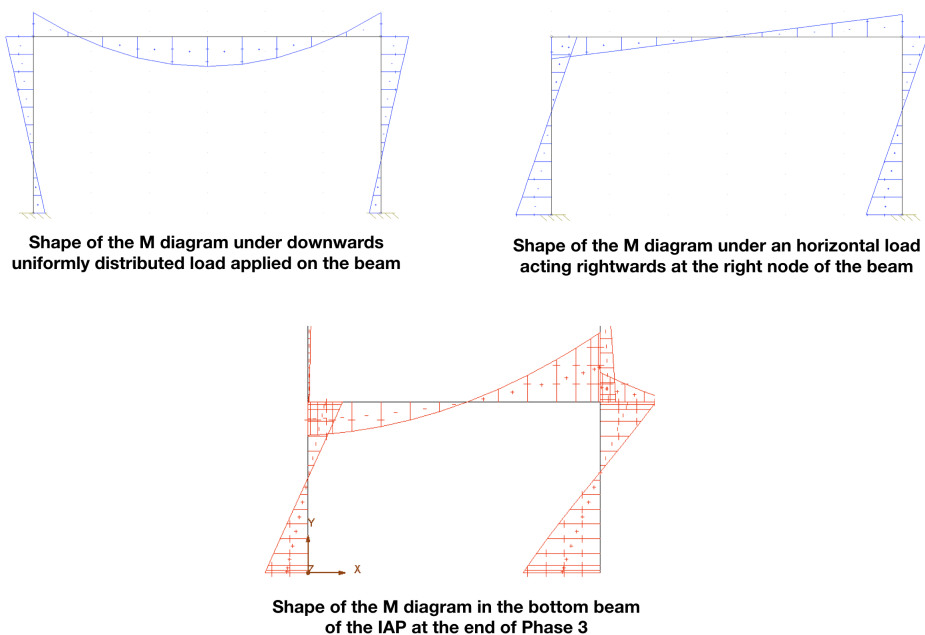


Figure IV.19: Shape of the bending moment diagram in the bottom beam of the IAP

As known, during Phase 2 and especially during Phase 3, the normal forces in the beams of the DAP are changing. Thus, the horizontal force acting on the right node of the bottom beam of the IAP is increasing. As shown on the top right of figure IV.19, the application of a rightwards horizontal load on the right node of the beam leads to the shown bending moment diagram.

As a consequence, the combination of the effects leading respectively to the two bending moments diagrams at the top of the figure IV.19 gives the shape of the bending moment diagram in the bottom beam of the IAP, i.e. the one at the bottom of figure IV.19.

These latter considerations explain why the value of the moment is increasing at the extreme right cross-section of the bottom beam of the IAP during Phase 2 and especially during Phase 3 as shown on figure IV.18.

Conclusion:

As long as the IAP remains indefinitely elastic, the evolutions of internal forces in the structure presented previously are not influenced by a potential yielding of the elements in the IAP. This will be investigated through the next section.

IV.2.2 DAP elastic-perfectly plastic - IAP elastic-perfectly plastic

The real behaviour of the frame under the loss of its central column will logically fit better the results obtained through simulations taking into account the yielding of the IAP than simulations where the IAP remains elastic as in the previous section.

In the present section, the influence of the yielding of the IAP on the global response of the frame will be analysed. More particularly, the order of formation of plastic hinges in the IAP as well as their locations will be determined. As previously detailed, the aim is to determine if the formation of the first hinges in the IAP induces a quick reach of the collapse of the structure through a chain formation of hinges.

The $(u; N_{AB})$ curve for an IAP elastic-perfectly plastic and a DAP elastic-perfectly plastic is given on figure IV.20. The latter is superposed with the one for an IAP remaining fully elastic. As shown, when the IAP is elastic-perfectly plastic, the structure is apparently not robust enough to reach the complete loss of the column (i.e. $N_{AB}=0\text{kN}$). Moreover, the development of the catenary actions during Phase 3 seems to be significantly limited by the yielding of the IAP.

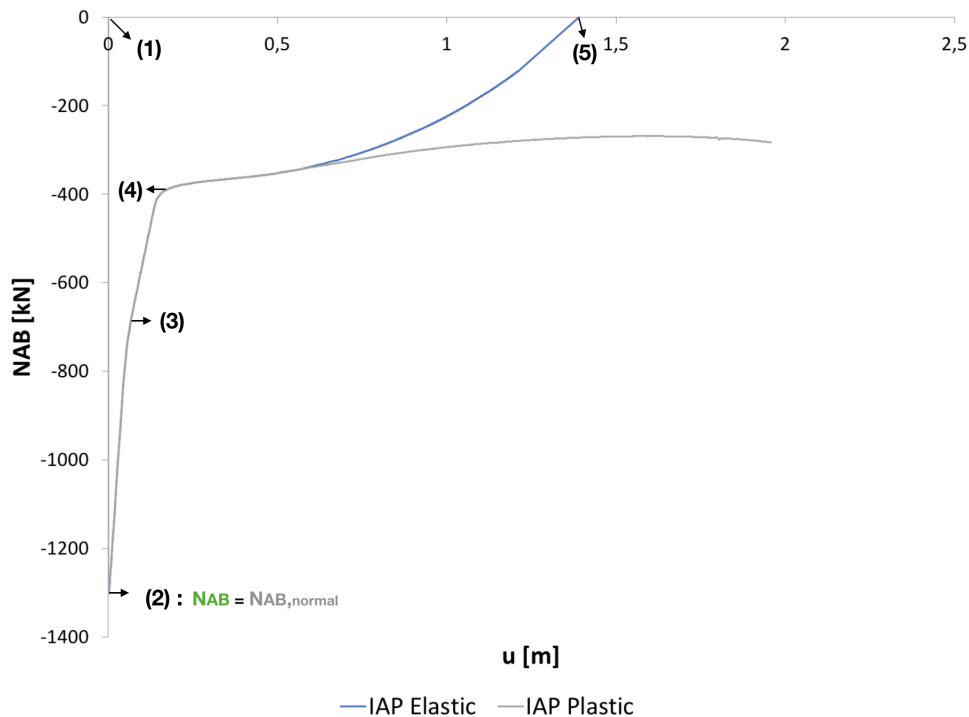


Figure IV.20: DAP elastic-perfectly plastic - IAP elastic-perfectly plastic

IV.2.2.1 Identification of successive phases in the behaviour of the structure

As shown on figure IV.20, Phases 1 and 2 are exactly the same for an IAP remaining fully elastic than for an IAP that may yield. The difference between the two curves occurs only during Phase 3. Thus, the yielding of the IAP in the present situation, i.e. the loss of a central column of the frame, only impacts the global response of the frame during Phase 3. As a consequence, the behaviour of the frame during Phase 1 and 2 will not be reminded here and the focus will be turned towards the global response of the frame during Phase 3.

Phase 3 : Progressive removal of the column (4) -> ...

As it is the case for the situation where the IAP remains elastic, the beginning of Phase 3 starts with an increase of the slope of the $(u; N_{AB})$ curve implied by the second order stiffness coming from the IAP allowing the activation of the catenary actions, i.e. the increase of the tensile forces into the bottom beams of the DAP. While the slope of the curve is increasing until the complete loss of the column (point (5)) for the frame with an IAP elastic, the slope of the curve for an IAP that may yield starts to decrease when the IAP yields. It means that the lateral stiffness brought by the IAP is progressively decreasing since the latter is progressively yielding through the development of several plastic hinges. Thus, for the present situation, the catenary actions are not able to develop significantly. Indeed, the increase of N_{lost} inducing an increase of the tension in the bottom beams of the DAP (catenary actions) is quickly stopped by the yielding of the IAP. It will be explained and illustrated further.

The identification of the development of plastic hinges in the IAP will be done through the next section since it needs the analysis of the evolution of the internal forces of the elements in the IAP.

IV.2.2.2 Analysis of the internal forces' distribution in the elements of the structure

As for the situation with an IAP remaining elastic, the problem is still symmetric for an IAP that may yield and only the half of the structure will thus be analysed.

Determination of a criterion to fix the moment of formation of hinges in the IAP:

A criterion was chosen to define when a cross-section of a beam or column can be considered as a plastic hinge. The criterion is based on the evaluation of the M-N interaction curve on which a considered cross-section yields. The adopted formulations to derive the M-N interaction curve were defined by M. Villette in his Phd thesis [20].

For a bending around the strong axis,

If $0 \leq \frac{N}{N_{pl}} \leq \frac{A_w}{A}$:

$$M_N = M_{pl} \left[1 - \left(\frac{N}{N_{pl}} \right)^2 \frac{1}{2 \left(\frac{h-t_f}{h-2t_f} \right) \left(1 - \frac{A_w}{A} \right) \frac{A_w}{A} + \left(\frac{A_w}{A} \right)^2} \right] \quad (IV.1)$$

It has to be noted that the previous formula does not take into account the fillets of the cross-section. Indeed, the A_w is the area of the web without taking into account the fillets. A is the total area of the cross-section.

If $\frac{A_w}{A} \leq \frac{N}{N_{pl}} \leq 1$:

$$M_N = bt_f(h - t_f)f_y - \frac{1}{2}(N - A_w f_y) \left[(h - 2t_f) + \frac{N - A_w f_y}{2bf_y} \right] \quad (IV.2)$$

It has to be noted that the previous formula takes into account the fillets of the cross-section. Indeed, A_w is given by the total area of the cross-section minus the area of the two flanges. Thus, A_w includes the area of the fillets.

Thus, the evolution of M and N in each cross-section presenting a hinge will be compared to the M-N interaction curve in order to determine the moment when each hinge is fully formed.

Figure IV.21 shows the M-N interaction curve derived for the cross-section of an HEB-240, i.e. the profile of the beside column. It shows as well the evolution of the internal forces M and N in the top cross-section and in the bottom cross-section of the beside column (the M and N are numerical results from the software FINELG).

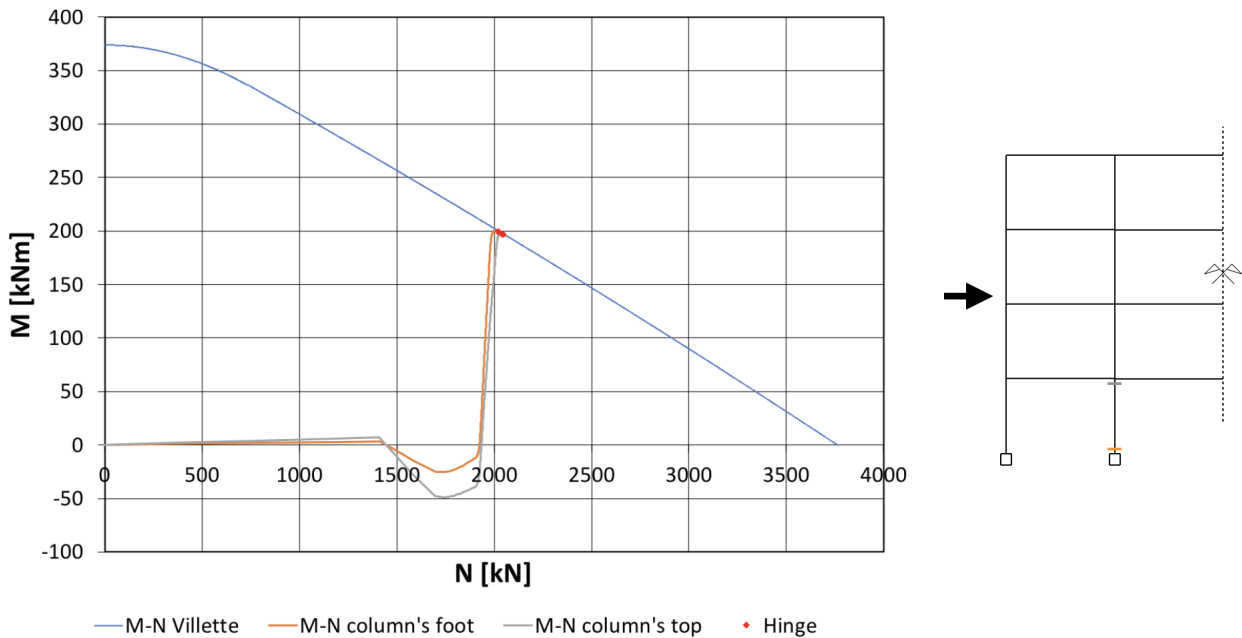


Figure IV.21: M-N curves

Thus, as shown on figure IV.21, the moment when the hinges are considered fully formed is determined when the $(N;M)$ curves hit the M-N interaction curve derived from the formula of Villette (shown by red dots). The same task was achieved for every cross-section presenting a hinge in the IAP.

Identification of the order of formation of hinges in the IAP:

It is now possible to identify the order of formation of plastic hinges in the IAP since a criterion was defined previously to determine the moment when a plastic hinge is formed in a cross-section.

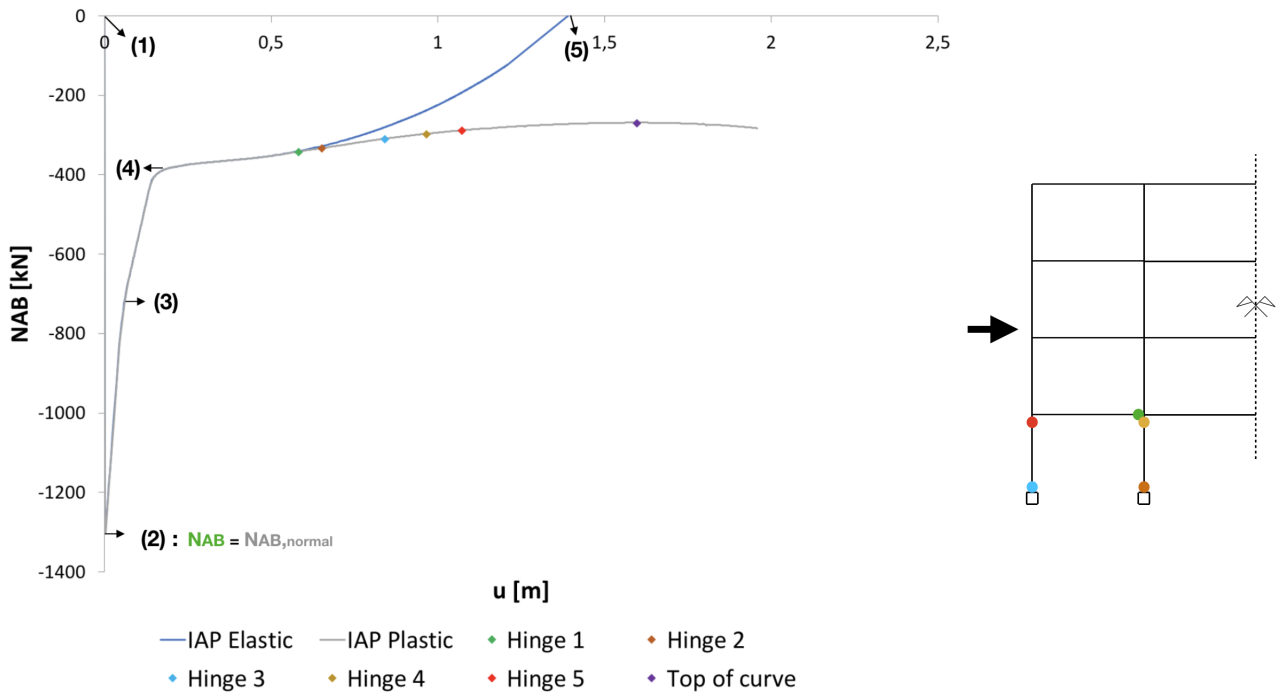


Figure IV.22: Order of formation of plastic hinges in the IAP

Each hinge is represented by a dot of a certain color on the $(u; N_{AB})$ curve for an IAP that may yield and on the structure on the right of figure IV.22.

The first hinge develops at the right extremity of the bottom beam of the IAP. Then, the other hinges are developing in the columns of the IAP. When the fifth hinge is formed at the top of the side column, a full plastic mechanism is attained (formed by the four hinges in the columns). The latter plastic mechanism is called a panel plastic mechanism. As shown on the $(u; N_{AB})$ curve, when the full plastic mechanism is reached (red dot) the top of the curve is not yet reached (purple dot). Thus, it is as if some lateral resistance was still remaining in the IAP when the panel plastic mechanism is fully formed. This point will be investigated further.

The N_{lost} causing the formation of the first plastic hinge in the IAP (green dot) is equal to 961 kN while the one causing the formation of the full plastic mechanism (red dot) is equal to 1014 kN. Thus the difference between the two is about 5,2 %. It may be concluded that the formation of the first plastic hinge in the IAP leads to a quick reach of the plastic mechanism. The N_{lost} corresponding to the top of the curve (purple dot), i.e. the one leading to the collapse of the structure, is equal to 1034 kN. Thus, the difference between the N_{lost} causing the formation of the plastic mechanism and the one corresponding to the top of the curve is about 1,9 %. Finally, the difference between the N_{lost} causing the formation of the first hinge and the N_{lost} corresponding to the top of the curve is 7,1 %.

To understand why there is a difference between the N_{lost} leading to the formation of the plastic mechanism and the one corresponding to the collapse of the structure, it is necessary to analyse the evolution of the normal forces into the beams of the DAP. Indeed, we saw earlier that an arch effect could occur.

Evolution of the normal forces into the beams of the DAP:

The evolution of the normal forces into the four beams sections of the DAP considered is shown on figure IV.23. On each of the latter, the moments of formation of each hinge are indicated.

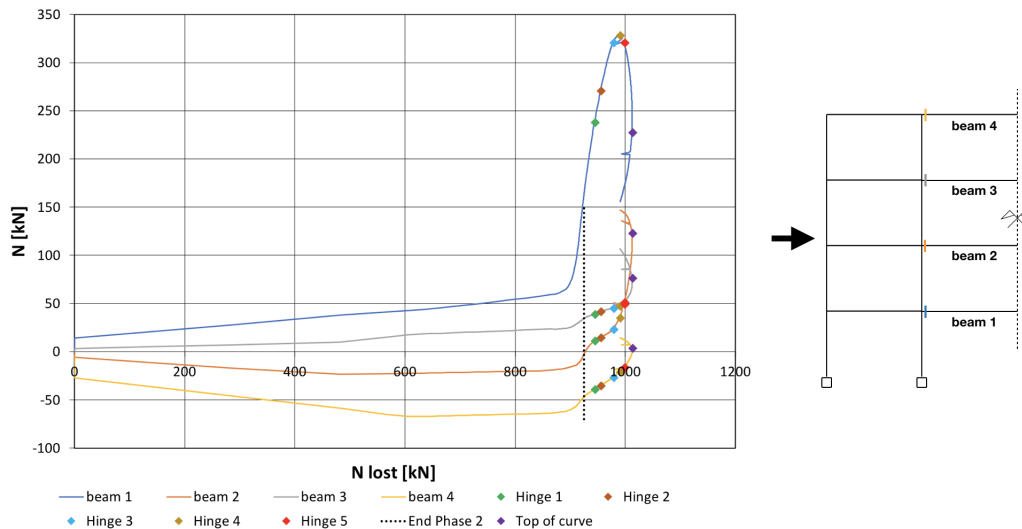


Figure IV.23: Evolution of the normal forces into beams' cross-sections of the DAP

After the end of Phase 2, marked by a vertical black dotted line shown on figure IV.23, the evolution of the normal forces is not the same than the one presented for an IAP remaining elastic. Instead of continuing to increase, the axial force into the beam 1 decreases after the formation of most of the plastic hinges. In parallel, beams 2, 3 and 4 are put in tension at the point corresponding to the collapse of the structure (purple dot) while only beams 2 and 3 were put in tension at the end of Phase 3 for the case of an IAP remaining elastic.

The goal of analysing the evolution of these forces was to understand why the structure is still standing when the panel plastic mechanism is formed. When the plastic mechanism is fully developed (red dot), the tension in beam 1 decreases since there is no more lateral resistance at the level of the plastic mechanism. In parallel, the tensions in beams 2 and 3 increase. It is as if there was still some lateral anchorage allowing an increase of these latter tensile forces. It may be understood by analysing the evolution of the normal force in beam 4. Indeed, when the plastic mechanism is formed (red dot), the beam is still in compression and is progressively decompressed until the collapse of the structure (purple dot). Thus, this "remaining" lateral restraint is brought by the beam which is put into compression. This latter effect is called the arch effect and was previously detailed.

As it was described previously in the analysis of the global trend of the $(u; N_{AB})$ curve in section IV.2.2.1, the yielding of the IAP limits the development of the catenary actions. It is well illustrated on figure IV.23 showing the decrease of the tension into beam 1 after the formation of the plastic mechanism in the IAP.

The shape of the evolution of the bending moment into the considered beams' cross-sections of the DAP is similar to the one already presented for the IAP remaining elastic. As it does not bring additional informations, it will not be exposed for the present situation. Moreover, the shape of the bending moment diagram in the structure shown on figures IV.10, IV.11 and IV.13, are similar to the ones where the IAP may yield. Therefore, they will not be added herein as it does not bring additional informations.

The evolution of the internal forces M and N will be analysed for the columns and for the bottom beam of the IAP in order to understand how the loss of the central column affects them.

Evolution of the normal forces into columns of the IAP:

The evolution of the normal forces into the side and beside columns has the exact same shape as the one presented and explained for the case where the IAP remains elastic.

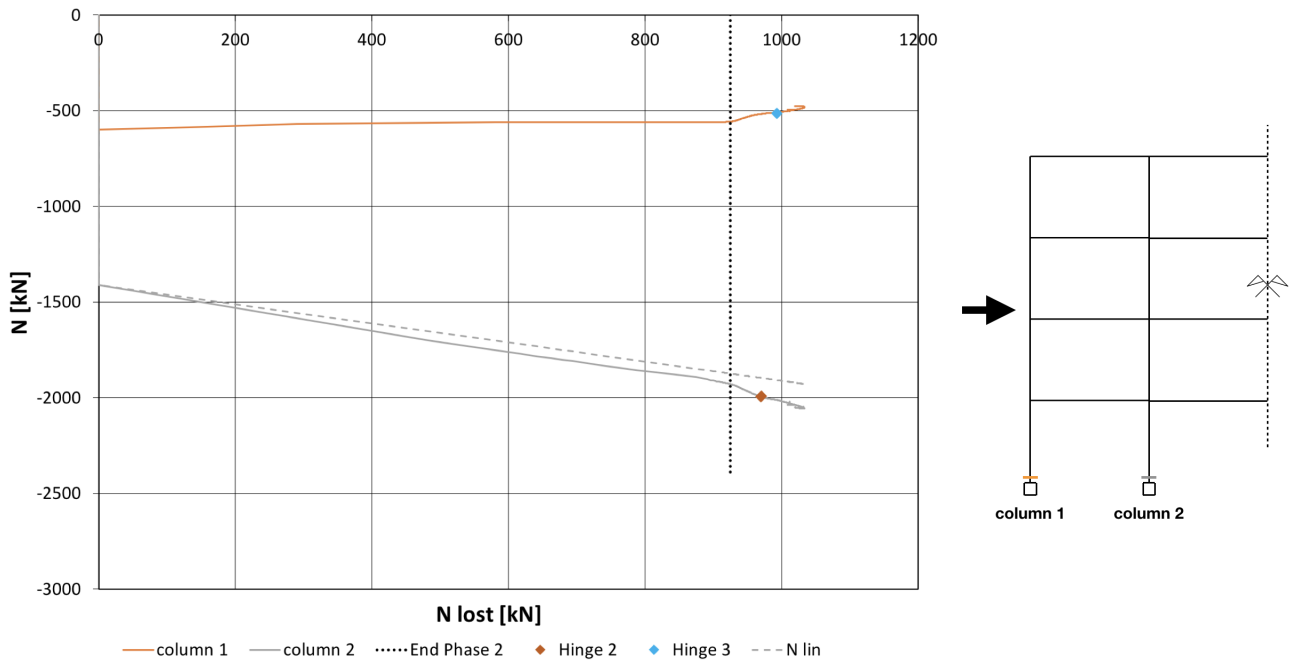


Figure IV.24: Evolution of the normal forces into columns' cross-sections of the IAP

The conclusion drawn is that the evolution of the normal force into column 1 is almost constant while the one for the column 2 is almost linear. As a consequence, column 1 almost does not feel the event "loss of the central column". The compression load previously supported by the lost column is again entirely redistributed in the beside columns.

During Phase 3, the slope of the evolution of N changed for the reasons previously detailed for the case where the IAP remained elastic. The difference between the values of N in column 2 and the values of N from the "N lin" curve never exceeds 5,7%.

The moment of formation of hinges in the two considered cross-sections in the columns are marked by a blue dot for the hinge forming in the bottom cross-section of column 1 and by a brown dot for the hinge developing in the bottom cross-section of column 2.

Evolution of the bending moments into columns of the IAP:

The shape of the evolution of the bending moments into the columns of the IAP is similar to the ones previously presented corresponding to an IAP remaining elastic (as announced at the beginning of section IV.2.2.1, the focus is turned towards Phase 3). The only difference is that during Phase 3, the bending moments do not continue to increase but are stopped when the hinges are forming into the columns, as shown by the reach of a certain "plateau" for the bending moments during Phase 3.

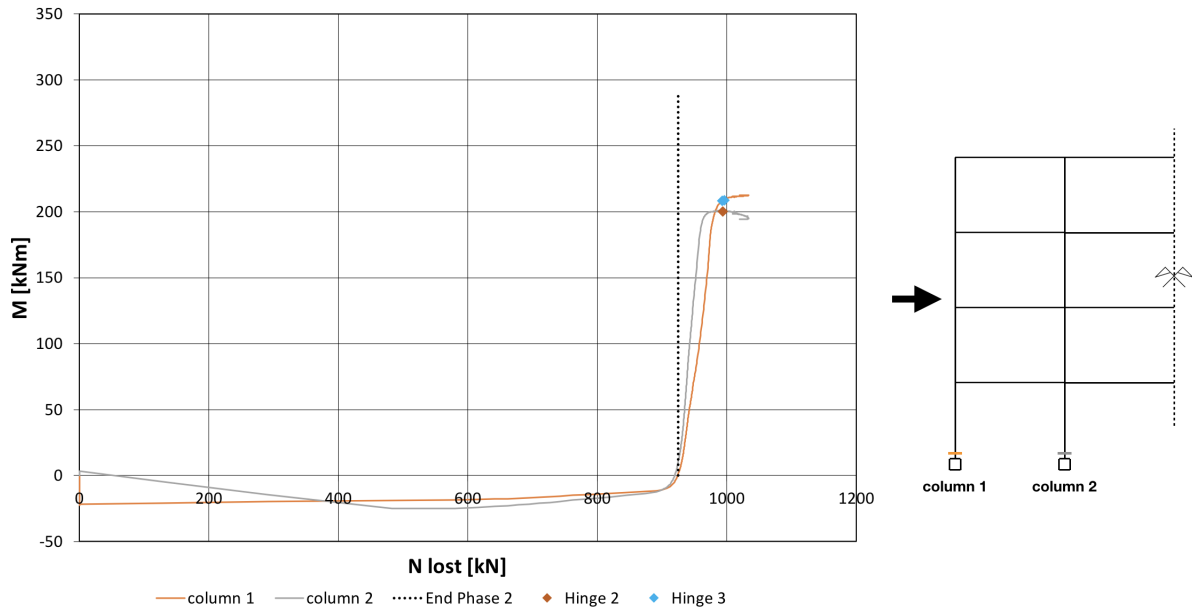


Figure IV.25: Evolution of the bending moments into columns' cross-sections of the IAP

The respective developed hinges in the considered cross-sections of the two columns are shown on the figure.

Evolution of the normal force into the bottom beam of the IAP:

During Phase 3, the tension into the beam follows the same shape than the evolution of N in the beam 1 of the DAP.

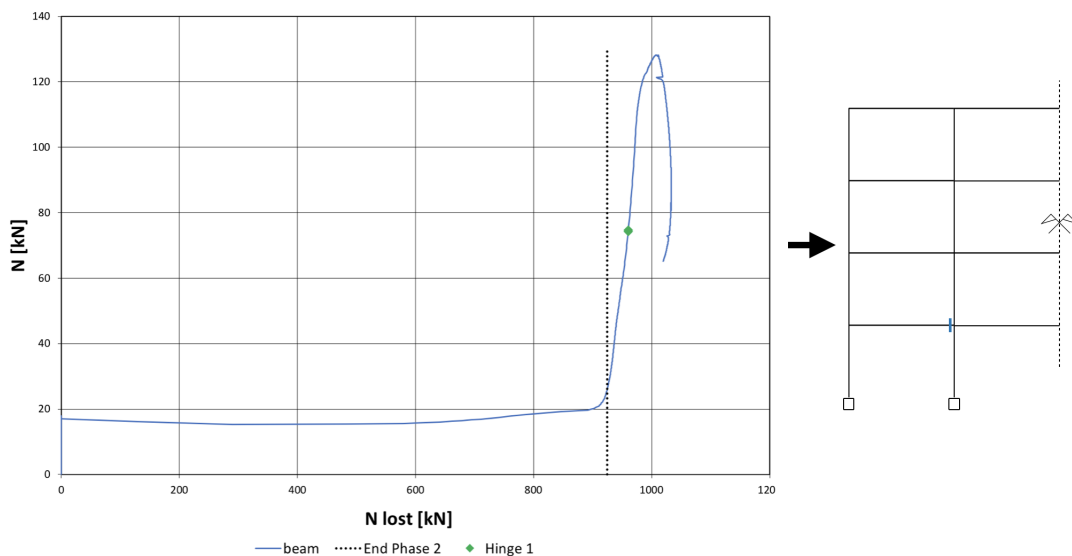


Figure IV.26: Evolution of the axial force into bottom beam's section of the IAP

The value of N for which a hinge is formed in the considered cross-section in the bottom beam of the IAP is marked on the graph by a green dot.

Evolution of the bending moment into the bottom beam of the IAP:

As the elements in the IAP may yield in the present situation, the bending moment diagram stop to increase when the cross-section is yielded as shown on the figure. The formation of the hinge in the cross-section is marked by a green dot on the graph.

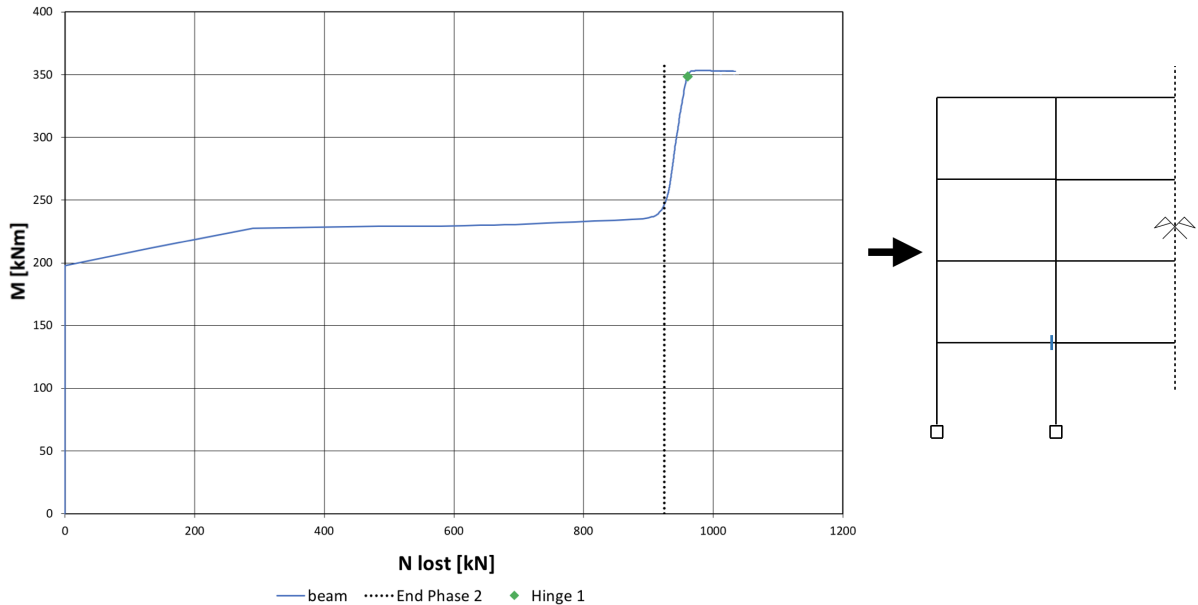


Figure IV.27: Evolution of the bending moment into bottom beam's cross-section of the IAP

Conclusion:

By considering the yielding of the IAP, the structure appeared not to be robust enough to attain the complete loss of the column.

The formation of the first hinges induces a chain formation of hinges in the IAP bringing to a quick collapse of the structure. It was shown by the difference of N_{lost} between the one inducing the first hinges and the one corresponding to the full plastic mechanism (5,2%) and with the one corresponding to the top of the curve (7,1%).

Moreover, it was highlighted that the yielding of the IAP limits significantly the development of catenary actions.

Finally, from the previous analyses, everything is now gathered to be able to identify a series of failure modes of the structure under the event "loss of a central column". This is the subject of the next section.

IV.2.3 Identified failure modes

As the full global response of the frame under the event "loss of a central column" is known during the three Phases and especially until the collapse of the latter, it is now possible to summarize the identified failure modes. Thus, knowing the potential failure modes, it is now possible to give recommendations on which elements that need to be verified during the considered event.

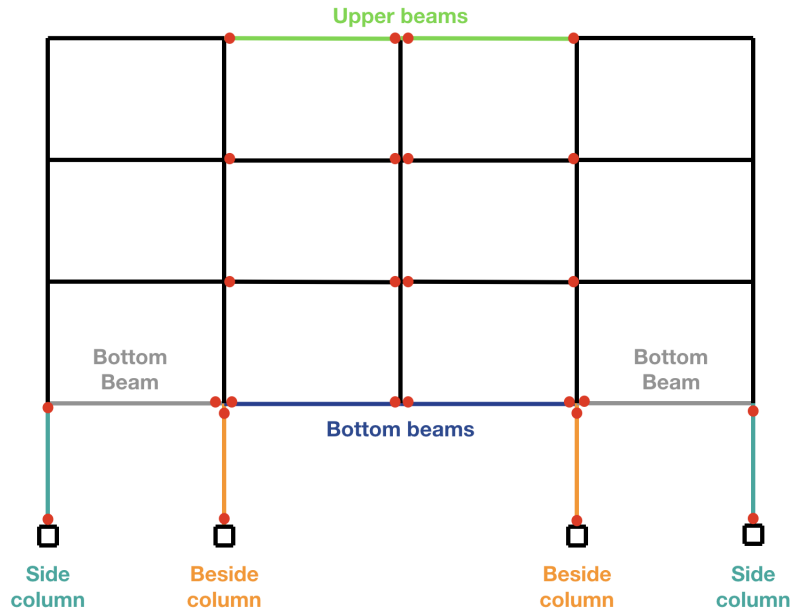


Figure IV.28: Identified failure modes and elements needed to be verified

At the end of Phase 1, the frame is fully loaded. The structure was designed and verified initially under a series of combination of actions including permanent loads, variable loads and accidental loads. Thus, the structure was designed initially to withstand a series of combination of actions including the one applied on the structure at the end of Phase 1 and does not need any further verifications.

During Phase 2, Muller has already identified the elements that need to be verified. This was recalled in the introduction section I.4.2. The same conclusions may be drawn during Phase 2 in the present situation.

The upper beams of the DAP present the biggest increase of their compression forces until the end of Phase 2 in comparison with the other beams in the DAP as seen earlier. Thus, the buckling of these latter needs to be checked (even if the compression forces in the upper beams remain rather small).

The bottom beams of the DAP present the biggest increase of their tension forces until the end of Phase 2 in comparison with the other beams in the DAP as seen earlier. The resistance of the bottom beams as well as the resistance of their joints need to be sufficient to sustain the tensile forces. The bottom beams and their joints need thus to be verified under the tensile forces at the end of Phase 2.

The beside columns are seeing their compression forces significantly increasing during Phase 2. Moreover their internal bending moments are increasing as it was explained earlier. Thus, the buckling of the beside columns needs to be checked.

Finally, as known, the end of Phase 2 is characterized by the full development of a beam plastic mechanism in the DAP reached by the successive formations of plastic hinges in each beam of the DAP and especially at their extremities, see figure IV.28. The beams cross-sections need to have a

sufficient rotational capacity in order to able the development of the full plastic mechanism and thus perform a plastic analysis. Thus, the cross-sections of the beams need to be of class 1. In the case where the hinges develop in the beam to column joints, the joints have to be properly designed to have a sufficient rotational capacity for the previously cited reasons and a sufficient resistance to withstand the applied forces.

During Phase 3, the bottom beams of the DAP are submitted to a significant increase of their tensile forces as detailed earlier and may break under an excessive yielding. These beams and their joints need to have sufficient resistance not to break under these forces. If these latter should not have sufficient resistance to withstand these forces, that would lead first to a break of the bottom beams. The forces would then be reported in the beams of the second floors which will neither be able to withstand them and thus will break as well and so on. This leads to a break of each beam of the DAP and to a progressive collapse of the latter. It is illustrated on figure IV.29. This failure mode may happen for regular buildings. However, in the case where upper beams in the DAP are mega beams, the failure mode will be different. Indeed, the mega beams will avoid the development of significant displacements at the top of the lost column and thus avoid the development of significant tensile forces in bottom beams of the DAP.

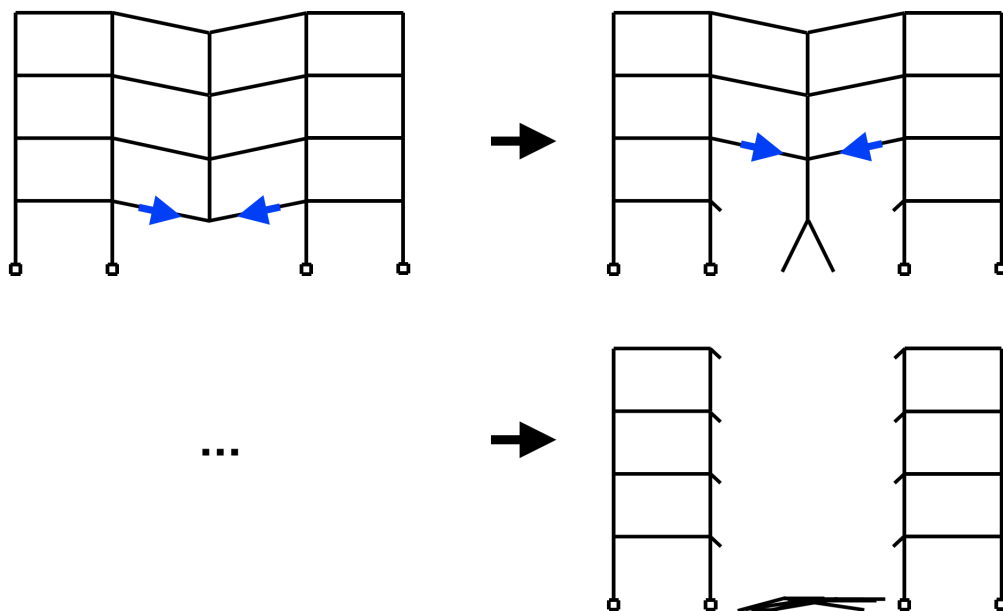


Figure IV.29: Progressive collapse of the DAP

The deformations of the hinges in the DAP are still increasing during Phase 3. Thus, the cross-sections presenting those hinges still need a sufficient rotation capacity (i.e. to be class 1) to allow those deformations to happen. The classification of the cross-sections is defined according to the behaviour related to the bending moment resistance [15]. Thus, they do not take into account the M-N interaction.

In robustness considerations, during Phase 3, it was highlighted that forces acting in bottom beams of the DAP are not only bending moments but significant tensile forces as well. In his Master thesis, Hjeir F. presents a method allowing to determine the rotation capacity of a steel cross-section defined by Gioncu [21]. However, as it was explained in the Master thesis of Farah [11], the rotation capacity calculated through this method is mainly used for seismic design, i.e. where the dominant forces are the bending moments. Thus, a method taking into account the M-N interaction and its influence on the rotation capacity should be determined in the future. This point could be the subject of further researches and is addressed in the perspectives. The rotation capacity calculated through the method of Gioncu will not be compared with the present numerical results as this method does not take into

account the M-N interaction. Thus, it is not known if the estimation of the rotation capacity from this method is fairly good in the context of robustness.

During Phase 3, a panel plastic mechanism develops in the IAP. The cross-sections of the beside and side columns of the IAP need to be of class 1 to have a sufficient rotational capacity to develop the latter panel plastic mechanism and thus perform a plastic analysis. This has to be satisfied in the case where the hinges are developing in the columns and not in the joints, i.e. in the case where the joints are fully resistant. In the case where the joints are not fully resistant (i.e. partially resistant), the hinges will develop in these latter. Indeed, for a partially resistant joint, its resistance is smaller than the ones of its connected elements. In that case, the joints will need to be designed to have a sufficient rotation capacity and a sufficient resistance to withstand the applied forces.

Moreover, as detailed earlier, it was explained that it may be considered that the side columns (in blue on figure IV.28) do not feel the loss of the column in terms of the value of their compression forces. All the compression force previously supported by the central column is redistributed in the beside columns. As a result, the buckling of the beside columns needs to be checked.

Finally, the cross-sections of the bottom beams of the IAP need to be of class 1 because they need a sufficient rotation capacity to perform a plastic analysis as they present a plastic hinge, see figure IV.28.

IV.3 Analysis of the reference structure under the loss of an intermediate column

In the present section, the global response of the frame will be detailed in both cases where the IAP remains elastic and where the IAP may yield under the event "loss of an intermediate column". On figure IV.30, the DAP is highlighted in red while the IAP is highlighted in blue.

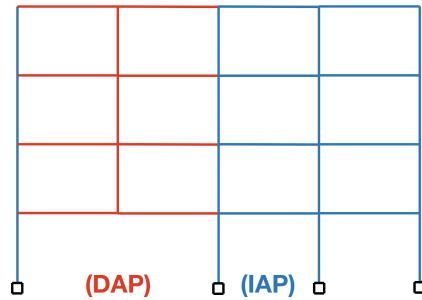


Figure IV.30: DAP and IAP of the reference structure under the loss of an intermediate column

IV.3.1 DAP elastic-perfectly plastic - IAP elastic

The $(u; N_{AB})$ curve for an IAP remaining elastic and a DAP elastic-perfectly plastic is shown on figure IV.31. The curve does not go until point (5) because of problems of convergence with the software FINELG. During Phase 3, starting at point (4), the curve should present a similar increasing slope characterizing the catenary actions than the one corresponding to the case of the loss of a central column for an IAP remaining elastic previously presented.

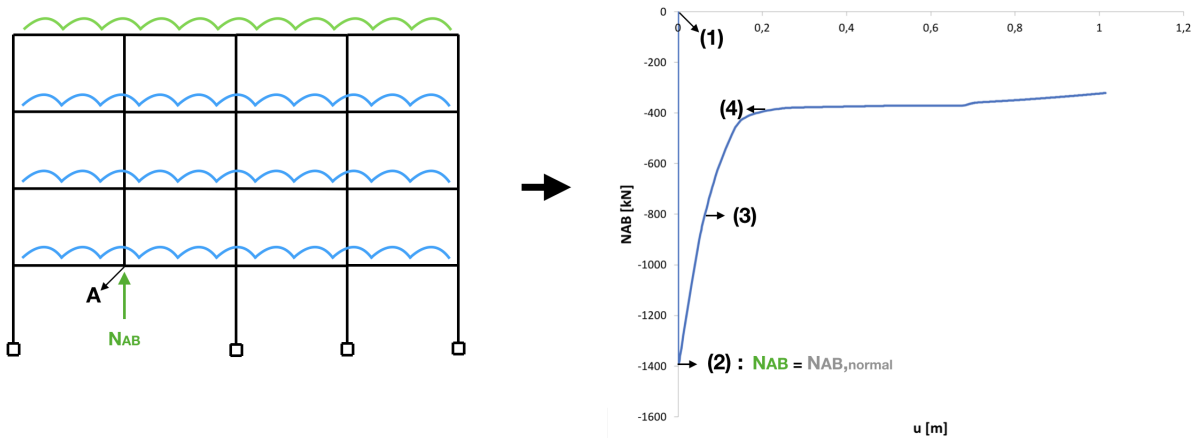


Figure IV.31: DAP elastic-perfectly plastic - IAP elastic

IV.3.1.1 Identification of successive phases in the behaviour of the structure

The description of the three successive Phases for the present situation is similar than the one exposed in section IV.2.1.1 and will thus not be reminded. Similarly, under the event "loss of an intermediate column" and for an IAP remaining elastic, the end of Phase 2 is characterized by the formation of a complete beam plastic mechanism as shown on figure IV.32.

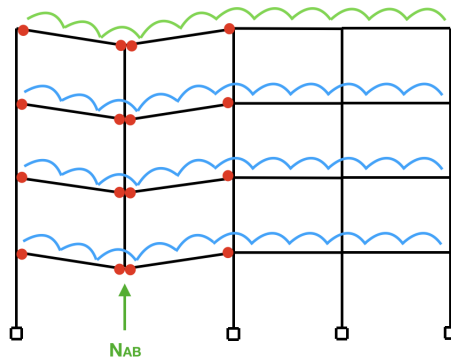


Figure IV.32: Beam plastic mechanism in the DAP

IV.3.1.2 Analysis of the internal forces' distribution in the elements of the structure

As the frame lost an intermediate column, the global response is no longer symmetrical. Thus, the whole structure is under investigation.

The evolution of internal forces will be analysed for critical cross-sections of the elements as for instance the locations where the hinges develop in the DAP to understand how the loss of an intermediate column affects the distribution of forces in the whole structure and thus finally being able to conclude regarding the identified failure modes.

Evolution of the normal forces into beams of the DAP:

The evolution of the normal forces into the beams' cross-sections presented on figure IV.33 are similar to the one corresponding to the beams' cross-sections marked by the vertical black dashes. Small differences between these latter are observed on their values since the behaviour is no longer symmetrical. But, the evolution of normal forces into the cross-sections marked by black dashes will not be exposed since it does not bring additional informations. Moreover, as previously announced, the forces until the end of Phase 3 are not represented because of problems of convergence in FINELG.

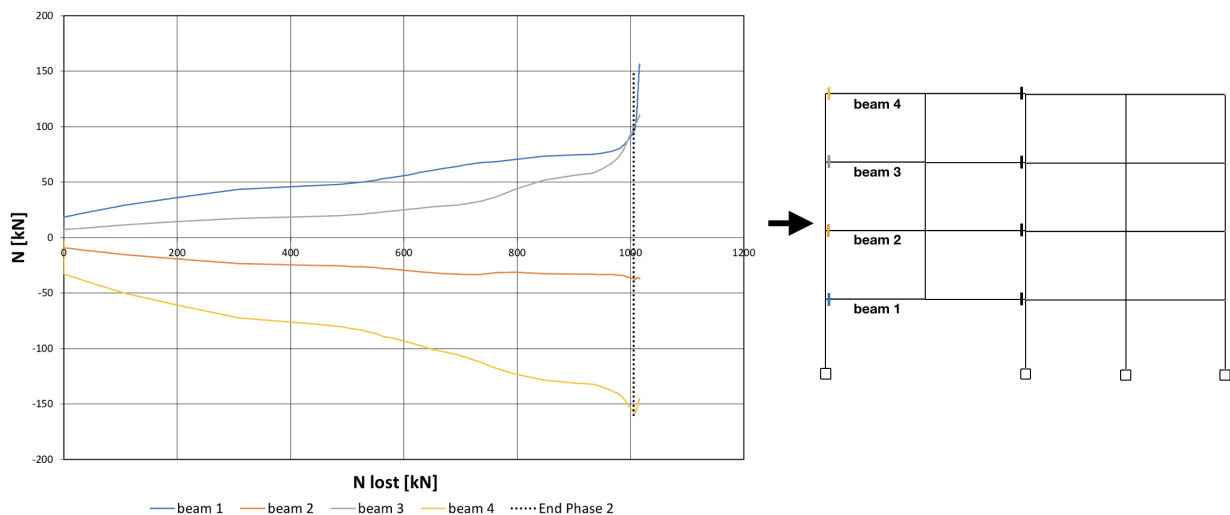


Figure IV.33: Evolution of the normal forces into beams' cross-sections of the DAP

As shown on figure IV.33, beams 1 and 3 are in tension while beams 2 and 4 are in compression as it was the case for the loss of the central column. A schematic representation of the deformation of the structure at the end of Phase 2 is shown on figure IV.34. As the tension is increasing into beams 1 and 3, the pulling forces acting on the IAP are increasing. The IAP from the left of the structure is only

made up of one series of columns while the IAP from the right is made up of three series of columns and two spans. As a result the lateral stiffness brought by the IAP from the left is smaller than the one brought by the IAP from the right. It explains why the IAP from the left is led to the center of the DAP and implies compression forces in beams of the DAP. These latter are pushing against the IAP from the right and induce rightwards displacements of the latter.

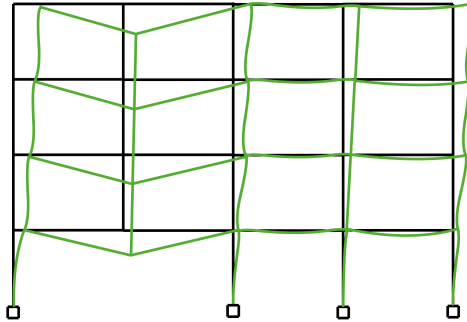


Figure IV.34: Schema of the frame's deformation (End Phase 2)

At the end of Phase 2, i.e. the beginning of Phase 3, the tension is significantly increasing in beam 1 (catenary actions). It remains thus globally similar in terms of the evolution of the normal forces in beams of the DAP in comparison with the loss of the central column situation.

The shape of the evolution of the bending moments in the considered beams' sections are similar to the ones presented for the loss of the central column in the case where the IAP remains elastic. Thus, it will not be detailed for the present situation.

Evolution of the normal forces into columns of the IAP:

As shown on figure IV.35, the loads previously supported by the lost column are entirely redistributed in the beside columns (i.e. columns 1 and 2) as the compression forces in the inter column (column 3) and in the side column (column 4) are remaining almost constant while N_{lost} is increasing. The differences between the N from the curve "N lin" and the ones in columns 1 and 2 do not exceed 4%. The evolutions of N in the beside columns are thus almost linear.

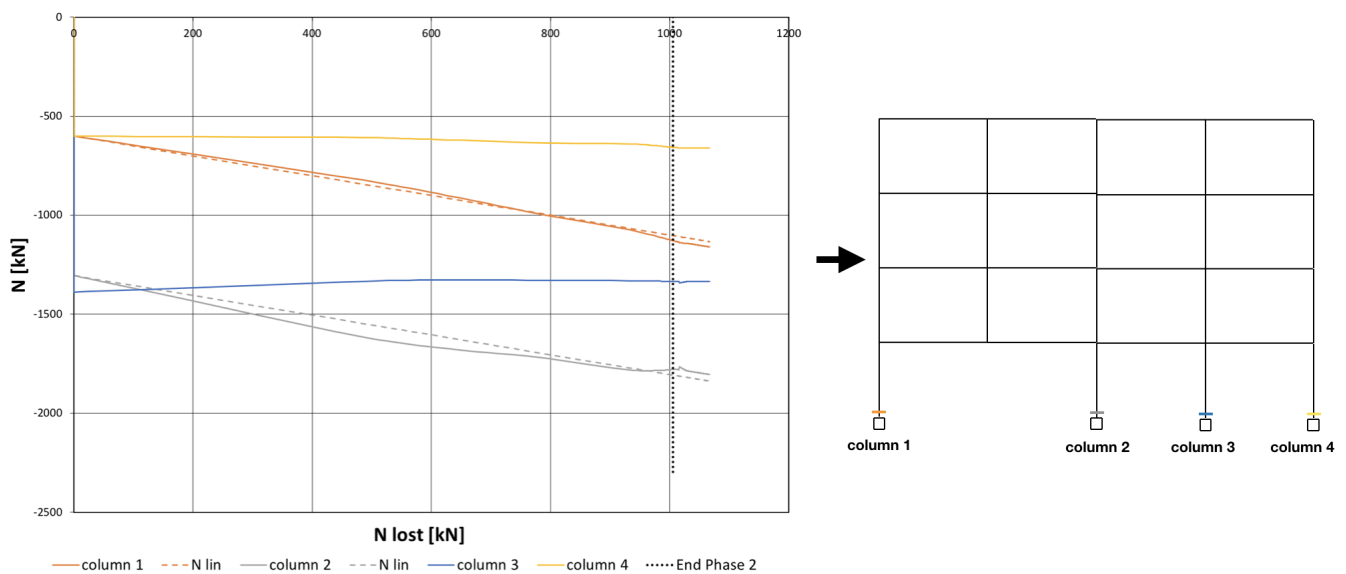


Figure IV.35: Evolution of the normal forces into columns' cross-sections of the IAP

The shape of the evolution of the bending moments into columns of the IAP, i.e. columns 1, 2, 3 and 4, are similar to the one already presented for the situation of the loss of the central column. It will thus not be explained for the present situation as it does not bring additional informations.

Moreover, both the evolutions of the normal force and of the bending moment into the bottom beams' cross-sections of the IAP are similar to the ones presented on figures IV.17 and IV.18. As it was already explained, it will not be reminded here.

Conclusion:

The influence of the loss of another column than the central one was investigated in the present section considering the IAP remaining elastic. The influence of the yielding of the latter will be studied through the next section.

IV.3.2 DAP elastic-perfectly plastic - IAP elastic-perfectly plastic

The $(u; N_{AB})$ curve obtained for a DAP elastic-perfectly plastic and an IAP elastic-perfectly plastic is given on figure IV.36. The latter is superposed with the curve obtained for an IAP remaining fully elastic.

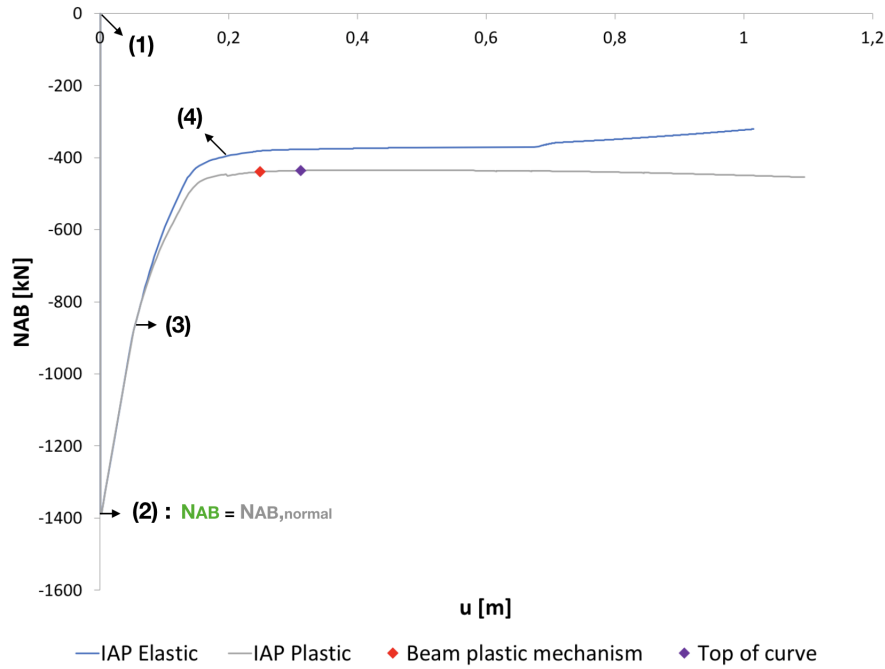


Figure IV.36: DAP elastic-perfectly plastic - IAP elastic-perfectly plastic

IV.3.2.1 Identification of successive phases in the behaviour of the structure

As shown on figure IV.36, Phase 2 is different for an IAP that may yield. The end of Phase 2 is theoretically defined as the reach of a plastic mechanism in the DAP as presented in Chapter I. In the present situation, the plastic mechanism is reached by a combination between yielding of the DAP and yielding of the IAP. Indeed, the mechanism is reached by the development of hinges in the beams of the DAP and in the left columns of the IAP, see figure IV.37.

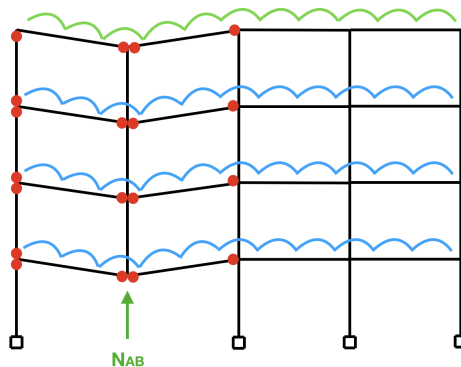


Figure IV.37: Plastic mechanism

This plastic mechanism corresponds to the red dot on figure IV.36. The last obstacle to the complete collapse of the structure is the beside column of the IAP located on the left of figure IV.37 since plastic hinges are formed at each extremity of the upper columns. The failure of the latter column is quickly reached, see purple dot (top of the curve) on figure IV.36. Thus, the collapse of the structure is attained at this point. At that stage, the IAP at the right of the DAP remains fully elastic.

IV.3.2.2 Analysis of the internal forces' distribution in the elements of the structure

As shown on figure IV.38, the bending moments at the extremities of the columns in the IAP from the left are significant. The hinges are developing there and not in the left extremities of the beams of the DAP because their resistant plastic bending moments are smaller than the ones of the beams. Moreover, in these columns, there are M-N interactions that decrease the resistant plastic bending moments of the columns.

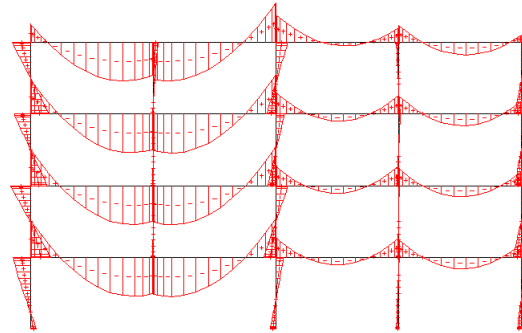


Figure IV.38: Bending moment diagram in the structure when the beam plastic mechanism is fully developed

To determine the red dot on figure IV.36, i.e. the moment where the complete beam plastic mechanism is reached, the M-N interaction curves established by M. Villette is used for the cross-sections where the hinges are developing. It is illustrated for one cross-section on figure IV.39. When the numerical (N;M) curve given by FINELG hit the M-N interaction curve from Villette, the hinge is formed. This logic was followed for all the cross-sections where the hinges are developing. The hinges in the columns of the IAP are developing almost at the same moment.

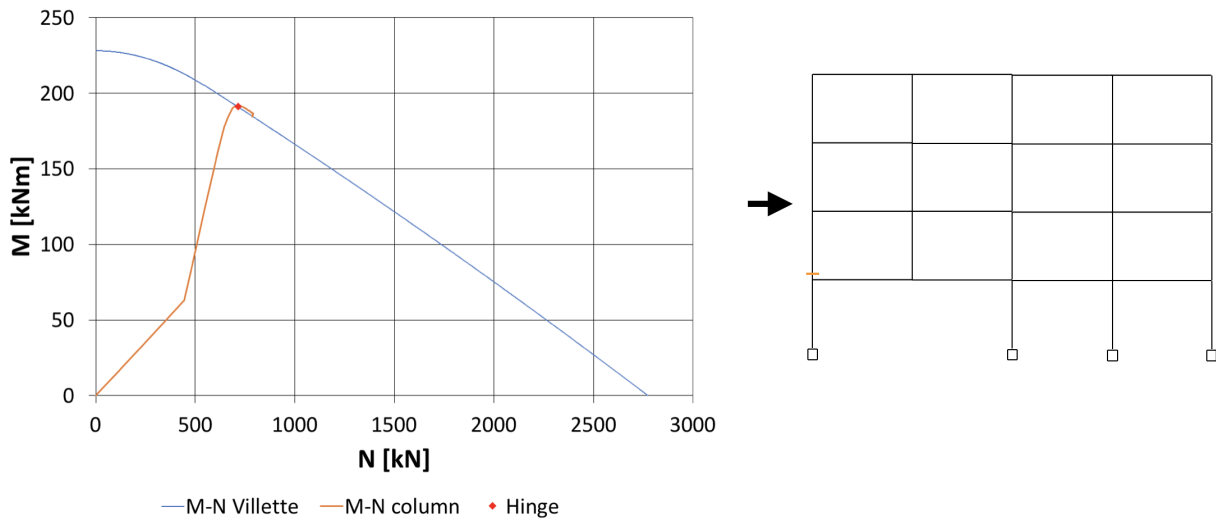


Figure IV.39: M-N curves

Evolution of the normal forces into beams of the DAP:

As shown on figure IV.40, the catenary actions characterized by a significant increase of the tension in beams of the DAP and especially in beam 1 are not able to develop freely in the present situation. Indeed, the collapse of the structure (purple dot), i.e. the failure of the left beside column of the IAP, does not allow it.

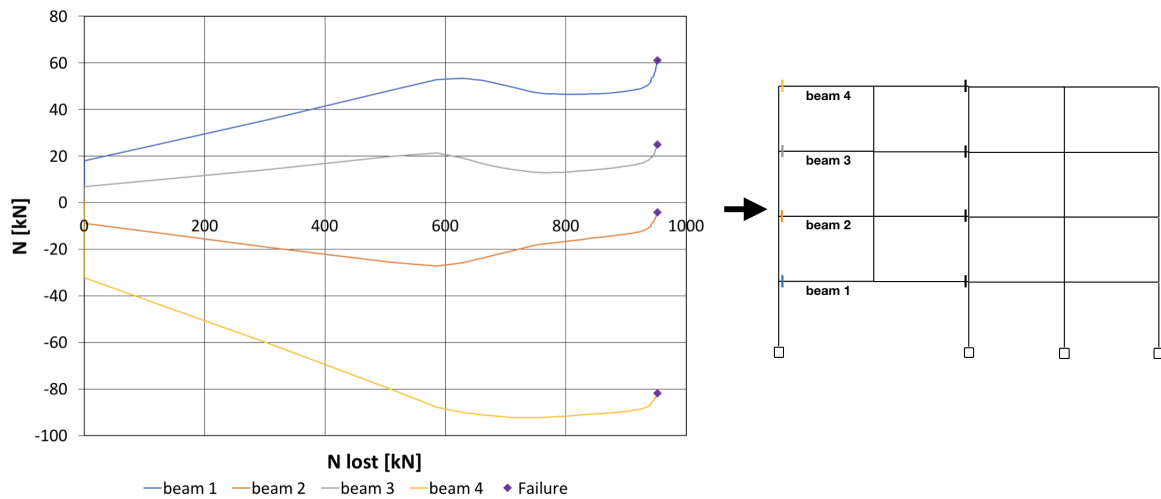


Figure IV.40: Evolution of the normal forces into beams' cross-sections of the IAP

The decrease of the tension forces into beams 1 and 3 are induced by the progressive formation of hinges in the left columns of the IAP. Then, a slight increase of the latter tension forces is observable. Indeed, there is still a remaining lateral stiffness coming from the beside left column of the IAP and a restraint coming from the geometric effect previously detailed as the arch effect inducing the compression of beams of the DAP as the beam 4.

The shape of the evolutions of the normal forces into the sections marked by vertical black dashes on figure IV.40 is similar to the one previously exposed. It differs slightly on the values of the latter as the problem is not symmetrical.

Evolution of the normal forces into columns of the IAP:

From figure IV.41, it may be concluded that the N_{lost} is again fully redistributed in the beside columns. Indeed, the differences between the N from the curve "N lin" and the ones from the N in columns 1 and 2 do not exceed 4%. Thus the evolutions of N in the beside columns are almost linear.

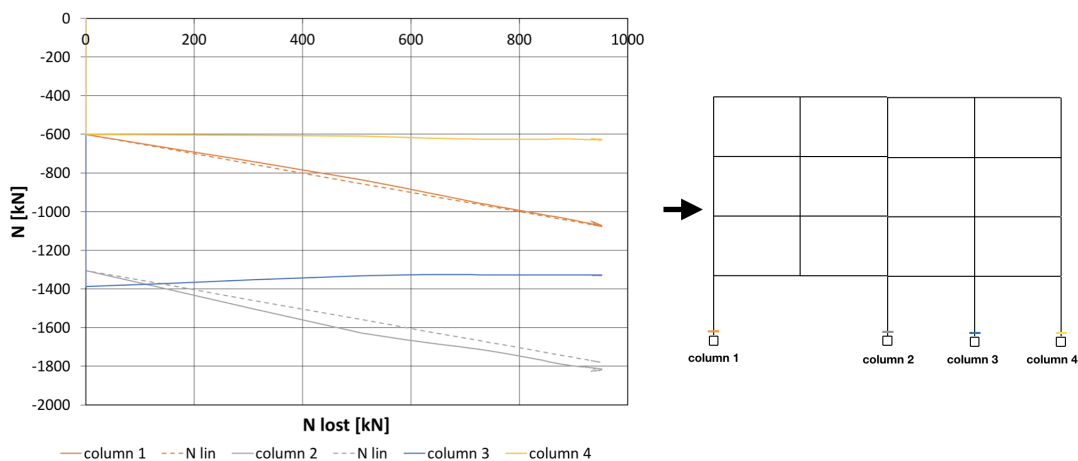


Figure IV.41: Evolution of the normal forces into columns' cross-sections of the IAP

Conclusion:

Everything is now gathered to be able to list a series of identified failure modes of the structure under the event "loss of an intermediate column". It is the subject of the next section.

IV.3.3 Identified failure modes

As the global response of the frame is known under the event "loss of an intermediate column" until the collapse of the structure, it is now possible to summarize the identified failure modes. Thus, it is possible to give recommendations on which elements that need to be verified during the considered event.

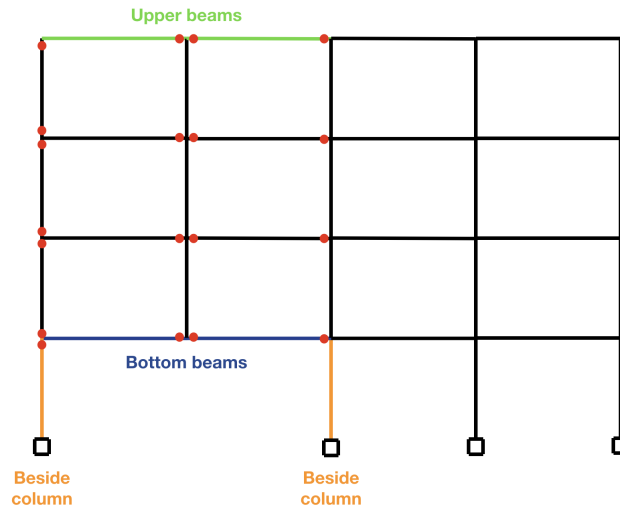


Figure IV.42: Identified failure modes and elements needed to be verified

As previously explained, the upper beams of the DAP present the maximum compression forces and thus their buckling needs to be checked.

The bottom beams present the maximum tension forces. The resistance of these latter and their joints needs to be checked for the given forces.

As a plastic mechanism develops through the formation of hinges in the beams of the DAP and in the left columns of the IAP, their cross-sections where the hinges develop need to have a sufficient rotation capacity to allow the development of the complete plastic mechanism and thus perform a plastic analysis. As a consequence, these cross-sections need to be class 1. In the case where the joints are partially resistant, the hinges will develop in the joints. Thus, they need to be designed to have sufficient rotation capacity and sufficient resistance under the given loads.

As the deformations of the hinges are still increasing after the formation of the plastic mechanism, it is necessary to check if these latter hinges are able to endure those deformations. A method calculating the rotation capacity of the hinges under M-N should be determined (previously explained in the section corresponding to the failure modes of the reference structure under the loss of a central column). It is a point addressed in the perspectives.

As the compression initially withstood by the lost column is entirely redistributed in the beside columns, their buckling needs to be checked.

As the IAP at the right of the DAP does not show any yielding, no further recommendations will be given.

IV.4 Analysis of the reference structure under the loss of an exterior column

In the present section, the global response of the frame will be detailed in both cases where the IAP remains elastic and where the IAP may yield under the event "loss of an exterior column". On figure IV.30, the DAP is highlighted in red while the IAP is highlighted in blue.

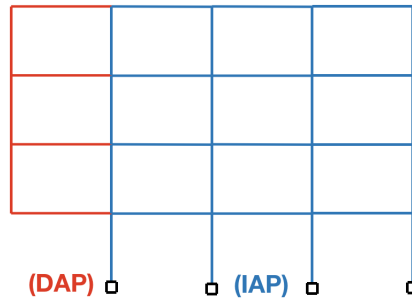


Figure IV.43: DAP and IAP of the reference structure under the loss of an exterior column

IV.4.1 DAP elastic-perfectly plastic - IAP elastic & elastic-perfectly plastic

The $(u; N_{AB})$ curve for a DAP elastic-perfectly plastic and an IAP elastic and elastic-perfectly plastic is shown on figure IV.44. In the present situation, the global response of the frame is exactly the same in both situations. Thus, the yielding of the IAP has no influence on the global response until the observed displacement u .

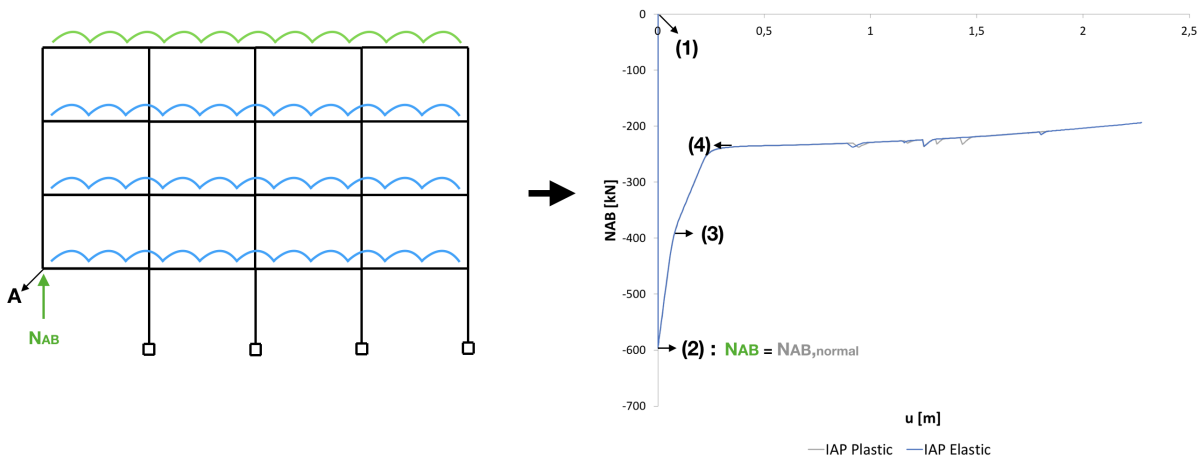


Figure IV.44: DAP elastic-perfectly plastic - IAP elastic & elastic-perfectly plastic

Since the goal of the present work is to study the influence of the yielding of the IAP on the global response of the frame, the present scenario "loss of an exterior column" is not really interesting to be detailed. However, some particularities will be presented in the following subsections.

IV.4.1.1 Identification of successive phases in the behaviour of the structure

The Phases 1 and 2 are the same than the ones presented in the previous sections. Indeed, the Phase 1 corresponds to the loading of the frame and the Phase 2 corresponds to the progressive formation of hinges in the DAP until the reach of a plastic mechanism. The differences observed show that the

upper beam of the DAP presents the maximum tensile forces while the bottom beam is put into compression during the progressive loss of the column. Moreover, it may be observed that the catenary actions are not developing a lot during Phase 3.

IV.4.1.2 Analysis of the internal forces' distribution in the elements of the structure

Obviously, the arch effect as the one previously exposed will not develop in the present situation. The evolution of the normal forces into the beams of the DAP will not be exposed.

The evolution of the normal forces in the columns of the IAP is shown on figure IV.45 in the case where the IAP is elastic-perfectly plastic. It reveals that the vertical load previously supported by the lost column is entirely redistributed in the beside column.

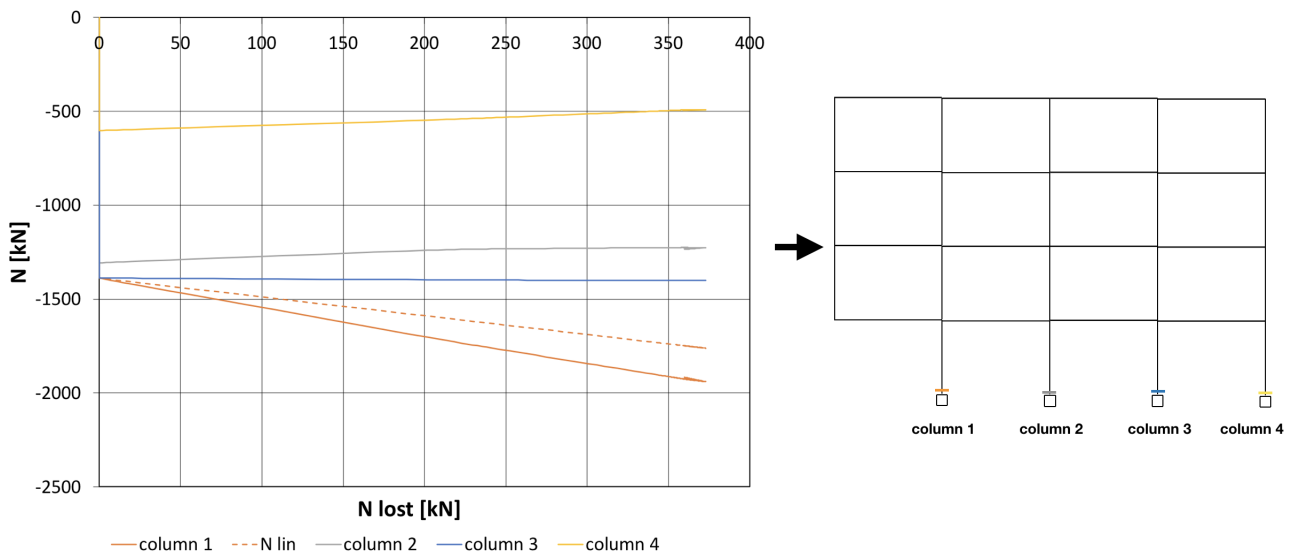


Figure IV.45: Evolution of the normal forces into columns' cross-sections of the IAP

The N in the beside column never differs more than 9% than the values of N from the "N lin" curve.

IV.4.2 Identified failure modes

In the present situation, the upper beam of the DAP is submitted to the higher tensile force. Thus, the resistance of the upper beam of the DAP and its joints needs to be sufficient to sustain the given forces.

The bottom beam of the DAP is submitted to compression forces. Thus the buckling of the latter needs to be checked.

The vertical load previously supported by the lost column is entirely redistributed in the beside column. Thus, the buckling of the beside columns needs to be checked. If the beside column fails, its neighbour from the right will neither be able to sustain the vertical loads and so on until the failure of each columns of the IAP at damaged level.

The cross-sections of the elements where the hinges are developing in the DAP are highlighted on figure IV.46. Again, the cross-sections where a hinge develops need to have a sufficient rotation capacity as explained earlier. Thus these cross-sections need to be class 1. In the case where the joints are partially resistant, the hinges will develop in the joints. Thus, they need to be designed to have sufficient rotation capacity and sufficient resistance under the given loads.

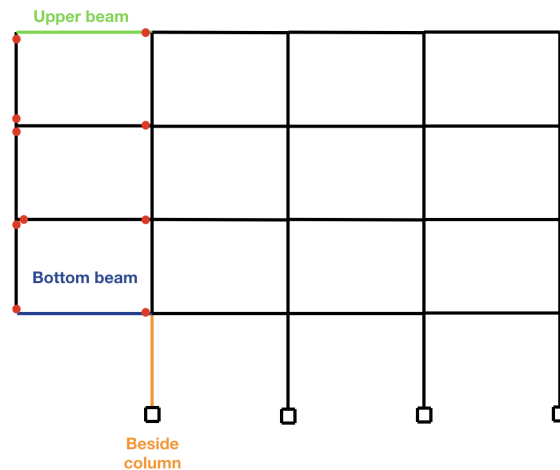


Figure IV.46: Identified failure modes and elements needed to be verified

IV.5 Conclusion

From the analysis of the three previous scenarios in the reference structure, it was seen that the evolution of N in the beside columns was mainly due to the full redistribution of N_{lost} . Indeed, in the most realistic behaviours of the frames, simulated by an IAP elastic-perfectly plastic, the differences between the values of N in the beside columns and the N from the "N lin" curves never exceed 6 to 9%. In the next chapter, this will be investigated for frames with more spans.

It shown globally that the formation of first hinges in the IAP induces a chain formation of hinges leading to the development of plastic mechanisms bringing to the collapse of the structure. This was quantified on the basis of the differences between N_{lost} inducing the first hinges, the complete plastic mechanisms and the collapse of the structure. It will be investigated for other structures in the next chapter.

Moreover, as seen, the yielding of the IAP limits significantly the development of the catenary actions. This point will be checked for other structures in the next chapter.

The influence of an arch effect was highlighted previously. This point will also be investigated in the next chapter.

The checks and recommendations in the previously investigated cases may be summarized as follows:

- In each cross-section presenting a hinge, the cross-section is recommended to be class 1;
- The buckling of the upper beams in the DAP needs to be checked;
- The resistance in tension of the bottom beams and of their joints needs to be checked;
- The buckling of the beside columns in the IAP needs to be checked;
- In the case where the joints are partially resistant, these latter have to be designed to have sufficient rotation capacity and sufficient resistance.

When it is an exterior column that is lost, the checks differ only on the two following points:

- The upper beam in the DAP and its joints need to be checked under the given tensile forces;
- The buckling of the bottom beam in the DAP needs to be checked under the given compression forces.

The failure modes of other structures will be investigated in the next chapter.

Chapter V

Parametric study (numerical analysis)

V.1 Introduction

The global response of the reference structure was studied in the last chapter through three scenarios, the loss of a central column, the loss of an intermediate column and the loss of an exterior column. It is within the latter scenarios that the study of influence of yielding of the IAP took place.

Through the present chapter, the goal is to verify whether the behaviour of the frame remains the same if the number of spans is increased.

The $(u;N_{AB})$ curve will still be presented both for an IAP remaining elastic and for an IAP that may yield.

The identification of the successive formations of hinges will be performed to check if the formation of the first hinges induces a chain formation of hinges and thus if the collapse of the structure is quickly attained. It will also be determined if the hinges are forming in the same locations as in the reference structure and if it leads to the formation of a panel plastic mechanism in the IAP as was the case in the reference structure. The difference between the N_{lost} inducing the formation of the first hinges with the one inducing the collapse of the structure will be determined for the new structures. Indeed, it is a good means to quantify the influence of the increase in the number of spans on the global response of the structure as well as the influence of the yielding of the IAP.

The evolution of the internal forces within the structures will be also analysed. The goal is finally to conclude and generalize on how the loads are redistributed during the loss of a column in the investigated frames. The latter will be shown for an IAP elastic-perfectly plastic. Indeed, the results corresponding to the IAP remaining elastic do not bring any additional information to what was presented in previous chapter.

The influence of the location of the lost column on the global response of these frames will be investigated as well.

Finally, identified failure modes for the new structures will be compared to the ones presented for the reference structure.

The two structures under investigation have respectively 6 and 8 spans while the reference structure has 4 spans. The number of storeys remains the same (4 storeys) since the goal is to analyse the effect of an increase in the number of spans. The design of the two latter structures is shown in Annex A page 119. The loading applied on these two latter structures is the same as the one applied on the reference structure defined in section III.2 page 31.

V.2 Increase in the number of spans from 4 to 6

In the present section, the event "loss of a column" will be investigated in four different locations, see figure V.1.

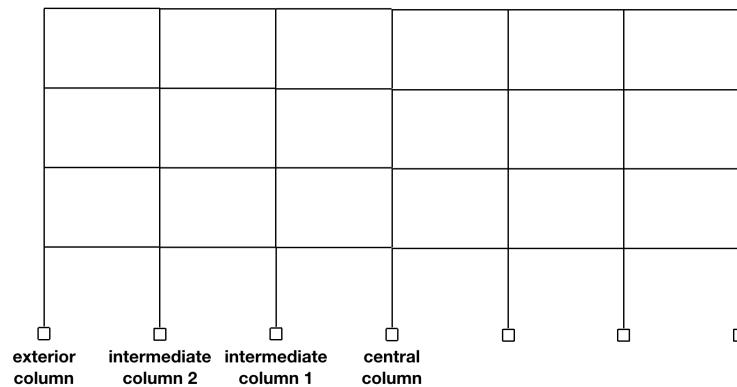


Figure V.1: Lost columns' designations

V.2.1 Loss of the central column

In the case of the loss of the central column, the behaviour of the frame is symmetrical. Thus, only half of the structure will be studied. As shown on figure V.2, the global response of the structure with 6 spans is globally the same as the one with 4 spans in the case of the loss of the central column. The successive formations of hinges in the IAP are shown on figure V.2. The hinges developed in the DAP are not represented on the schema as the focus is turned to Phase 3, i.e. when hinges are developing in the IAP.

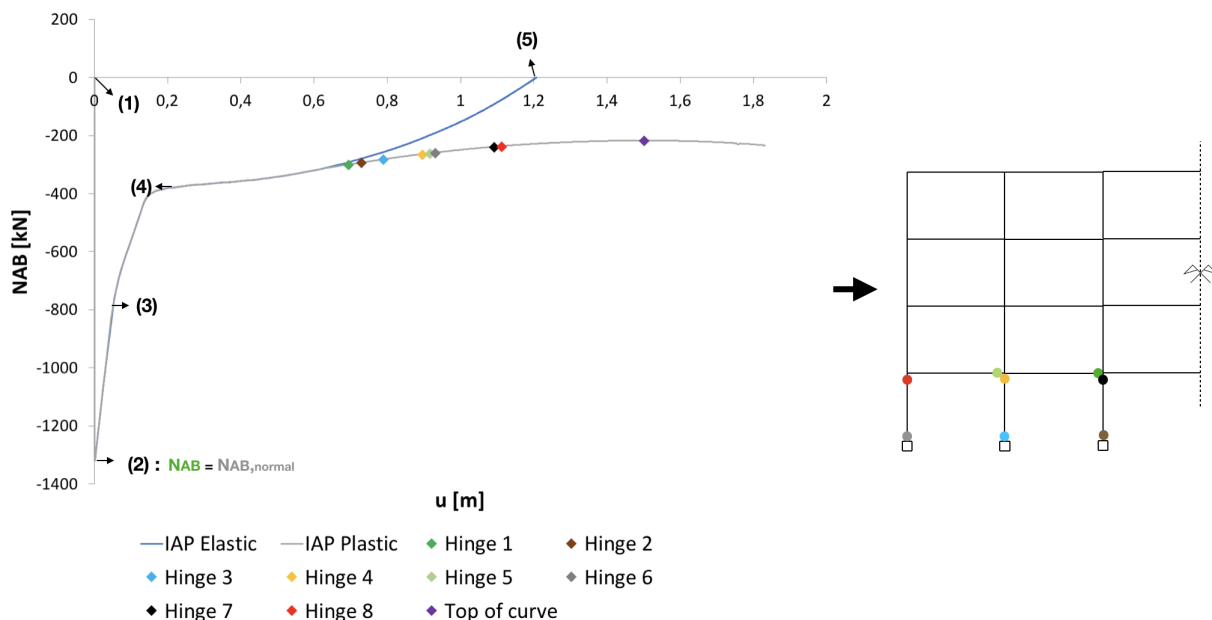


Figure V.2: $(u; N_{AB})$ curves for an IAP elastic and an IAP elastic-perfectly plastic

In the case where the IAP is elastic-perfectly plastic, during Phase 3 (i.e. from point (4)), the hinges are still developing in the extremities of the columns at the damaged level and at the right cross-sections of the bottom beams in the IAP. The N_{lost} inducing the formation of the first hinge (green dot) is equal to 1019 kN and the one inducing the formation of the full plastic mechanism (red dot) is equal to 1082 kN. The difference between the latter values is about 5,8%. In the case of the structure

with 4 spans, this difference was about 5,2%. Thus, by increasing the number of spans, the lateral stiffness brought about by the IAP increases and it consequently induces an increase in the difference between the considered N_{lost} . Thus, increasing the number of spans allows reaching the full plastic mechanism to be delayed when the first hinge is formed in the IAP.

The N_{lost} corresponding to the top of the curve (purple dot) is equal to 1101 kN. Thus, the difference between the latter N_{lost} and the one inducing the complete formation of the panel plastic mechanism is about 1,7%. In the case of the structure with 4 spans, it was about 1,9%. Thus, it seems that the influence of the arch effect on the value of N_{lost} is slightly decreasing.

Evolution of the normal forces into beams of the DAP:

The trend of the evolution of the tension and compression in the beams of the DAP, in the case where the IAP is elastic-perfectly plastic, is similar to the one obtained for the reference structure (4 spans) in the case of the loss of the central column. The tension in beam 1 is higher in the present situation. Indeed, there are more spans and thus the resistance of the IAP is bigger for the structure with 6 spans than the one with 4 spans. Then, the pulling forces acting on the IAP need to be bigger to attain the panel plastic mechanism.

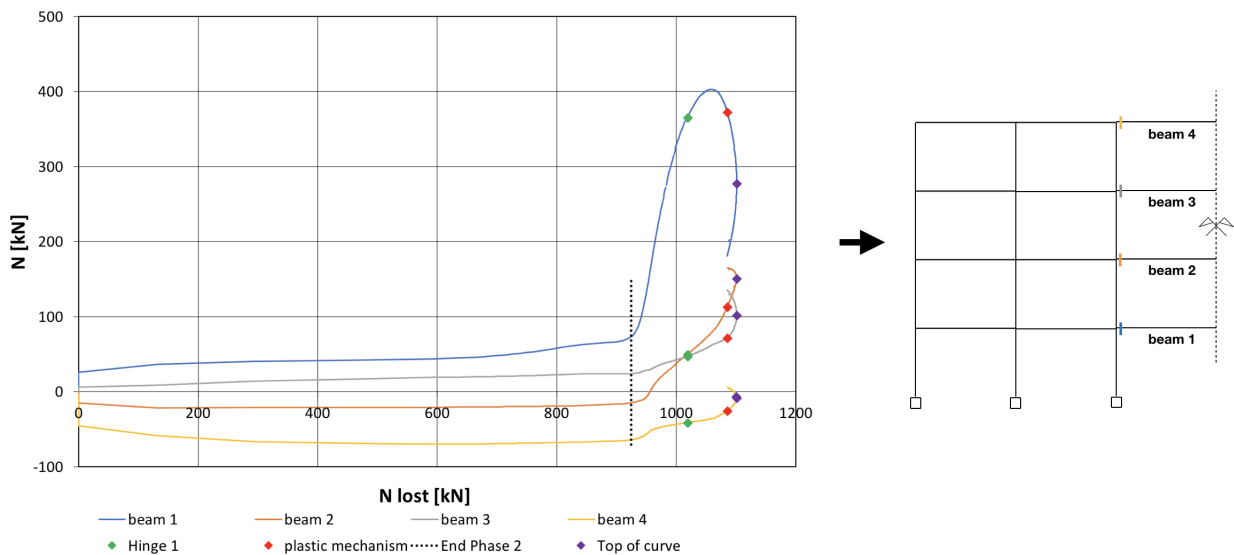


Figure V.3: Evolution of the normal forces into beams' cross-sections of the DAP

As shown in figure V.3, the plastic mechanism (panel plastic mechanism) is not reached at the maximum value of the N in the beam 1 as might have been expected but slightly after reaching the latter peak. Instead of checking individually the normal forces in each beam, it is rather their sum that needs to be analysed. Indeed, the plastic mechanism is expected to be reached when the pulling force acting on the IAP reaches its maximum.

As shown on figure V.4, the panel plastic mechanism (red dot) is developed when the sum of the normal forces in the beams reaches its peak ($\sum_{i=1}^4 N_{beam,i}$)¹.

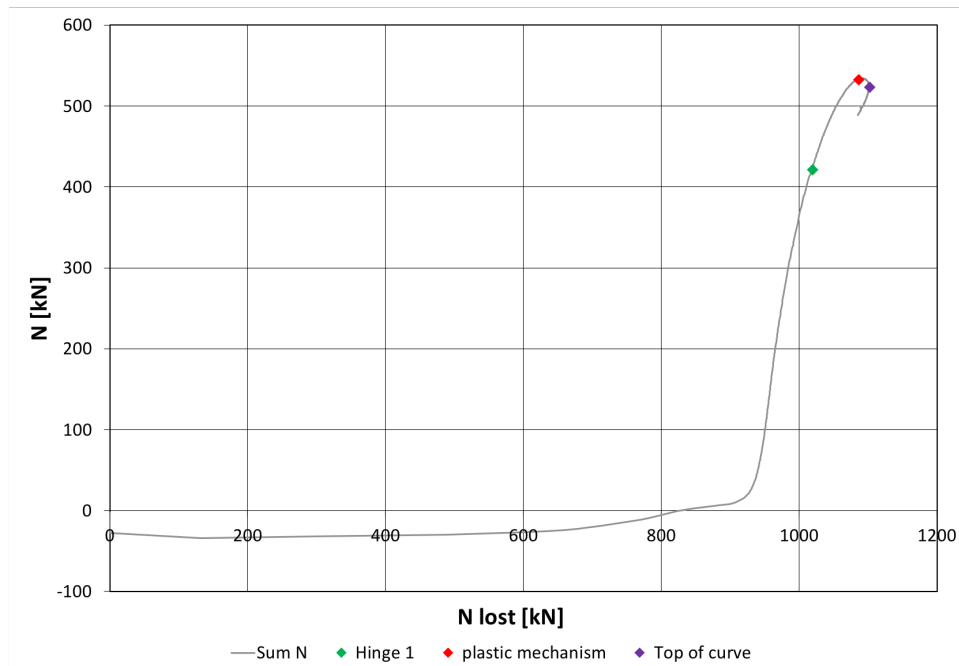


Figure V.4: Sum of the normal forces into beams' cross-sections of the DAP

Evolution of the normal forces into columns of the IAP:

As was the case for the reference structure, the load previously supported by the lost column is entirely redistributed in the beside columns. The evolution of N in column 3 is almost linear. The differences between the N in the column 3 and the N of the "N lin" curve never exceeds 7%.

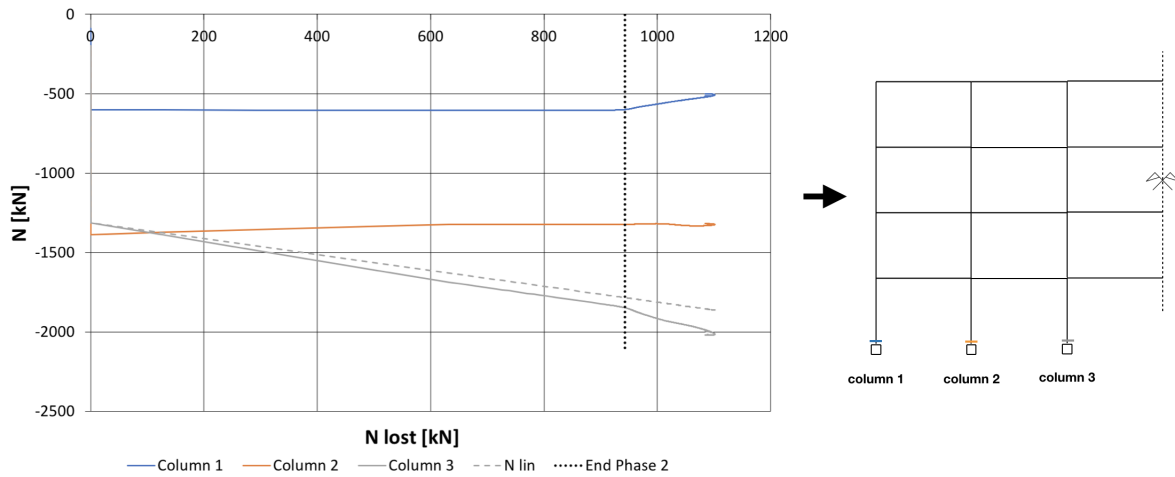


Figure V.5: Evolution of the normal forces into columns' cross-sections of the IAP

¹This sum is calculated since the beams in the IAP present almost the same inclination.

V.2.2 Loss of the intermediate column 1

The $(u; N_{AB})$ curves for an IAP elastic and an IAP elastic-perfectly plastic are shown on figure V.6 in the case of the loss of an intermediate column. The hinges developed in the IAP are shown on the figure and marked by coloured dots. The yielding only occurs in the IAP from the left. The IAP from the right remains fully elastic during the loss of the column. Indeed, the yielding occurs where the lateral resistance is the smallest, i.e. in the IAP at the left of the lost column.

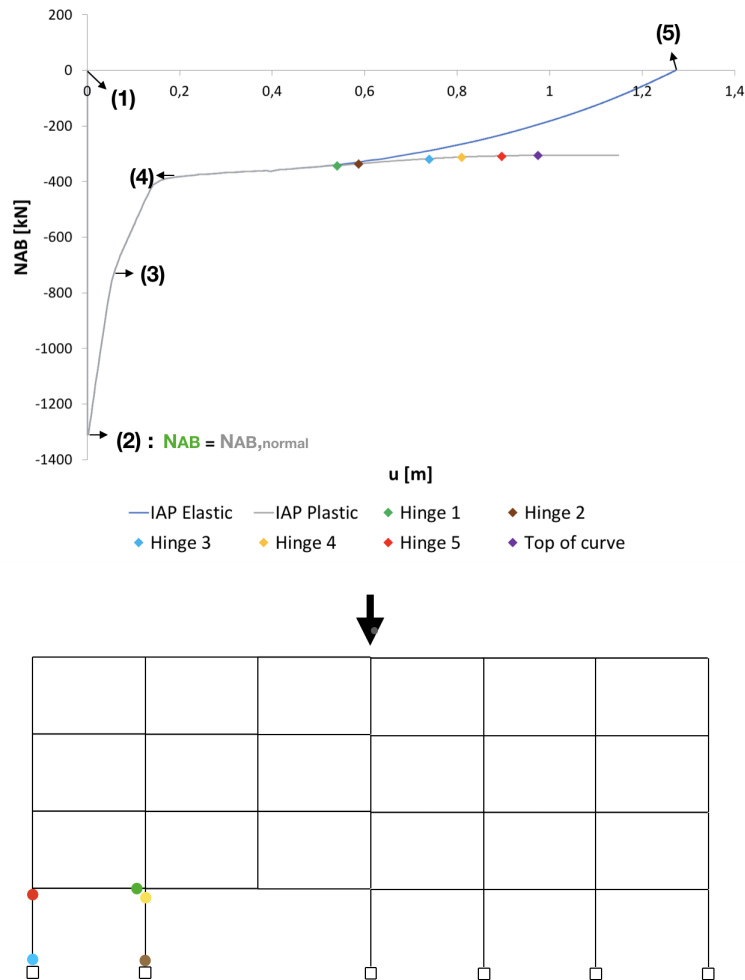


Figure V.6: $(u; N_{AB})$ curves for an IAP elastic and an IAP elastic-perfectly plastic

The order of formation of the hinges is exactly the same as the one presented for the loss of the central column for the reference structure. Indeed, the first hinge develops at the right extremity of the bottom beam and the other hinges develop at the extremities of the columns of the left IAP.

The N_{lost} inducing the formation of the first hinge (green dot) is equal to $967,5 \text{ kN}$ and the one inducing the formation of the complete panel mechanism (red dot) is equal to $1002,1 \text{ kN}$. The difference between the latter values is about $3,5\%$. For the loss of the central column, the difference was about $5,8\%$. The plastic mechanism is thus developed faster after the formation of the first hinge in the case of the loss of the considered intermediate column. Indeed, only 4 hinges are needed to form the panel plastic mechanism in the present situation while a total of 12 hinges (6 from the left and 6 from the right of the IAP) are needed to form the panel plastic mechanism in the case of the loss of the central column for the present structure (6 spans).

The N_{lost} corresponding to the top of the curve (purple dot) is equal to $1004,8 \text{ kN}$. The difference between the last value of N_{lost} with the one corresponding to the formation of the plastic mechanism

is about 0,3%. The collapse of the structure is thus quickly reached after the complete formation of the panel plastic mechanism.

The shape of the evolution of the normal forces into the beams of the DAP are similar to the ones presented for the loss of the central column and will thus not be recalled here.

Evolution of the normal forces into columns of the IAP:

The loads previously supported by the lost column are again entirely redistributed in the beside columns. Indeed, the N in the other columns remains almost constant as shown in figure V.7.

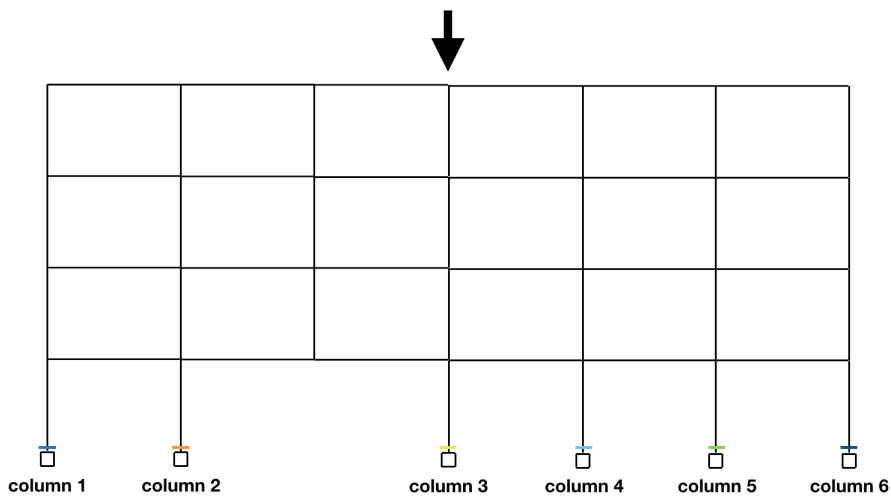
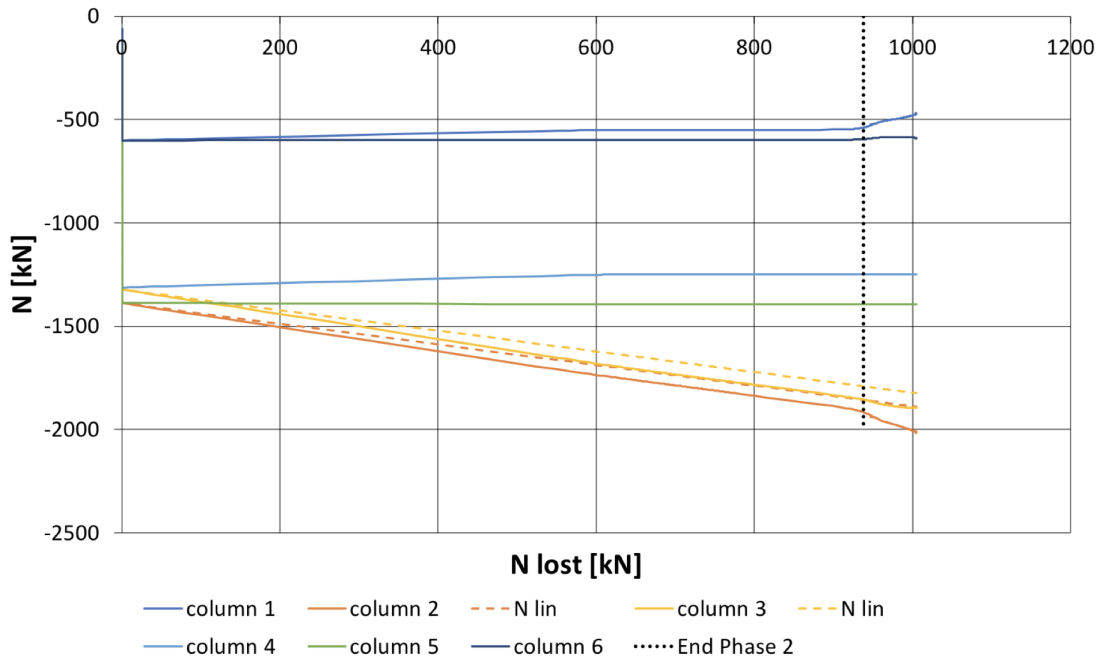


Figure V.7: Evolution of the axial forces into columns' cross-sections of the IAP

The differences between the N in the beside columns (columns 2 and 3) and the N from the "N lin" never exceed 6%.

V.2.3 Loss of the intermediate column 2

The global response of the frame under the loss of the intermediate column 2 is similar to the one presented in chapter IV and will thus not be recalled here. A comparison is shown further in section V.4.2.

V.2.4 Loss of the exterior column

The global response of the frame under the loss of the exterior column is similar to the one presented in chapter IV for the loss of the exterior column in the reference structure. It will thus not be recalled here.

V.3 Increase in the number of spans from 6 to 8

In the present section, the event "loss of a column" will be investigated in five different locations, see figure V.8.

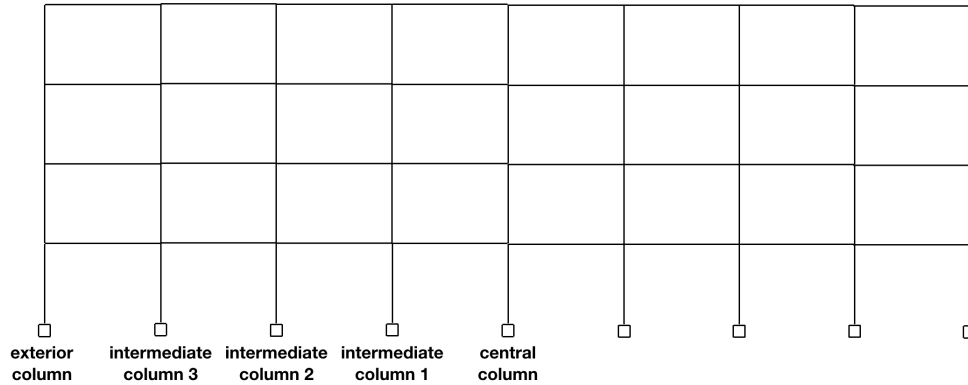


Figure V.8: Lost columns' designations

V.3.1 Loss of the central column

In the case of the loss of the central column for the structure with 8 spans, the hinges are developing in the exact same locations in the IAP, i.e. at the extremities of the columns at the damaged level and at one extremity in each bottom beam in the IAP. The choice made was to highlight the moments corresponding to the formation of the first plastic hinge (green dot) in the IAP, the formation of the full plastic mechanism (red dot) and the attaining of the top of the curve (purple dot), see figure V.9.

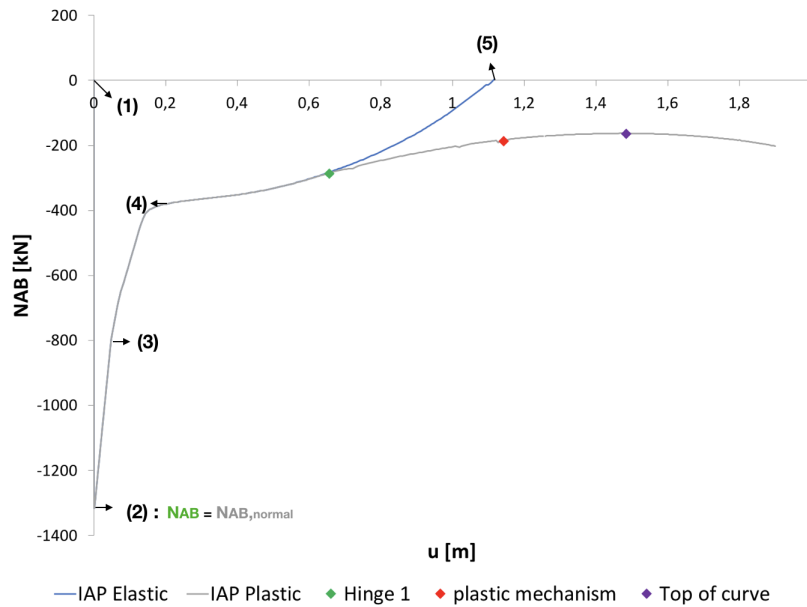


Figure V.9: $(u; N_{AB})$ curves for an IAP elastic and an IAP elastic-perfectly plastic

The N_{lost} inducing the formation of the first hinge (green dot) is equal to 1031 kN and the one inducing the formation of the full plastic mechanism (red dot) is equal to 1132 kN. The difference between the latter values is about 8,9%. In the case of the structure with 4 spans, this difference was about 5,2% and with 6 spans, it was about 5,8%. It confirms again that an increase in the number of spans allows reaching the full plastic mechanism to be delayed when the first hinge is formed in the IAP.

The N_{lost} corresponding to the top of the curve (purple dot) is equal to 1154 kN. Thus, the difference between the latter N_{lost} and the one inducing the complete formation of the panel plastic mechanism is about 1,9%. In the case of the structure with 4 spans, it was about 1,9% as well and in the case of the structure with 6 spans, it was about 1,7%. So, the influence of the arch effect does not change significantly when the number of spans increases. The increase in the number of storeys would most likely increase the influence of the arch effect on the latter results.

The shape of the evolution of the normal forces into the beams of the IAP is similar to the one presented for the 6 spans structure in the case of the loss of a central column and will thus not be exposed for the present situation. It differs only on the values of the normal forces. For instance, the tension into the beam 1 will be higher in the present situation. It is logical since the resistance of the IAP is higher as there are more spans and thus the pulling forces acting on the IAP need to be higher to develop the complete panel plastic mechanism.

Evolution of the normal forces into columns of the IAP:

Again, as shown in figure V.10, the loads previously supported by the lost columns are entirely re-distributed in the beside columns. The evolution of the N in the beside columns is near the linear evolution "N lin". Indeed, the differences between the N in the beside columns and the one from "N lin" never exceed 7,5%.

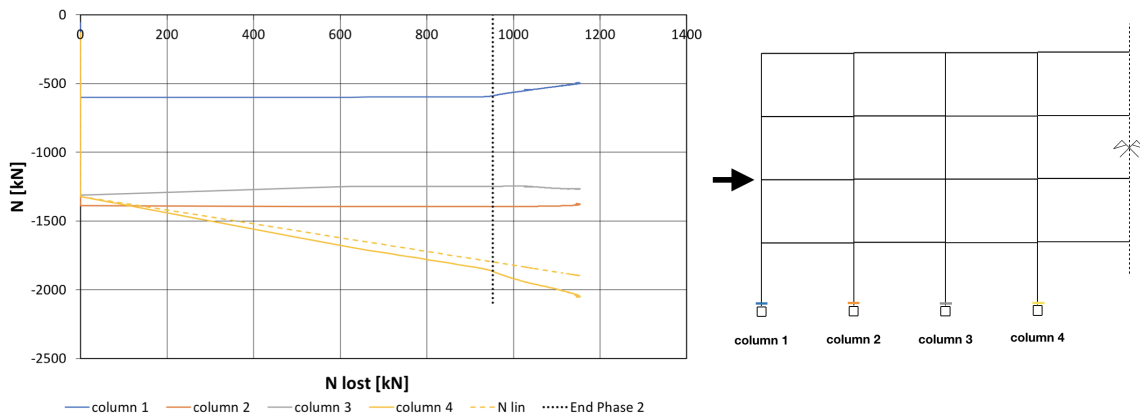


Figure V.10: Evolution of the normal forces into columns' cross-sections of the IAP

V.3.2 Loss of the intermediate column 1

In the present situation, it is again the side of the IAP which is the less resistant (fewer spans in the present case) that will yield and thus present a panel plastic mechanism, i.e. the left side of the IAP. The right side of the IAP remains fully elastic. This case is not presented herein because it does not bring new information.

V.3.3 Loss of the intermediate column 2

The global response of the frame (8 spans) in the case of the loss of the intermediate column 2 is exactly the same as the one corresponding to the loss of the intermediate column 1 for the structure with 6 spans when the IAP is elastic-perfectly plastic. It will thus not be recalled here.

V.3.4 Loss of the intermediate column 3

The global response of the frame (8 spans) in the case of the loss of the intermediate column 3 is exactly the same as the one presented in chapter IV and as the one corresponding to the loss of the intermediate column 2 for the structure with 6 spans in the case where the IAP may yield (elastic-perfectly plastic) and will thus not be recalled here.

V.3.5 Loss of the exterior column

The global response of the frame under the loss of the exterior column is similar to the one presented in chapter IV for the loss of the exterior column in the reference structure. It will thus not be recalled here.

V.4 Comparison between the numerical results for 4, 6 and 8 spans

Thanks to the analysis of all the previous simulations of the loss of a column in different locations for three structures, it was noticed that it is always the side of the IAP which is the less resistant (fewer spans) that presents hinges while the other side remains fully elastic. This is valid until the collapse of the structures (purple dot on all the previous graphs). Moreover, the hinges are forming in the exact same locations in the IAP, i.e. at one extremity of each bottom beam and at the top and bottom of the columns.

Through this section, a comparison will be achieved concerning the loss of the central column between the three structures. Indeed, this comparison is judged adequate to illustrate and to summarize the influence of the increase in the number of spans (i.e. increase in lateral stiffness and resistance coming from the IAP) on the global response of the structures. This is the aim followed in section V.4.1.

Then, a comparison will be made between the loss of the intermediate column in the 4 spans structure with the loss of the intermediate column 2 in the 6 spans structure and the loss of the intermediate column 3 in the 8 spans structure in order to highlight that their global responses are the same when the IAP is elastic-perfectly plastic. A comparison between the loss of the intermediate column 1 for the 6 spans structure and the loss of the intermediate column 2 for the 8 spans structure will also be achieved in order to highlight that their global responses are the same when the IAP is elastic-perfectly plastic. These are the aims followed in section V.4.2.

The scenario of the loss of an exterior column implies the exact same global response in each structure. This will thus not be exposed here.

A conclusion will be drawn on the evolution of N in the columns of the IAP through section V.4.3.

Finally, the identified failure modes will be compared between the investigated situations and finally generalized. This is the aim pursued in section V.4.4.

V.4.1 Loss of a central column

In the case of the loss of the central column in each of the three structures (4, 6 and 8 spans), the $(u; N_{AB})$ curves are drawn on the figures V.11 and V.12 respectively for an IAP elastic and an IAP elastic-perfectly plastic.

As shown on figure V.11, the Phases 1 and 2 are similar for the three structures since the beam plastic mechanism in the DAP is the same in each structure. A difference appears during Phase 3, the more spans the bigger the slopes of the curves are. Indeed, the slope of the curve during Phase 3 is ruled by the lateral stiffness coming from the IAP as was previously explained. Thus, the more spans there are, the higher the stiffness of the IAP and thus the bigger the slopes during Phase 3. As a consequence, the displacement at the top of the lost column (u) will be smaller in the case of the structure with 8 spans than in the structures with 6 and 4 spans during Phase 3.

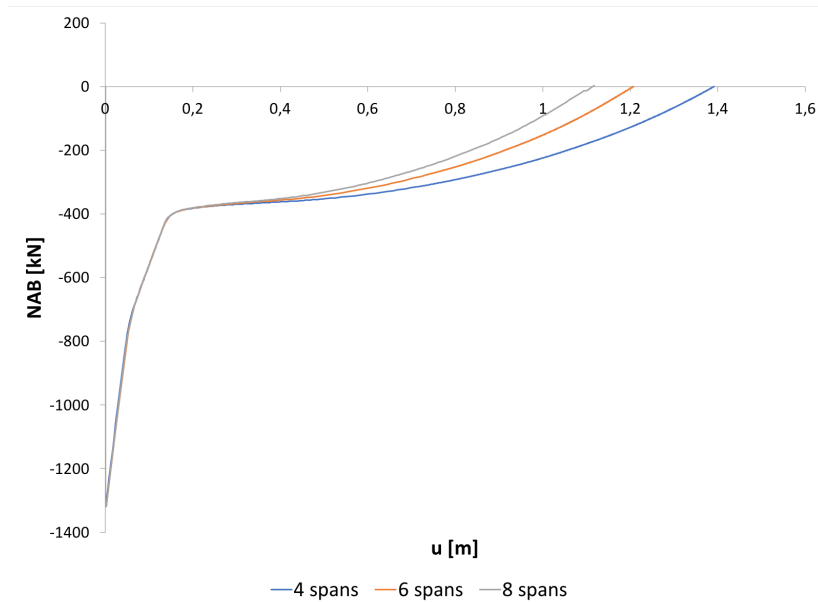


Figure V.11: Comparison of the $(u; N_{AB})$ curves between the three structures for an IAP elastic

As shown in figure V.12, the more spans there are, the higher the top of the $(u; N_{AB})$ curve will be, i.e. the bigger the value of N_{lost} . Thus, by increasing the number of spans, the structure tends to be more and more able to withstand the complete loss of the column when the IAP may yield. In other words, it becomes more and more able to reach N_{AB} equals to 0 and thus N_{lost} equals to $N_{AB,normal}$. Indeed, as previously explained, by increasing the number of spans, the lateral resistance increases.

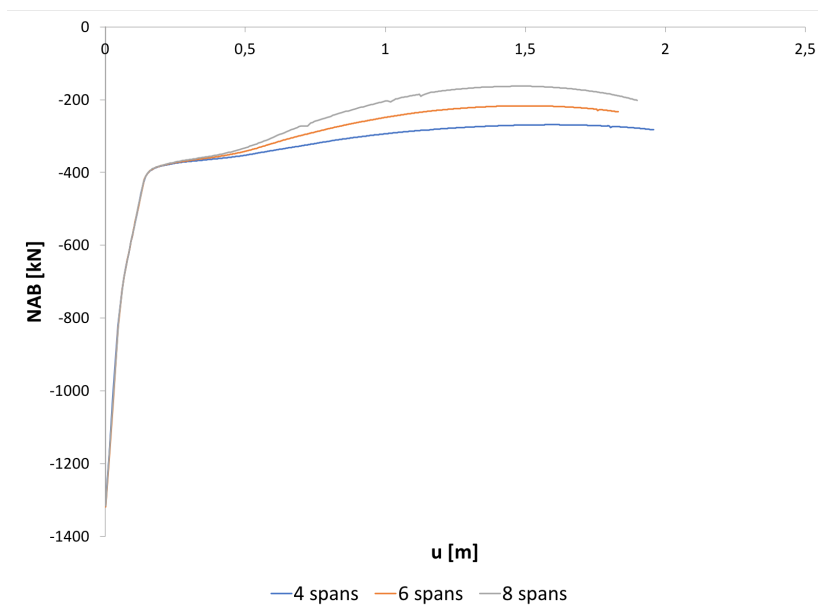


Figure V.12: Comparison of the $(u; N_{AB})$ curves between the three structures for an IAP elastic-perfectly plastic

The N_{lost} for each structure are gathered in table V.1. $N_{lost,1}$ is the value of N_{lost} corresponding to the formation of the first hinge in the IAP, $N_{lost,2}$ is the one corresponding to the formation of the complete panel plastic mechanism and $N_{lost,3}$ is the one corresponding to the top of the $(u; N_{AB})$ curve when the IAP is elastic-perfectly plastic. The differences between the previous values are listed in the table. The latter were calculated as $\%N_{lost,1,2} = \frac{N_{lost,2} - N_{lost,1}}{N_{lost,2}} * 100 = 5,2\%$ for the structure with 4 spans for instance.

	4 spans	6 spans	8 spans
$N_{lost,1}$ [kN]	961	1019	1031
$N_{lost,2}$ [kN]	1014	1082	1132
$N_{lost,3}$ [kN]	1034	1101	1154
$\neq N_{lost,1,2}$ [%]	5,2	5,8	8,9
$\neq N_{lost,2,3}$ [%]	1,9	1,7	1,9
$\neq N_{lost,1,3}$ [%]	7,1	7,5	10,7

Table V.1: Comparison of the values of N_{lost} between the three structures

Each N_{lost} is logically increasing with the increase in the number of spans since more resistance is brought about by the increase in the number of spans, see table V.1.

The attaining of the complete panel mechanism in the IAP when the first hinge is developed is delayed by increasing the number of spans. Indeed, the value of $\neq N_{lost,1,2}$ is increasing with the number of spans.

By analysing the values of $\neq N_{lost,2,3}$, it may be concluded that the influence of the arch effect remains the same for the three structures. Thus, the arch effect is not influenced by an increase in the number of spans. It would be most likely influenced by an increase in the number of storeys. The checking of an increase in the number of storeys is a point addressed in the perspectives.

The values of $\neq N_{lost,1,3}$, i.e. the differences between the N_{lost} corresponding to the top of the curve and the N_{lost} inducing the formation of the first hinge in the IAP, are increasing with the number of spans.

As a consequence, the evolutions of $\neq N_{lost,1,2}$ and $\neq N_{lost,1,3}$ seem to be ruled by the lateral resistance coming from the IAP since they are both increasing with the increase in the number of spans.

V.4.2 Loss of an intermediate column

In the case of the loss of the intermediate column shown on figure V.13, the $(u; N_{AB})$ curves are exactly the same for the three structures. As the response was described for the case of the structure with 4 spans in chapter IV, it was not recalled for the other structures.

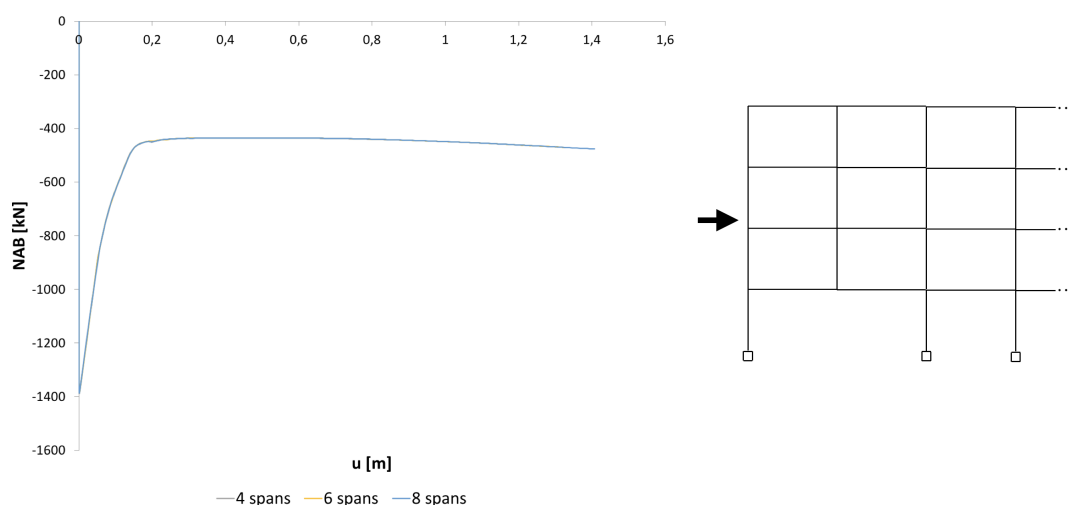


Figure V.13: Comparison of the $(u; N_{AB})$ curves between the three structures for an IAP elastic-perfectly plastic

Similarly, in the case of the loss of the intermediate column shown in figure V.14, the $(u; N_{AB})$ curves are exactly the same for the 6 and 8 spans structures. The global response of the 6 spans structure under the loss on the considered column with an IAP that may yield was detailed earlier. Thus, that is why the situation was not detailed for the 8 spans structure.

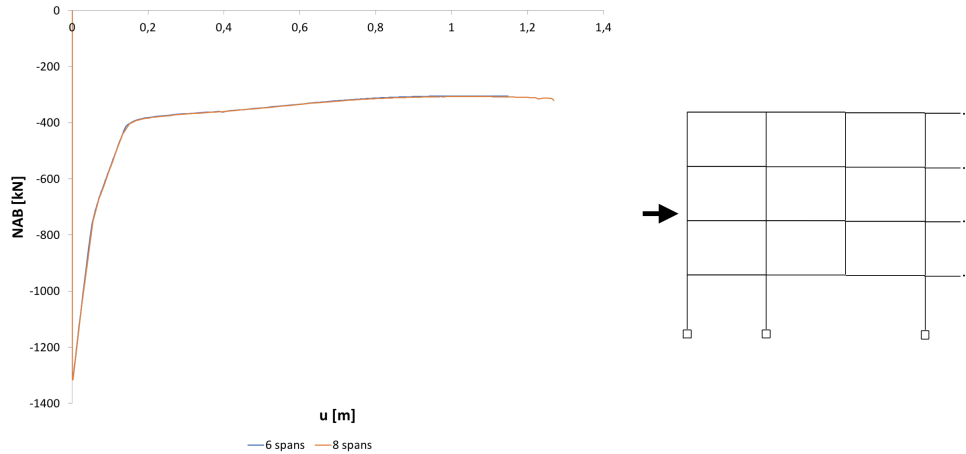


Figure V.14: Comparison of the $(u; N_{AB})$ curves between the 6 and 8 spans structures for an IAP elastic-perfectly plastic

V.4.3 Redistribution of loads during the loss of a column

For all the three structures and for all the "loss of a column" scenarios investigated, the N_{lost} is entirely redistributed in the beside columns. The differences observed between the values of N in the beside columns and the values of N from the linear curves "N lin" never exceed 8 to 9 %.

The final goal at the end of chapter VI is to give a method to predict the failure modes of structures that suffer the loss of a column based on the results of the complete analytical model presented in chapter I. In that way of thinking, it would have been perfect to be able to predict the exact value of N in the beside columns to check their stability based on the values of N_{lost} analytically predicted. As seen earlier, the increase of N in the beside columns is not only due to the redistribution of N_{lost} since the values of N differ in the extreme situations from 8 to 9% in the investigated situations. Since the general aim is to give a simplified method for practitioners to check the robustness of structures, a coefficient could be calibrated to evaluate properly the true values of N in the beside columns. However, there are not enough simulations achieved in the present thesis to be able to evaluate such a coefficient. It is a point addressed in the perspectives.

V.4.4 Failure modes

As previously explained, the behaviour of all the investigated frames that lose the intermediate column shown on figure V.15 are equivalent for the case where the IAP may yield. The failure modes and thus the verification recommendations are exactly the same in the 4, 6 and 8 spans structures. They were presented and explained in section IV.3.3 for the case of the 4 spans structure.

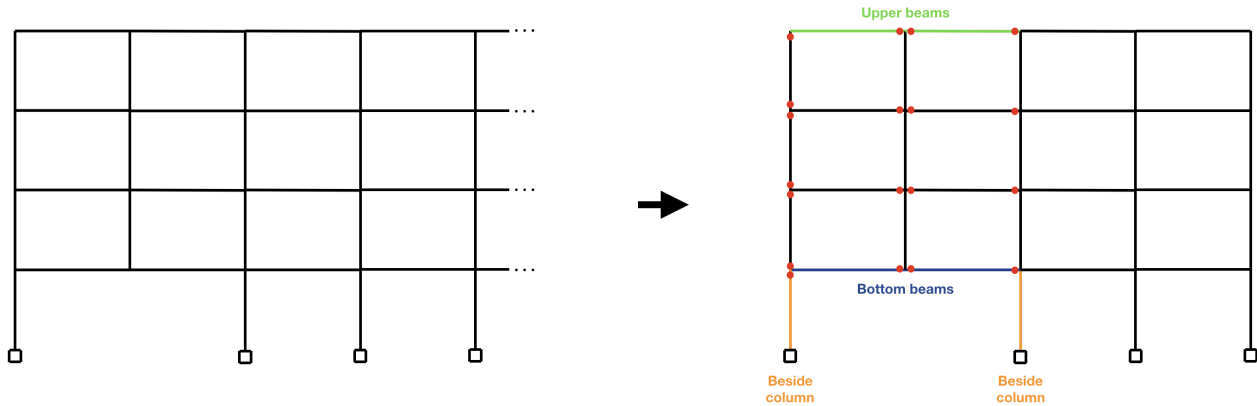


Figure V.15: Loss of intermediate column

The verification recommendations for the loss of the intermediate columns shown on figures V.16 and V.17 follow the same logic as the one presented in chapter IV concerning the reference structure.

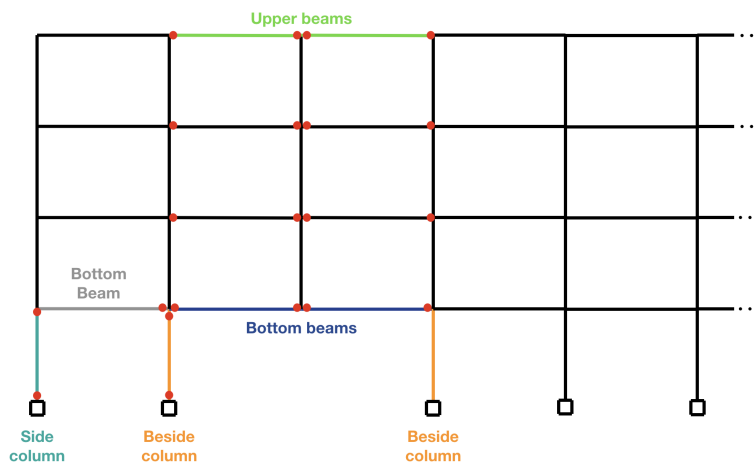


Figure V.16: Loss of intermediate column

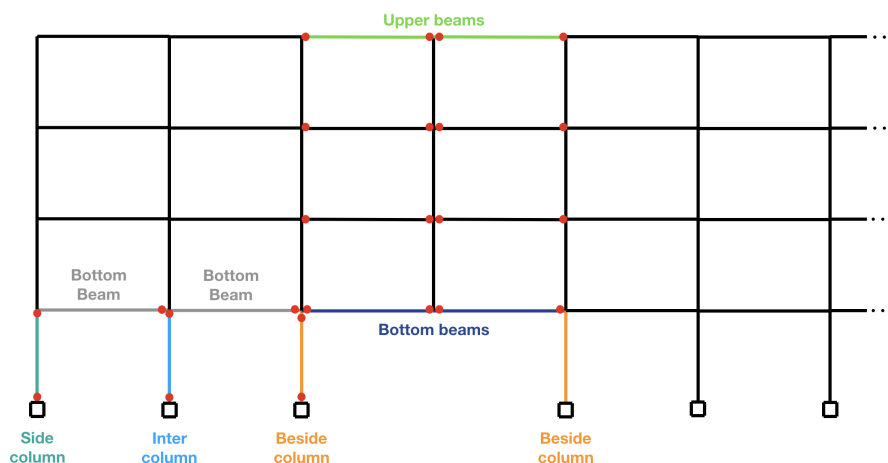


Figure V.17: Loss of intermediate column

In the case of the loss of a central column, the failure modes are exactly the same as the ones presented for the reference structure. The differences lay in the number of hinges developing in the IAP. Indeed, by increasing the number of spans, the number of hinges needed to form the full panel plastic mechanism in the IAP increases. But the locations of the cross-sections in which the hinges are developing

do not change. Indeed, the hinges in the IAP are still developing at the inner extremity of the bottom beams and at the top and bottom of each columns.

Moreover, as previously said, the behaviour under the loss of an exterior column in each of the three structures is similar. The associated failure modes are then equivalent to those presented in section IV.4.2.

For all the investigated situations, verification recommendations remain similar:

- The cross-sections of the elements where the hinges are developing need to be class 1;
- The buckling of the upper beams of the DAP needs to be checked;
- The resistance of the bottom beams and their joints needs to be checked under the tensile forces in action;
- The buckling of the beside columns needs to be checked;
- In the case where the joints are partially resistant, the latter have to be designed to have sufficient rotation capacity and sufficient resistance.

In the case of the loss of an exterior column, the only checks that differs are:

- The resistance of upper beam of the DAP and its joints needs to be checked under the tensile forces;
- The buckling of the bottom beam of the DAP needs to be checked.

V.5 Conclusion

The influence of the yielding of the indirectly affected part (IAP) was investigated on the global response of three structures within several "loss of a column" scenarios. The latter shown that the hinges are developing in the exact same locations in the three structures. Thus, the increase in the number of spans does not affects the locations of formation of hinges. Moreover, it shown that the formation of first hinges in the IAP led to a chain formation of hinges inducing a quick reach of the collapse of the structure through the formation of plastic mechanism. It was highlighted that the reach of the collapse of the structure after the formation of first hinges in the IAP is delayed when the number of hinges needed to form the mechanism increases. Indeed, the differences between the N_{lost} inducing the first hinges and the one corresponding to the collapse of the structure are increasing with an increase in the number of hinges needed to form the mechanism in the IAP.

The influence of an arch effect was detailed and it was concluded that the increase in the number of spans does not affect the latter. It would most likely have been influenced by an increase in the number of storeys. It is a point addressed in the perspectives.

The real behaviour of the investigated structures is known within the considered scenarios. The evolution of internal forces in the structure was detailed. More particularly, it was shown that the loads previously supported by the lost column are entirely redistributed in the beside columns. The associated identified failure modes of the structures were also presented and it was shown that the verification recommendations to assess robustness checks were similar for the three structures. The latter were recalled in section V.4.4.

The goal now would be to predict the latter on the basis of the complete analytical procedure presented in chapter I. This is the aim pursued through the next chapter.

Chapter VI

Analytical study

VI.1 Introduction

The first goal of this chapter is to identify analytically the point of collapse of the structure. A comparison between the analytical results and the numerical ones will be achieved in order to validate the analytical predictions. This is the aim followed through section VI.2.

Then, the goal is to establish a simple method allowing to predict as accurately as possible the latter collapse of the structure based on the complete analytical method detailed in chapter I. To achieve that, the task is to find a way to combine the analytical prediction of the collapse of the structure determined in section VI.2 with the complete analytical method in order to identify a breakpoint on the $(u; N_{AB})$ curve (or $(u; \lambda)$ curve) analytically predicted. Indeed, the complete analytical procedure can derive those curves for a DAP elastic-perfectly plastic and an IAP elastic. Then, the task is to determine if the latter breakpoint would be a good approximation of the real collapse of the structure in terms of the value of N_{lost} and in terms of the value of the displacement u of the top of the lost column. Thus, the differences between the N_{lost} corresponding to the identified breakpoint on the $(u; \lambda)$ curve for an IAP elastic and the N_{lost} corresponding to the real collapse of the structure (i.e. on the $(u; \lambda)$ curve for an IAP that may yield) will be established. The differences between the observed values of u will be also determined. This is done in order to quantify the accuracy of the approximation of the collapse of the structure through the identified breakpoint. This is the aim pursued through section VI.3.

The final goal of this chapter is to give methods allowing to predict the identified failure modes of the structures based on the extracted results from the complete analytical model and especially the ones corresponding to the previously determined breakpoint. This is the aim pursued through section VI.4.

VI.2 General method for the calculation of the plastic mechanism in the IAP

As was presented in the previous chapters, the collapse of a structure that loses its central column may be induced by the development of a panel plastic mechanism in the IAP. Thus, the goal followed in the present section is to predict analytically the formation of the panel plastic mechanism. This will be investigated for the case of the loss of the central column of the reference structure (4 spans). In other words, the goal is to predict analytically the red point on figure VI.1 corresponding to the formation of the panel plastic mechanism in the IAP.

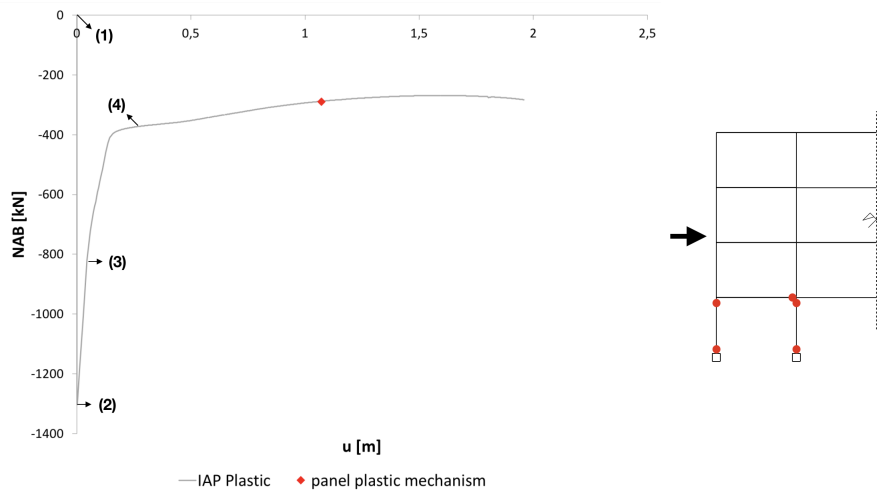


Figure VI.1: Panel plastic mechanism point on the $(u; N_{AB})$ curve

Since the behaviour of the frame is symmetrical under the loss of its central column, the panel plastic mechanism in the IAP from the left (illustrated on figure VI.1) develops in the exact same way and in the exact same moment as the one in the IAP from the right. Thus, since the latter two are equivalent, only one needs to be investigated, see figure VI.2.

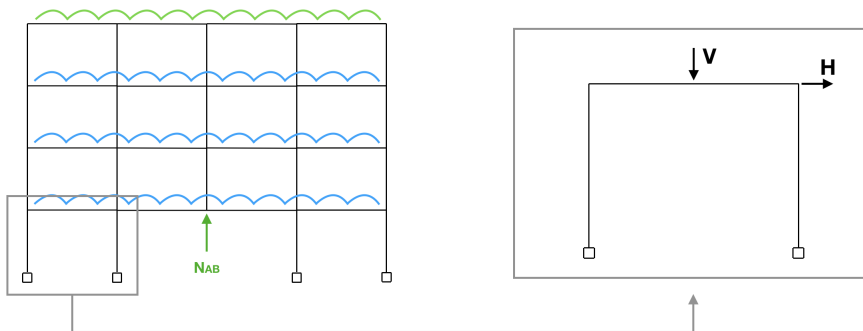


Figure VI.2: Studied substructure

There is a simple way to evaluate the loads V and H acting on the substructure which cause the formation of the plastic mechanism. Indeed, H may be calculated by the sum of the horizontal reactions at the supports of the substructure and V may be calculated by the sum of the vertical reactions.

The second order effects may have a destabilizing influence on the development of the panel plastic mechanism when the columns are compressed. These effects are explained in pages 415, 416 and 417 in the book "Calcul plastique des constructions" (Massonnet and Save [22]) through the explanation of the effects of deformations on the post-limit behaviour. The calculation of the panel plastic mechanism will be achieved on the basis of the theory defined in this book. Its application is made through

the assumption of infinitely rigid bars composing the considered frame shown on figure VI.3.

In the present situation, the value of β is finite since the numerical results have shown that non negligible angles appear at these locations (figure VI.3). The horizontal and vertical displacements, δ_h and δ_v , are given as:

$$\delta_h = h \sin \beta \quad \text{and} \quad \delta_v = h(1 - \cos \beta) \quad (\text{VI.1})$$

in accordance with the configuration of the substructure on figure VI.3.

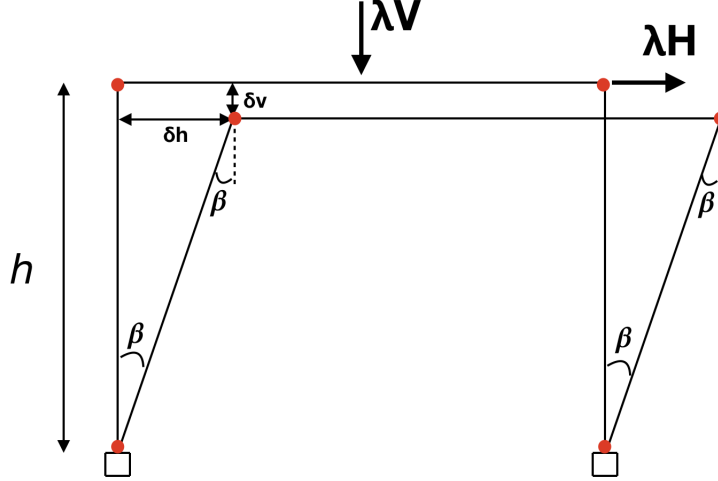


Figure VI.3: Panel plastic mechanism

The theorem of virtual works says that the limit multiplier λ for the frame deformed with an angle β is obtained by giving a virtual deformation infinitely small $d\beta$ to this frame, during which δ_h and δ_v undergo variations [22] as:

$$d\delta_h = h \cos \beta d\beta \quad \text{and} \quad d\delta_v = h \sin \beta d\beta \quad (\text{VI.2})$$

Thus, the external work w_E and the internal work w_I are respectively given as:

$$w_E = \lambda H h \cos \beta d\beta + \lambda V h \sin \beta d\beta \quad (\text{VI.3})$$

$$w_I = \left(\sum_{i=1}^4 M_{pl,i} \right) d\beta \quad (\text{VI.4})$$

Where $M_{pl,i}$ is the resistant plastic moment of the cross-section i where a hinge develops. It has to be noted that the reduction of $M_{pl,i}$ because of N (normal forces) has to be taken into account.

The equalization of the internal and external works gives:

$$\lambda = \frac{\sum_{i=1}^4 M_{pl,i}}{h [H \cos \beta + V \sin \beta]} \quad (\text{VI.5})$$

Thus, when λ is equal to 1, it indicates that the panel plastic mechanism is completely developed.

The latter λ will be evaluated based on the values of H , V , β and $M_{pl,i}$ corresponding to the red dot on figure VI.1, i.e. the formation of the panel plastic mechanism (thus for an IAP elastic-perfectly plastic). These data are taken from the numerical results calculated through Finelg. The calculated λ is about 1,028. It is thus almost equal to 1. The adopted formula seems to fit for the formation of the

panel plastic mechanism for the reference structure.

In the case of the loss of the central column for the structure with 6 spans, the panel plastic mechanism is formed by 6 hinges. The corresponding λ is equal to 0,997. And finally, for the loss of the central column of the 8 spans structure, the panel plastic mechanism is formed by 8 hinges. The corresponding λ is equal to 0,995.

	Lambda [-]	Error [%]
4 spans	1,028	2,8
6 spans	0,997	0,3
8 spans	0,995	0,5

Table VI.1: Lambda for the three structures and the associated errors

Each λ are gathered in the table VI.1 and their respective errors compared to the value of λ equals 1. As shown, the errors remain small. The point of formation of the panel plastic mechanism in each of the three structures is thus well estimated by the analytical formula of λ previously presented.

VI.3 Combination of the previous general method with the complete analytical procedure

Thanks to the complete analytical model detailed in chapter I, the response of the frame is known for a DAP elastic-perfectly plastic and an IAP elastic, i.e. the blue curve on the figure VI.4.

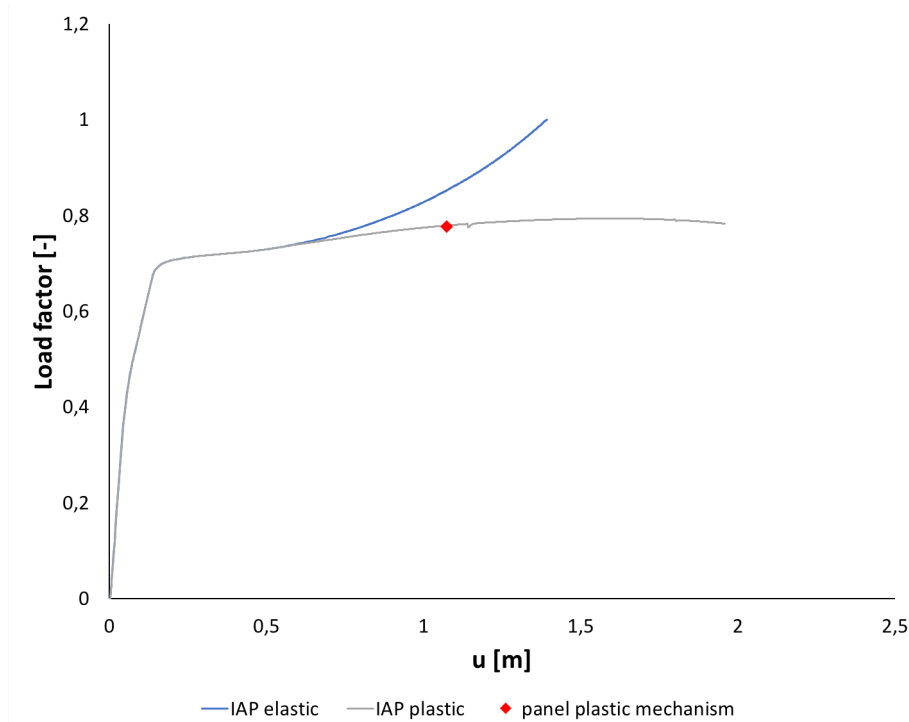


Figure VI.4: $(u;\lambda)$ curves for the loss of the central column in the reference structure

In chapter III, λ was presented as the multiplier of N_o to get N_{lost} , i.e. $N_{lost} = \lambda N_o$ ($N_o = N_{AB,normal}$).

In the previous section, it was shown that the estimation of the formation of the plastic mechanism was made with a pretty good accuracy. In the present section, the goal is to be able to find a break-point on the curve that may be calculated by the complete analytical model (i.e. the blue curve on figure VI.4). Then the task will consist of determining how well this latter point estimates the real

development of the plastic mechanism leading to the collapse of the structure (i.e. the red dot on the grey curve of figure VI.4¹).

On the basis of the numerical results obtained through Finelg, we were able to determine if the λ obtained through the formula VI.5 was equal to 1 corresponding to the formation of the panel plastic mechanism. The formula VI.5 allows to draw a second order rigid plastic ($u;\lambda$) curve as the orange one shown on figure VI.5. The latter was calculated on the basis of the H , V , β and the $M_{pl,i}$ obtained through Finelg for the case where the IAP is elastic-perfectly plastic.

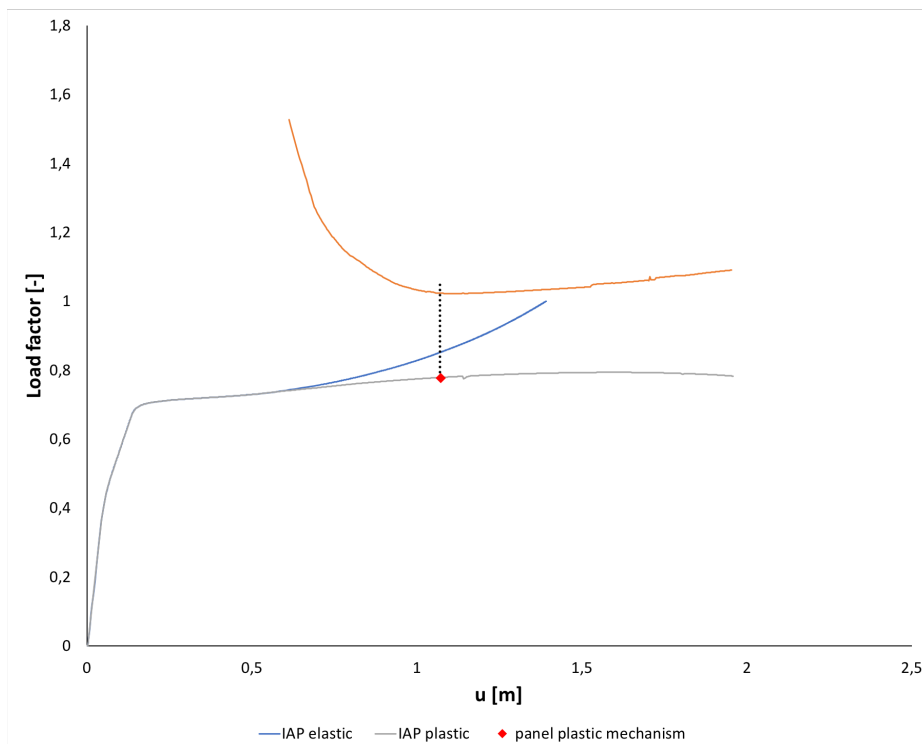


Figure VI.5: ($u;\lambda$) curves for the loss of the central column in the reference structure and the second order rigid plastic curve

It is shown that the red dot corresponding to the formation of the panel plastic mechanism is in a good accordance with the minimum of the second order rigid plastic curve (orange curve) where λ equals 1,028. Indeed, the formation of the panel plastic mechanism occurs on both curves for the same displacement (u) as highlighted by the vertical dotted black line.

The goal is now to derive a second order rigid plastic curve on the basis of the internal forces obtained through the complete analytical model (and thus where the IAP is elastic). The model gives all the internal forces in the DAP since it resolves the DAP. Based on the normal forces and the shear forces into the beams of the DAP (i.e. the N and T on figure VI.6) and their inclination θ , it is possible to have a good evaluation of H and V . H and V were previously determined by the sum of the horizontal reactions and the sum of the vertical reactions respectively in the IAP. But, the latter reactions are not given by the complete analytical model.

¹It has to be reminded that the point of formation of the panel plastic mechanism is not the point where the structure will collapse. Indeed, in the previous chapters it was highlighted that the top of the curve and thus the collapse of the structure occurs a bit further.

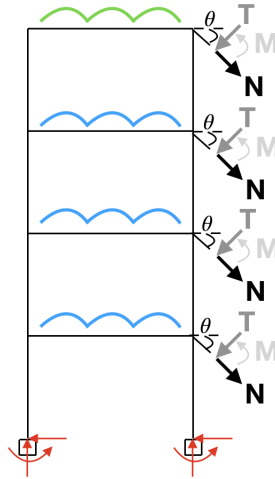


Figure VI.6: Cut in the reference structure in the case of the loss of its central column

Thus, based on N , T and θ in each left extremity of the beams of the DAP, it is possible to calculate the H and V . The H is thus calculated by the horizontal projection of N and T and by summing the latter. And V may be calculated by summing the vertical projections of N and T , by adding the applied loads on the IAP shown in blue and green on figure VI.6 and by adding the self-weight of the elements of the IAP shown on the latter figure.

The two remaining unknowns are β and the $M_{pl,i}$. The complete analytical model gives the displacement at each extremity of the DAP. Thus, by knowing the horizontal displacement of the left extremity of the bottom beam in the DAP (i.e. the lowest extremity where the N and T are represented in figure VI.6) and by knowing the height of the columns h (equals 3,5 meters in the present situation), it is possible to determine β .

To determine the $M_{pl,i}$, the formulas of Villette presented in chapter IV will be used. To achieve that, the values of N have to be known in the columns where the panel plastic mechanism develops. As was detailed in the previous chapters, the only columns that feel the loss of the column (i.e. that see their normal forces changing) are the beside columns. Thus, it was shown that the N_{lost} was fully redistributed in the beside columns, i.e. $\frac{N_{lost}}{2}$ in the beside column from the left and $\frac{N_{lost}}{2}$ in the beside column from the right.

The N in the columns are known when the frame is fully loaded (i.e. at the end of Phase 1) and thus for N_{lost} equals zero. Thus, when N_{lost} is increasing, since the complete analytical model gives the values of N_{lost} , the task consists simply of redistributing manually the N_{lost} in the beside columns.

The calculated values of N where the hinges are developing are then introduced in the formulas of Villette to get the successive $M_{pl,i}$.

It is now possible to derive the second order rigid plastic curve based on the complete analytical model results and thus for the case where the IAP remains elastic. The curve will be drawn based on the numerical results for the reference structure with a DAP elastic-perfectly plastic and an IAP elastic. Indeed, these are equivalent to the results that would have been obtained through the application of the analytical model to the reference structure. The second order rigid plastic curve established through the calculation of the λ from the formula VI.5 is drawn in yellow in figure VI.7.

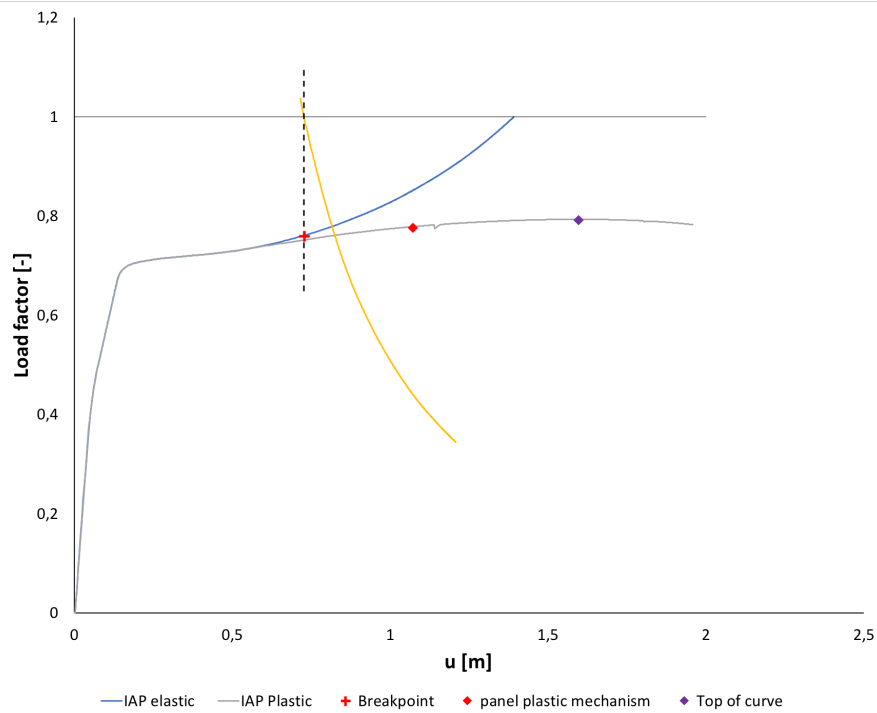


Figure VI.7: Identified breakpoint (4 spans structure)

Since the yellow and the blue curves are drawn on the basis of the same data, for a given u , the identified points on the two curves correspond to the same state of the structure under investigation (same internal forces, same deformations, etc.). Moreover, when the λ is equal to 1 on the yellow curve, it means theoretically that the plastic mechanism is developed. Therefore, by drawing the vertical black dashed line that intersects the yellow curve on the point where λ is equal to 1, it is possible to determine a point on the blue ($u;\lambda$) curve. The identified point called the breakpoint characterizes theoretically the point of formation of the panel plastic mechanism determined on the basis of displacements and internal forces for the structure with an IAP elastic.

It is thus now possible to determine analytically a breakpoint for which the collapse of the structure is assumed to be reached. It is thus where the calculations will be stopped (where the blue curve will be stopped). It has to be noted that the corresponding internal forces and the displacements are those associated with an IAP remaining elastic. The ones occurring at the real formation of the plastic mechanism (red dot) and at the real collapse of the structure (purple dot) are obviously different. But, the N_{lost} estimated at the breakpoint will be compared to the ones at the real formation of the plastic mechanism (red dot) and at the real reaching of the collapse of the structure (purple dot) in order to quantify the accuracy of the estimated failure point. The displacements u at each of the latter points will be also compared.

The N_{lost+} is equal to 991,3 kN, the $N_{lost\blacklozenge}$ is equal to 1014,2 kN and the $N_{lost\blacklozenge}$ is equal to 1033,5 kN. Thus, the difference between the breakpoint (+) and the red dot (◆) is about 2,3%. The difference between the breakpoint (+) and the top of the curve (◆) is about 4%. It is thus concluded that those differences are rather small and that the breakpoint is a good estimation of the collapse of the structure in terms of N_{lost} . Moreover, it is even on the safe side.

On the contrary, in terms of deformations, the differences are significant as shown in figure VI.7. The deformations are underestimated. It is thus not on the safe side. Further investigations are thus needed to better evaluate these deformations, i.e. the real u . It is a point addressed in the perspectives.

Breakpoint for the loss of the central column in the 6 and 8 spans structures:

Now, the task is to apply the same approach on the other structures to check if the observations remain similar. This will first be analysed for the loss of the central column of the 6 spans structure on the basis of the figure VI.8. Secondly, it will be investigated for the case of the loss of the central column of the 8 spans structure on the basis of figure VI.9.

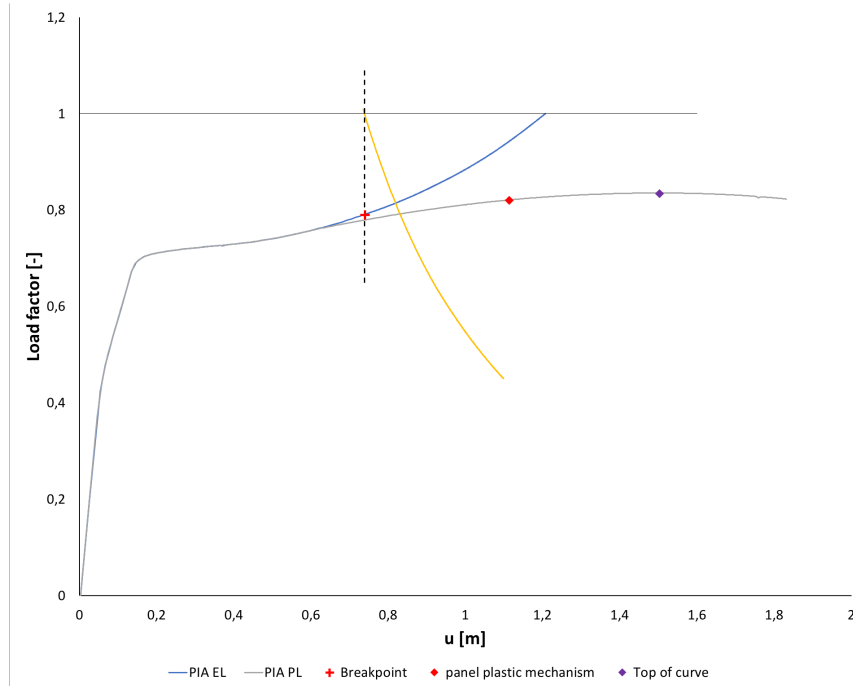


Figure VI.8: Identified breakpoint (6 spans structure)

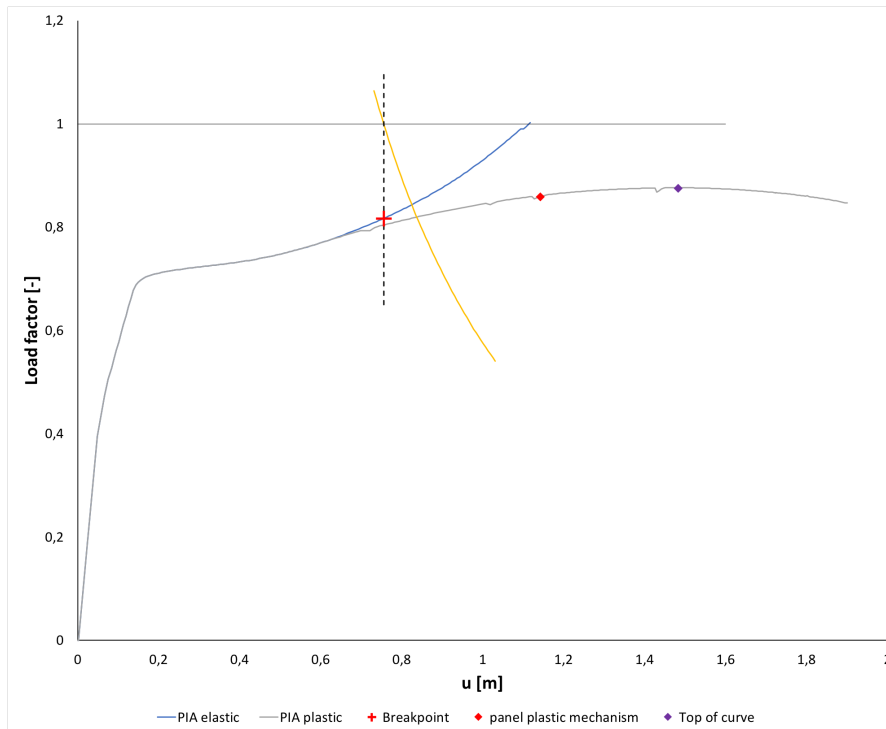


Figure VI.9: Identified breakpoint (8 spans structure)

The errors are summarised in table VI.2 for the three structures. Thus, by increasing the number of spans, the errors made on the estimation of the N_{lost} increase and thus become less and less negligible.

	4 spans	6 spans	8 spans
N_{lost}^{\blacklozenge} [kN]	991,3	1042,6	1075,8
$N_{lost}^{\blacktriangle}$ [kN]	1014,2	1082,1	1131,7
N_{lost}^{\blacklozenge} [kN]	1033,5	1101,2	1153,7
$\neq_{N_{lost}}^{\blacklozenge, \blacktriangle}$ [%]	2,3	3,7	4,9
$\neq_{N_{lost}}^{\blacklozenge, \blacklozenge}$ [%]	4	5,3	6,8

Table VI.2: Errors made on N_{lost}

The increase of the number of storeys should have also the same effect, i.e. increasing the difference between the estimated N_{lost} on the breakpoint and the one corresponding to the top of the curve. It should be investigated. It is a point addressed in the perspectives.

In terms of deformations (u), the differences observed for each of the three structures are almost the same. That is to say the differences between the u of the breakpoint and the u of the panel plastic mechanism (red dot) and the top of the curve (purple dot) are almost the same for the three structures. These errors made on the u are not negligible at all.

Thus, the errors made on the N_{lost} seem to be a function of the number of hinges developed to form the panel plastic mechanism. It would be interesting to check the case of the loss of an intermediate column

Breakpoint for the loss of an intermediate column:

In the situation shown in figure VI.10, the N_{lost+} is equal to 986,3 kN, the $N_{lost\blacklozenge}$ is equal to 1002,1 kN and the $N_{lost\blacklozenge}$ is equal to 1005 kN. Thus, the difference between the breakpoint (+) and the red dot (◆) is about 1,6%. The difference between the breakpoint (+) and the top of the curve (◆) is about 1,9%. The u is still significantly underestimated but the differences are smaller for the present case than for the ones investigated previously.

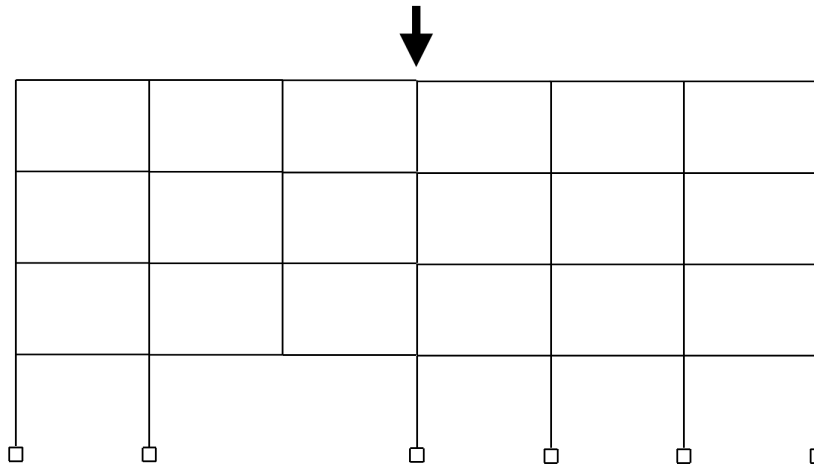
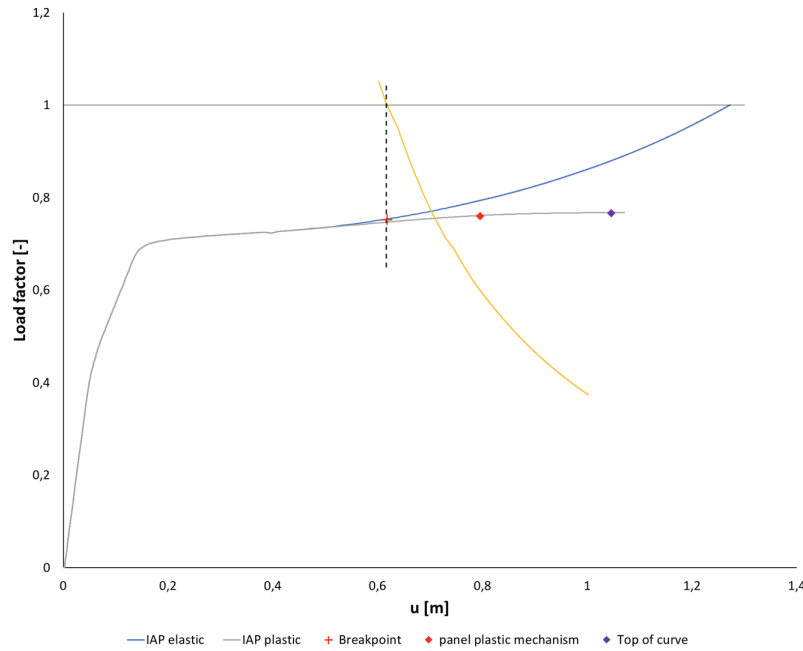


Figure VI.10: Identified breakpoint (6 spans structure)

In this situation, the number of hinges needed to form the panel plastic mechanism is equal to 4. In the situation of the loss of the central column in the 4 spans structure, the number of hinges needed to form the panel plastic mechanisms at the left and at the right of the lost column is equal to 8. For the loss of the central column in the 6 spans structure, the number of hinges needed to form the panel plastic mechanisms is equal to 12. Finally, for the loss of the central column in the 8 spans structure, the number of hinges needed to form the panel plastic mechanisms is equal to 16.

Knowing the errors made of the N_{lost} by considering the breakpoint as the collapse of the structure, it may thus be concluded that the latter depend in a certain manner on the number of hinges developed.

Conclusion:

In this section, it was demonstrated that it is now possible to determine with a fairly good accuracy the collapse of the structure on the basis of the results of the complete analytical procedure for most of the investigated scenarios.

However, it was highlighted that the approach still has several weaknesses. Indeed, the errors made on the value of N_{lost} by considering the breakpoint as the collapse of the structure are increasing with the number of hinges needed to form the panel plastic mechanism. But, in the previously investigated situations, the values of those errors remained rather acceptable. It was also said that the N_{lost} of the breakpoint remains on the safe side.

Moreover, another weakness is the significant underestimation of the displacement u .

Further investigations are thus needed to make the analytical predictions more accurate in terms of the displacement u . Making it more accurate in terms of the N_{lost} is questionable. It should be investigated for more structures and especially robust structures, i.e. which are capable to withstand the complete loss of a column.

The loss of an exterior column was not investigated because the analytical approach previously presented does not fit such a situation. It is a point addressed in the perspectives.

Similarly, in the case of the loss of an intermediate column when there is only one remaining column at one of the two sides of the IAP (such as the loss of the intermediate column in the reference structure), the developed approach does not fit such a situation either. It is a point addressed in the perspectives. In fact, the complete analytical model does not integrate the calculation of node mechanisms appearing at the left side of the DAP. Indeed, as was shown in figure IV.37, when the IAP is elastic-perfectly plastic, the hinges develop in the columns of the left IAP. The complete analytical model calculates only the beam plastic mechanism in the DAP through formation of hinges in beams of the DAP only. Thus, further improvement of the model is needed. This is also a point addressed in the perspectives.

VI.4 Method to predict the different failure modes on the basis of the available analytical model results

In the present section, methods will be given to perform the needed verifications of elements in the structure knowing a series of identified failure modes detailed in the previous chapters.

First, it was recommended that all the cross-sections of the elements where hinges are developing have to be class 1 (the reasons were previously detailed).

The buckling of the upper beams of the DAP needs to be checked. The complete analytical model returns the values of internal forces in each beams of the DAP. The compression forces in the upper beams of the DAP is thus known for each value of N_{lost} (called P in the complete analytical model). The verification of the buckling of the upper beams of the DAP is thus possible on the basis of the latter forces. In the case of the loss of an exterior column, the buckling of the bottom beam of the DAP needs to be checked.

Similarly, the resistance in tension of the bottom beams of the DAP and their joints needs to be verified because significant tensile forces are acting in these latter and they may break after excessive yielding induced by the tension. The internal tensile forces in the bottom beams of the DAP are returned by the complete analytical model. The latter verifications may thus be performed. In the case of the loss of an exterior column, the resistance of the upper beam of the DAP and of its joints needs to be checked under the given tensile forces.

Finally, as explained in the previous chapters, the buckling of the beside columns of the IAP needs to be checked. As it was demonstrated that the increase of their compression is mainly due to the full redistribution of the N_{lost} , it is thus possible to determine the compression forces in the latter beside columns. Indeed, the normal forces at the end of Phase 1 in the beside columns may be easily determined by implementing the frame in a linear elastic computation software such as Ossa2D and by applying the considered loading combination of actions. It is quick and easy to apply. Then, the goal is to know the values of N in the beside columns at the moment of collapse of the structure. In the previous section, it was explained that a N_{lost} estimating with a rather good accuracy the N_{lost} that would have occurred at the real collapse of the structure may be analytically determined. Thus, based on the previously analytically determined value of N_{lost} , the values of N in the beside columns at the moment of the estimated collapsed of the structure are known. Indeed, it was explained that the N in one beside column at the collapse of the structure may be obtained by adding the N at the end of Phase 1 to the $\frac{N_{lost}}{2}$ at the collapse of the structure.

However, it was explained that the values of N in the beside columns differ slightly from a true linear evolution shown by the determined "N lin" curves. Indeed, it was highlighted that considering that the evolution of N in the beside columns during Phases 2 and 3 is only due to the redistribution of N_{lost} is not always on the safe side. Indeed, the N from the "N lin" curves were most of the time slightly underestimating the true values of N in the beside columns. To have a perfect estimation of the N in the beside columns, it was said that a coefficient of amplification may be added to the redistributed N_{lost} . But, such a coefficient needs to be well calibrated by performing a significant amount of simulations. Not enough simulations were performed on this work to be able to determine such a coefficient.

Thus, on the basis of the previously determined values of N in the beside columns, it is possible to verify their stability.

The practitioner has thus everything in his hands to make robustness checks for the kind of frames within the loss column scenarios under consideration and investigated in the present work.

VI.5 Conclusion

In the present chapter, through section VI.2, an approach was first determined to evaluate the formation of panel plastic mechanisms in the structures within "loss of a column" scenarios. It was shown that the used formula was able to predict with a good accuracy the development of the mechanism.

Through section VI.3, a method allowing to combine the previously determined approach with the complete analytical model was determined to evaluate analytically the point of collapse of the structure. It shown that the N_{lost} corresponding to the analytically determined point was predicted with a fairly good accuracy. Moreover, the errors made on the value of N_{lost} increases with an increase in the number of hinges needed to attain the complete development of the plastic mechanism. These errors were established on the basis of the predicted values of N_{lost} in comparison with the values of N_{lost} corresponding to the real formation of the plastic mechanism (for an IAP elastic-perfectly plastic) and finally with the values of N_{lost} corresponding to the real collapse of the structure. Moreover, the investigations shown that the predicted values of u were significantly underestimated.

This approach still presents several weaknesses. It should first be seen if there is a way to improve the accuracy of the predicted N_{lost} (which is actually fairly good). Seen the u is significantly underestimated, research are needed to determine the latter more accurately.

Moreover, the complete analytical model is not yet able to predict the failure of the structure in the case of the loss of an intermediate column when only one column remains in one of the two sides of the IAP as the situation shown on figure V.15.

The analytical model is neither able to predict the behaviour of a frame that loses an exterior column. Indeed, the model works for hinges developing in the beams of the DAP when forming the plastic mechanism in the DAP. It was seen that in the case of the loss of an exterior column, the hinges develop as well in the columns of the DAP. Thus, the model needs to be improved to integrate such a situation.

Since the two latter situations are not well treated by the complete analytical model, the developed approach in the present chapter is not applicable to them for the moment.

However, the developed approach gives a first opportunity to practitioners to integrate robustness checks when designing a structure. Through section VI.4, it was explained how to predict the different identified failure modes on the basis of the approach results. In other words, it was presented how to apply the verification recommendations prescribed in the previous chapters.

Chapter VII

General conclusions and perspectives

VII.1 Conclusions

Past research at the University of Liège led to the development of a complete analytical procedure allowing the prediction of the behaviour of 2D frames within "loss of a column" scenarios. In particular, this model is made for reflecting the global response of frames losing a column with a directly affected part that may yield and an indirectly affected part remaining infinitely elastic. The developed approach consequently does not consider the potential yielding of the indirectly affected part and more particularly its influence on the global response of the frame. Knowing the indirectly affected part remains elastic, it was explained that the lateral restraint of the latter remains constant during the whole progressive loss of a column (the lateral restraint being characterized by the stiffness of the indirectly affected part). Thus, the obtained deformations of the structure being predicted analytically are underestimated in comparison to the situation where the indirectly affected part loses progressively its stiffness through its progressive yielding.

This is context in which the **first goal** of the present work is situated. The latter consisted of analysing the effect of the progressive yielding of the indirectly affected part on the global response of a 2D steel frame losing one column. More particularly, the study was aiming to evaluate how far the analytical predicted behaviour is from the realistic behaviour of a frame losing a column reflected by an indirectly affected part that may progressively yield. This was achieved by following several steps:

- The locations and the order of formation of plastic hinges in the indirectly affected part were firstly determined. This was done to qualify the effect of the yielding of the indirectly affected part generally (e.g. through the identification of the formation of a plastic mechanism in the indirectly affected part). Then, the values of N_{lost} corresponding to the first signs of yielding (first hinges) were compared to the values of the N_{lost} corresponding to the collapse of the structure. It was done to quantify the effect of the yielding of the indirectly affected part. More particularly, the goal pursued was to determine if the formation of first hinges led to a chain formation of hinges in the indirectly affected part inducing the collapse of the structure, which was rapidly attained;
- The influence of the yielding of the indirectly affected part on the redistribution of loads in the structure during the loss of a column was investigated. The goal was to identify which elements experience changes in their internal forces during the loss of the column in order to establish a series of verification recommendations to be performed to assess robustness checks. It was achieved by identifying a series of failure modes in the context where the indirectly affected may yield.

The latter steps were done first for the reference structure within three considered "loss of a column" scenarios. The loss of a central column, the loss of an intermediate column and the loss of an exterior column. Then, the effect of an increase in the number of spans was determined on the previously described global responses. This was studied firstly for an increase from 4 to 6 spans and secondly from 4 to 8 spans.

The conclusions of the **first goal** of the work are the following:

- Globally, it shown that the formation of first hinges in the indirectly affected part led to a chain formation of hinges where the collapse of the structure was rapidly attained through the formation of plastic mechanism. It was highlighted that the collapse of the structure attained after the formation of first hinges in the indirectly affected part is delayed when the number of hinges needed to form the mechanism increases (e.g. through an increase in the number of spans). Indeed, the differences between the N_{lost} inducing the first hinges and the one corresponding to

the collapse of the structure increase with an increase in the number of hinges needed to form the mechanism in the indirectly affected part;

- It was shown that the yielding of the indirectly affected part limits significantly the development of the catenary actions during Phase 3 in comparison to the situation where the indirectly affected part remains elastic;
- The analysis of the redistribution in the structure of the loads previously supported by the lost column showed that the latter were entirely redistributed in the beside columns (i.e. the N_{lost} is entirely redistributed in the beside columns);
- The influence of an arch effect delaying the collapse of the structure after the attaining of the complete formation of the plastic mechanism in the indirectly affected part was highlighted. The latter effect remains the same when the number of spans is increased;
- The study revealed a series of identified failure modes remaining similar in each investigated structure. It leads to a series of verification recommendations. For every location of the lost column except for the exterior one:
 - The buckling of the upper beams in the DAP needs to be checked;
 - The resistance in tension of the bottom beams and of their joints needs to be checked;
 - The buckling of the beside columns in the IAP needs to be checked;
 - In each cross-section presenting a hinge, the cross-section is recommended to be class 1;
 - In the case where the joints are partially resistant, the latter have to be designed to have sufficient rotation capacity and sufficient resistance.

When an exterior column is the column that is lost, the checks differ only on the two following points:

- The upper beam in the DAP and its joints need to be checked under the given tensile forces (indeed they may break under an excessive tension);
- The buckling of the bottom beam in the DAP needs to be checked under the given compression forces.

The **second goal** of the present work was to determine analytically the moment of collapse of the structure and the associated state of the latter (i.e. the internal forces and the deformations). Indeed, on the basis of the values of internal forces and displacements in the structure that would be analytically determined, it would then be possible to achieve the verification recommendations. The purpose is to give practitioners a tool to integrate robustness checks in the design of a structure. This was achieved by following several steps:

- First, the task consisted of the development of a method allowing the analytical determination of the plastic mechanism formation in the IAP;
- Then, the aim was to combine the latter method with the complete analytical procedure able to determine the $(u;\lambda)$ curve in order to identify a breakpoint on the latter predicting the true collapse of the structure. The task was then to determine if the latter breakpoint was predicting with enough accuracy the true collapse of the structure. It was achieved by comparing the predicted value of N_{lost} with the one corresponding to the collapse of the structure. The displacement u was also compared;
- Finally, on the basis of the analytical predicted results, methods were given to establish the verification recommendations.

The conclusions of the **second goal** of the work are the following:

- It was shown that the formula used to predict the formation of the mechanism in the IAP was able to do so with a good accuracy on the three investigated structures within the "loss of a central column" scenario, see table VI.1 in section VI.2 page 95;
- A breakpoint was determined on the $(u;\lambda)$ curve analytically determined. The latter breakpoint revealed a fairly good estimation of the N_{lost} corresponding to the collapse of the structure, see table VI.2 in section VI.3 page 100. It revealed that the accuracy of the predicted N_{lost} was less and less good when the number of hinges needed to develop the plastic mechanism increases. Moreover, it revealed that the predicted value of u associated with the breakpoint was significantly underestimated. The approach presented several weaknesses that are addressed to be improved and this is set out in the perspectives;
- Finally, general methods were given to establish the verification recommendations on the basis of the actual analytical model results, see section VI.4.

In conclusion, the analysis of the influence of the indirectly affected part yielding on the global response of 2D steel frames within "loss of a column" scenarios allowed an approach to be developed aiming to predict analytically the collapse of latter structures. Thus, the developed approach gives a first opportunity to practitioners to integrate full robustness checks within the design of a structure.

VII.2 Perspectives

Within the sections related to the identified failure modes of structures, it was highlighted that no method is evaluating properly the true rotation capacity of a cross-section submitted to M and N. Indeed, existing methods are evaluating the rotation capacity for cross-section where the dominant internal force is the bending moment (Gioncu [21]). In robustness considerations, and especially during Phase 3, it was shown that there were not only bending moments in the bottom beams of the DAP but also significant tensile forces. Thus, the development of a method predicting the rotation capacity of a cross-section submitted to M and N could be the subject of further research.

Within the analysis of the redistribution of the loads previously supported by the lost column, it was shown that the values of N in the beside columns differ up to 9% from the values of N that would have been obtained if the increase of normal forces in the beside columns was only due to the redistribution of N_{lost} . The values of N in the beside columns are not analytically determined but rather estimated based on the analytical results obtained in the DAP. Indeed, for sake of simplicity, it was assumed that the N in the beside columns may be obtained by redistributing manually the N_{lost} in each of the two beside columns. But, it was shown that this latter choice would lead to an underestimation of the compression in the beside columns up to 9%. This choice is thus not on the safe side. The idea would be to determine a coefficient which would be added to the redistributed N_{lost} in the beside columns allowing a safe estimation of the compression in the beside columns. Not enough simulations were performed in the present work to determine such a coefficient. It could then be determined in further research.

The complete analytical procedure presented in Chapter I does not take into account the formation of node mechanisms as the ones occurring in the situation presented in figure IV.37 in section IV.3.2.1 page 64. Indeed, the model only takes into account the formation of hinges in the beams of the DAP. The analytical procedure is neither able to calculate the plastic mechanism occurring in the DAP in the case of the loss of an exterior column. Indeed, the hinges are developing also in the columns of the DAP as shown in figure IV.46 in section IV.4.2 page 70. As a consequence, the developed approach in Chapter VI is not able to predict the estimated point of collapse of the structure for the latter two situations.

As presented, the approach exposed in Chapter VI allowing a point estimating the true collapse of the structure to be analytically determined has shown several weaknesses. Indeed, the values of the displacements of the top of the lost column u are significantly underestimated. Moreover, the more hinges needed to form the plastic mechanism in the indirectly affected part, the higher the errors made on the values of N_{lost} associated with the predicted breakpoint. Thus, the actual method needs further investigation mainly to estimate more accurately the u and also the N_{lost} . Moreover, the accuracy of the determined breakpoint was only investigated in the case of an increase in the number of spans. It would be interesting to see how it is influenced by an increase in the number of storeys and if the previous conclusions remain similar.

The influence of an arch effect allowing the increase of N_{lost} after the full development of the plastic mechanism was explained in the present work. It was shown that the latter remained almost the same in the three investigated structures (i.e. the structures with 4, 6 and 8 spans). Thus, it was concluded that an increase in the number of spans does not influence the arch effect. It would then be interesting to see how the increase in the number of storeys influences the latter effect.

The present work took place within the analysis of the behaviour of 2D steel frames losing a column. In further research, the effect of the yielding of the indirectly affected part on the behaviour of a 3D

structure losing a column should be analysed. Indeed, the 3D effects such as the presence of two-way concrete slabs or the presence of frames in the plane perpendicular to the plane considered for the treated 2D structures should be investigated. The identified failure modes could indeed be different.

Annex A

List of loads

All the loads used for the design will be listed in the following in order to highlight clearly the sources of the latter.

The **permanent loads** (G_k) include the weight of the concrete slab of 25 cm of thickness and considering the characteristic unit weight of concrete which is 25 kN/m^3 and a topping layer of $1,5 \text{ kN/m}^2$. The resultant permanent load is acting both on the roof and on other storeys. Then, the permanent load is:

$$G_k = 6 * (0,25 * 25 + 1,5) = 46,5 \text{ kN/m}$$

The self-weight of the steel elements is taken equal to 7850 kg/m^3 .

The **live load** for offices, i.e. buildings of category B (Table 6.1 page 21 from EN 1991-1-1 [16]), is found equal to 3 kN/m^2 in the Table 6.2 page 22 of EN 1991-1-1 [16]. The live load for the roof is defined as the load in accordance with a roof of category H (Roofs not accessible except for normal maintenance and repair) and is found equal to 1 kN/m^2 (Table 6.10 page 29 of EN 1991-1-1 [16]). The most unfavourable values of actions were chosen both for the roof and the floors.

The live load for the roof $Q_{k,roof}$ is:

$$Q_{k,roof} = 1 * 6 = 6 \text{ kN/m}$$

The live load applied at each floor $Q_{k,floor}$ is:

$$Q_{k,floor} = 3 * 6 = 18 \text{ kN/m}$$

where the 6 represents the spacing between the frames.

The **snow load** acting on the roof should be determined according to the formula (5.1) in the EN1991-1-3 page 18 [23] in the case of persistent/transient design situations:

$$S = \mu_i C_e C_t S_k$$

where $\mu_i = 0,8$ is the snow load shape coefficient taken for roofs with a slope equal to zero ($0^\circ \leq \alpha \leq 30^\circ$), C_e is the exposure coefficient, C_t is the thermal coefficient ($C_e = C_t = 1$ in Belgium) and S_k is the characteristic value of the snow on the ground. The value of S_k depends on the altitude of the location. For a building in Brussels (altitude of 13 meters above sea level) or in Liège (66 meters above sea level), the characteristic value of the snow is equal to $0,5 \text{ kN/m}^2$ for values of altitudes

lower than 100 meters above sea level.

The snow load acting on the roof is then:

$$S = 0,5 * 0,8 = 0,4kN/m^2$$

Then, as a lineic load:

$$S = 0,4 * 6 = 2,4kN/m$$

Internal and external **wind pressures** on surfaces at respective heights z_i and z_e are given by the following expressions:

$$w_i = q_p(z_i)c_{pi}$$

$$w_e = q_p(z_e)c_{pe}$$

Where c_{pi} and c_{pe} are the internal and external pressure coefficients and $q_p(z)$ is the peak velocity pressure at height z .

$$q_p(z) = C_e(z)q_b$$

$C_e(z)$ is the exposure pressure factor and is taken equal to 1,4 (In the case of terrain of class IV (table 4.1 in EN 1991-1-4) and see figure 4.2 in EN 1991-1-4 [24] for the value of $C_e(z)$). q_b is the basic velocity pressure:

$$q_b = \frac{1}{2}\rho v_b^2$$

Where the recommended value for ρ is $1,25kg/m^3$ and v_b is the basic wind velocity.

$$v_b = c_{dir}c_{season}v_{b,0}$$

The recommended values for c_{dir} and c_{season} is 1. $v_{b,0}$ is the fundamental value of the basic wind velocity and is found equal to $25m/s$ for Brussels area. Thus,

$$v_b = 25m/s$$

$$q_b = \frac{1}{2}\rho v_b^2 = \frac{1}{2} * 1,25 * 25^2 = 0,39kN/m^2$$

$$q_p(z) = C_e(z)q_b = 1,4 * 0,39 = 0,546kN/m^2$$

where z is the height above the terrain and is taken equal 14 meters which is the height of the reference frame. For the corresponding $z=14$ m, the value of $C_e(14) = 1,4$ is found on figure 4.2 in EN 1991-1-4 [24].

And, considering the spacing between the frames is equal to 6 meters, $q_p(14) = 6 * 0,546 = 3,281kN/m$.

It is now possible to calculate the value of $w_i = q_p(z_i)c_{pi}$ and $w_e = q_p(z_e)c_{pe}$. The external pressure coefficient c_{pe} is given in table 7.1 of EN 1991-1-4 and calculated based on the recommendations prescribed in the section 7.2.2 of EN 1991-1-4 [24]. For the wall on the left of figure 1 $c_{pe} = 0,744$

and for the wall on the right of $1 c_{pe} = 0,389$ (obtained through a linear interpolation of the values gathered in Table 7.1). The c_{pi} is taken equal to 0 in the situation where the area of openings of one side is bigger than 30% of the total area of that side (this has to be the case for 2 sides), see section 7.2.9 (2) in EN 1991-1-4 [24]. For office buildings, in the present case, c_{pi} is thus taken equal to 0.

Finally, the total wind pressure on the walls is calculated as follows:

$$w = (c_{pe} + c_{pi})q_p(14)$$

The characteristic values of w for the left and right walls are given on the figure 1. For the considered height of 14 meters, the pressure of the wind is uniformly distributed. For a bigger value of the height of the structure, the distribution may change, see figure 7.4 in EN 1991-1-4 [24].

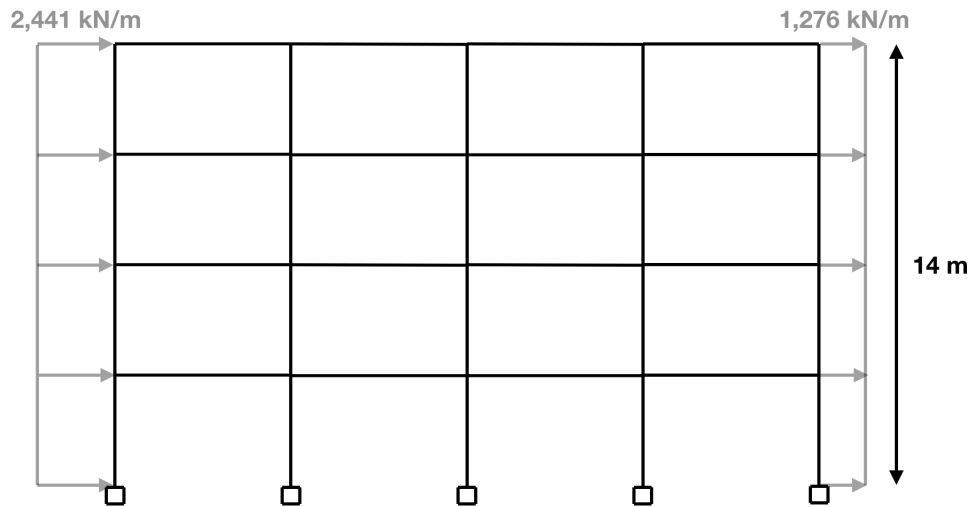


Figure 1: Wind actions

The structural imperfection is given as:

$$\phi = \alpha_h \alpha_m \phi_o$$

according to EN 1993-1-1.

- $\alpha_m = \sqrt{0,5(1 + \frac{1}{m})} \leq 1$
 $\alpha_m = 0,775 \leq 1$

where m is the number of columns per storey and is equal to 5 in our case.

- $\alpha_h = \frac{2}{\sqrt{h}}$ but $\frac{2}{3} \leq \alpha_h \leq 1$ and $h = 14m$ the height of the structure
 $\alpha_h = 0,53 \leq \frac{2}{3}$, thus $\alpha_h = \frac{2}{3}$
- $\phi_o = \frac{1}{200}$

Thus,

$$\phi = 0,775 * \frac{2}{3} * \frac{1}{200} = 2,583 * 10^{-3}$$

The consideration of the latter structural imperfection is achieved by introducing equivalent horizontal loads at each floor of the structure by multiplying ϕ by the vertical loads as it is illustrated on figure 2.

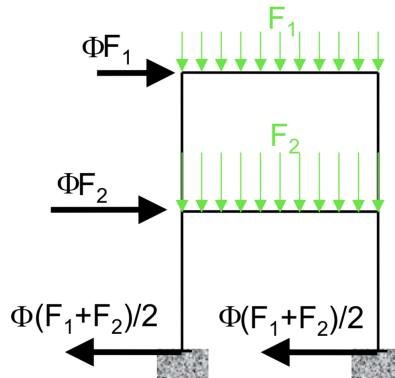


Figure 2: Equivalent horizontal loads [25]

Verification of the structure

A set of combinations are made based on the SLS and ULS combination of actions formula explicitly presented as the equation II.1 and the equation II.2 in section II.2 page 25. These latter combination are then implemented on OSSA2D (elastic linear software for 2D structures developed at the University of Liège [19]).

The verifications of the structure were made starting from the following choices:

- Rigid beam to column joints and fully resistant;
- Perfectly embedded columns in the ground;
- No out-of-plane instability;
- Elements' buckling occurs around their strong axis in the plane.

The initial design of the structure is given on figure 3 and it is the latter that will be verified in the following of the present section.

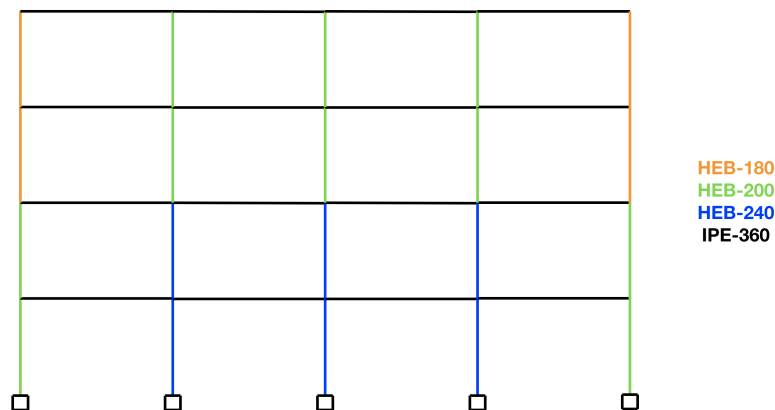


Figure 3: Design of the 2D reference frame

SLS

- Maximum transverse displacement for one storey (visual comfort) is equal to $4mm < \frac{3500}{250} = 14mm \rightarrow$ **OK**;
- Maximum transverse displacement for the entire structure is equal to $15mm < \frac{14000}{500} = 28mm \rightarrow$ **OK**;
- Maximum deflection for floor beams (visual comfort) is equal to $19mm < \frac{6000}{300} = 20mm \rightarrow$ **OK**;
- Maximum deflection for roof beams (visual comfort) is equal to $21mm > \frac{6000}{300} = 20mm \rightarrow$ **NOT OK**. But the deflection of $21mm$ is accepted.

The structure is thus verified under SLS.

ULS

1. Classification of the structure:

The classification of the structure is done through the evaluation of the ratio of the critical instability linear elastic load F_{cr} of the structure corresponding to the first lateral instability mode (see figure 4) to the total vertical design load F_{ED} acting on the structure [26]. Thus,

$$\alpha_{cr} = \frac{F_{cr}}{F_{Ed}}$$

All the α_{cr} for each combination of actions are given by the software OSSA2D. The results given by OSSA2D were compared by the results given by analytical expressions in [26] and it reveals that the results from OSSA2D are accurate enough, see page 86 of [26].

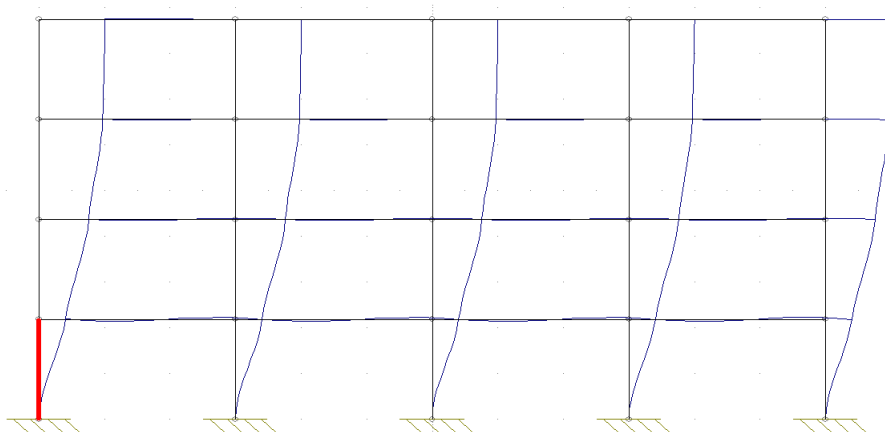


Figure 4: First lateral instability mode of the structure for a considered combination

The results from OSSA2D reveal values of α_{cr} smaller than 10 meaning that the structure is classified as a sway structure. It is true for all the considered combinations. In case of a sway structure, the second order effects $P - \Delta$ have to be included into the global process of analysis and design of the structure [26]. The method applied is to perform a second order analysis including the effects $P - \Delta$ and to verify the stability of the columns based on a buckling length established for the non sway mode of the structure, i.e. for nodes (for instance the extremities of the columns) that do not move horizontally. OSSA2D first calculates the structure by applying a first order elastic analysis. Then, the software allows to make a second order correction. Thus, in the case of α_{cr} smaller than 10, a

second order correction is made through OSSA2D. All the following internal forces as the internal moments, the internal normal forces and the internal shear forces will be given taking into account the second order correction.

2. Verification of the resistance and stability of beams:

The type of the beams is IPE-360 with steel S355 ($f_{yk} = f_{yd} = 355\text{Mpa}$), a Young Modulus $E = 205000\text{ Mpa}$ and the length of the beams is 6 meters. All the geometrical characteristics will not be recalled here, the reader is invited to go into catalogues.

The verifications of the beams were made based on the most critical situation concerning the internal efforts.

$$M_{Ed} = 332\text{ kNm}$$

$$N_{Ed} = -20\text{ kN}$$

$$V_{Ed} = 303\text{ kN}$$

- Classification of the cross-section:

In pure bending: Class 1

In pure compression: Class 4

Considering there is bending combined with compression, the class of the cross section has to be calculated under combined bending and compression.

$$x = \frac{N_{Ed}}{t_w f_y} = 7\text{ mm}$$

$$\alpha = \frac{\frac{d}{2} + x}{d} = 0,512$$

When $\alpha > 0,5$: Class 1 if and only if $\frac{d}{t_w} \leq \frac{396\epsilon}{13\alpha - 1}$

$$\text{where } \frac{d}{t_w} = \frac{298,6}{8} = 37,325$$

$$\text{and } \frac{396\epsilon}{13\alpha - 1} = \frac{396\sqrt{\frac{235}{355}}}{13\alpha - 1} = 57$$

Thus $37,325 < 57$ and the cross section is Class 1 in combined bending and compression.

- Resistance to shear:

$$V_{pl,Rd} = \frac{A_v f_y}{\sqrt{3}} = 719,41\text{ kN} > V_{Ed} = 303\text{ kN}$$

$$V_{Ed} = 303 < 0,5V_{pl,Rd} = 359,71\text{ kN} \text{ and } \frac{d}{t_w} = 37,325 < \frac{72\epsilon}{\eta} = \frac{72 * 0,814}{1,2} = 48,84$$

Thus, the impact of the shear stress on the bending resistance is negligible.

- Resistance of cross sections at the extremities of the beams:

$$N_{pl,Rd} = A f_y = 2580,85 \text{ kN}$$

$$N_{Ed} = 20 \text{ kN} < 0,25 * 2580,85 = 645,213 \text{ kN} \text{ and } N_{Ed} = 20 \text{ kN} < 0,5 \frac{h_w t_w f_y}{\gamma_{Mo}} = 424,012 \text{ kN}$$

So it is not necessary to take the influence of the normal load on the bending resistance.

$$M_{pl,Rd,y} = w_{pl,y,Rd} f_{yd} = 361,745 \text{ kNm}$$

$$\text{Then, } M_{Ed} = 332 \text{ kNm} < M_{pl,Rd,y}$$

Thus, the resistance of cross sections at the extremities of the beams is assured.

- Resistance to instabilities:

Only the buckling around the strong axis (in the plane) is considered as mentioned earlier.

For elements under compression and bending, the following expression has to be verified:

$$\frac{N_{Ed}}{\chi_y N_{pl,Rd}} + \mu_y \frac{1}{(1 - \frac{N_{Ed}}{N_{cr,y}})} \frac{c_{my} M_{y,Ed}}{c_{yy} M_{pl,y,Rd}} \leq 1$$

The beam under verification is the central beam illustrated on figure 5. It is necessary to evaluate the buckling length of the beam in the non sway mode, i.e. the nodes do not move horizontally (as already mentioned and explained earlier).

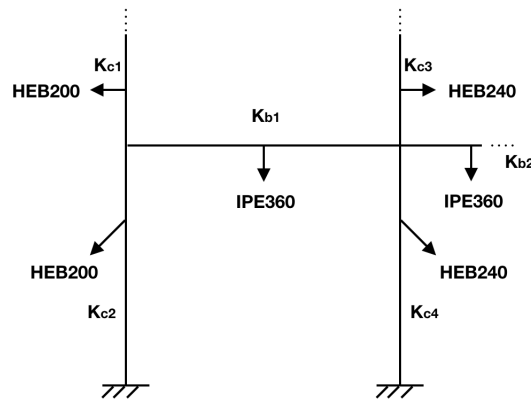


Figure 5: Evaluation of the buckling length of the beam

$$L_{buckling,y} = L_{beam} \left[\frac{1+0,145(k_1+k_2)-0,265k_1k_2}{2-0,364(k_1+k_2)-0,247k_1k_2} \right]$$

$$k_1 = \frac{K_{b1}+K_{c1}+K_{c2}}{K_{b1}+K_{c1}+K_{c2}} = 1$$

$$k_2 = \frac{K_{b1}+K_{b2}+K_{c3}+K_{c4}}{K_{b1}+K_{b2}+K_{c3}+K_{c4}} = 1$$

$$L_{buckling,y} = L_{beam} \left[\frac{1+0,145(k_1+k_2)-0,265k_1k_2}{2-0,364(k_1+k_2)-0,247k_1k_2} \right] = L_{beam} * 1 = 6 \text{ m}$$

$$N_{cr,y} = \frac{\pi^2 EI}{L_{buckling,y}^2} = 9144,1 \text{ kN}$$

$$\chi_y = \frac{1}{\phi + \sqrt{\phi^2 - \bar{\lambda}^2}}$$

$$\bar{\lambda} = \sqrt{\frac{N_{pl,Rd}}{N_{cr,y}}} = 0,531$$

$$\phi = 0,5(1 + \alpha(\bar{\lambda} - 0,2) + \bar{\lambda}^2)$$

For hot rolled profile with $\frac{h}{b} = 2,12 > 1,2$, $t_f = 12,7 < 40mm$ and axis y-y (strong axis), the chosen European buckling curve is the curve "a" and the coefficient α is equal to 0,21. Thus,

$$\phi = 0,5(1 + \alpha(\bar{\lambda} - 0,2) + \bar{\lambda}^2) = 0,676$$

$$\chi_y = \frac{1}{\phi + \sqrt{\phi^2 - \bar{\lambda}^2}} = 0,914$$

$$\mu_y = \frac{(1 - \frac{N_{Ed}}{N_{cr,y}})}{(1 - \chi_y \frac{N_{Ed}}{N_{cr,y}})} = 0,999$$

$$C_{my} = 1 + \left(\frac{\pi^2 EI_y |\delta_{max}|}{|M_{Ed,y}| L^2} - 1 \right) \frac{N_{Ed}}{N_{cr,y}} = 0,999$$

$$w_y = \frac{w_{pl,y}}{w_{el,y}} = 1,127$$

$$C_{yy} = 1 + (w_y - 1) \left[2 - \frac{1,6}{w_y} C_{my}^2 (\bar{\lambda} + \bar{\lambda}^2) \right] \frac{N_{Ed}}{N_{pl,Rd}} \geq \frac{1}{w_y}$$

Thus,

$$C_{yy} = 1$$

Finally,

$$\frac{N_{Ed}}{\chi_y N_{pl,Rd}} + \mu_y \frac{1}{(1 - \frac{N_{Ed}}{N_{cr,y}})} \frac{C_{my} M_{y,Ed}}{C_{yy} M_{pl,y,Rd}} \leq 1$$

gives

$$0,927 < 1$$

The resistance and the stability of the beam are thus verified. The exact same method was applied for the beams for every combination.

3. Verification of the resistance and stability of columns:

The exact same philosophy was followed to verify all the columns in the structure based on the method followed in the previous point. The calculation will not be recalled here to avoid redundancy.

Thus, all the elements of the initial design are verified. The initial design was thus verified under SLS and ULS and is illustrated on figure 3.

Design of the structure with 6 spans:

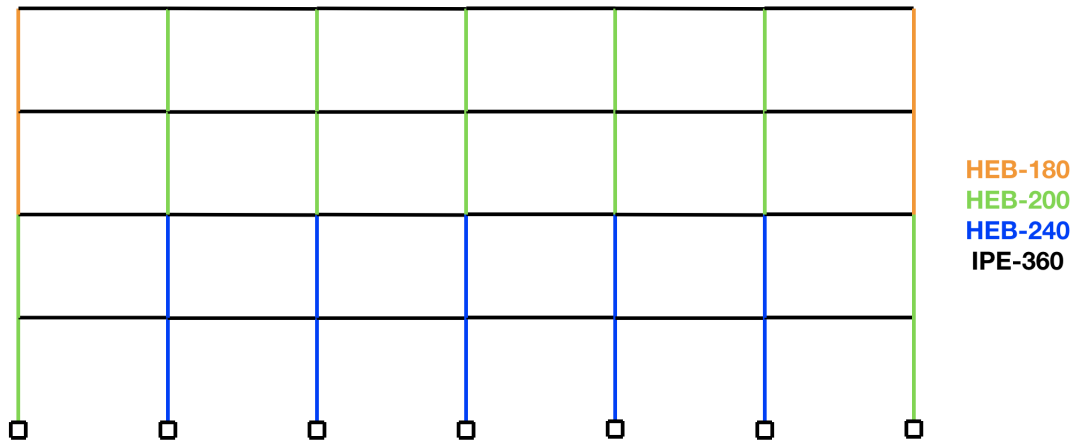


Figure 6: Design of the 2D 6 spans frame

Design of the structure with 8 spans:

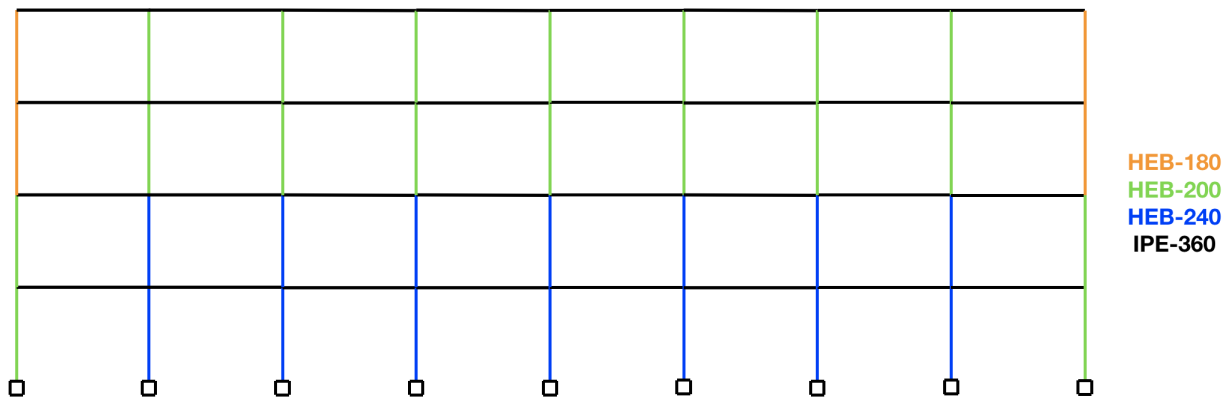


Figure 7: Design of the 2D 8 spans frame

Bibliography

- [1] Huvelle C. Contribution à l'étude de la robustesse des structures de bâtiments - Prise en compte de la plastification progressive de la partie "non directement affectée" par l'événement exceptionnel considéré, Master thesis presented at Liège University. Liège, Belgium, 2011.
- [2] Demonceau J-F and Dewals B. Natural and technological risks in civil engineering, course given at Liège University. Liège, Belgium.
- [3] Canisius T.D.G. (Editor). Cost tu0601-structural robustness design for practising engineers, September 2011.
- [4] European committee for standardization. EN 1991-1-7 : Eurocode 1 - Actions on structures - Part 1-7: General actions - Accidental actions. Brussels, Belgium, 2006.
- [5] Comelieu L., Rossi B., and Demonceau J.-F. Robustness of steel and composite buildings suffering the dynamic loss of a column. *Struct Eng Int J*, 22 (3) (2012), pp. 323-329.
- [6] Demonceau J-F. Steel and composite building frames : sway response under conventional loading and development of membrane effects in beams further to an exceptional action, PhD thesis presented at Liège University. Liège, Belgium, 2008.
- [7] Hai L.N.N. Structural response of steel and composite building frames further to an impact leading to the loss of a column, PhD thesis presented at Liège University. Liège, Belgium, 2008.
- [8] Huvelle C., Jaspart J.-P., and Demonceau J.-F. Robustness of steel building structures following a column loss, scientific article. Helsinki, Finland, 2013.
- [9] Huvelle C., Jaspart J.-P., Demonceau J.-F., and Hoang V.-L. Complete analytical procedure to assess the response of a frame submitted to a column loss, scientific article. Oxford, United Kingdom, 2015.
- [10] Comelieu L. Effets du comportement dynamique des structures de bâtiments en acier suite à la ruine accidentelle de l'une des colonnes portantes, Master thesis presented at Liège University. Liège, Belgium, 2009.
- [11] Hjeir Farah. Robustness of steel structures further to a column loss : Identification of the structural requirements through parametrical studies, Master thesis presented at Liège University. Liège, Belgium, 2015.
- [12] Lemaire F. Etude du comportement 3D de structures en acier ou mixtes lors de la perte d'une colonne, Master thesis presented at Liège University. Liège, Belgium, 2010.
- [13] Ghimire A. Robustness of 3D steel structures further to a column loss : Identification of structural requirements through parametrical studied, Master thesis presented at Liège University. Liège, Belgium, 2016.

- [14] Muller F. Application d'une approche globale d'étude des bâtiments en acier soumis à la perte d'une colonne, Master thesis presented at Liège University. Liège, Belgium, 2009.
- [15] Jaspart J.-P. Calcul d'éléments métalliques, course given at Liège University. Liège, Belgium, 2015-2016.
- [16] European committee for standardization. EN 1991-1-1 : Eurocode 1 : Actions on structures - Part 1-1 : General actions - Densities, self-weight, imposed loads for buildings. Brussels, Belgium, 2002.
- [17] European committee for standardization. EN 1990 : Eurocode - Basis of structural design. Brussels, Belgium, 2002.
- [18] MSM department Greisch info s.a. Finelg user's manual - Nonlinear finite element analysis program - Version 8.5. Liège, Belgium, 2002.
- [19] Duchêne Y. and Guisse S. WnOssa2D : computation software for 2D structures - User's manual (in French). Liège, Belgium, 1995.
- [20] Villette M. Analyse critique du traitement de la barre comprimée fléchie et propositions de nouvelles formulations, PhD thesis presented at Liège University. Liège, Belgium, 2004.
- [21] Gioncu V., Mosoarca M., and Anastasiadis A. Prediction of available rotation capacity and ductility of wide-flange beams, Journal of Constructional Steel Research, 2011.
- [22] Massonnet Ch. and Save M. Calcul plastique des constructions - Volume 1 - Structures dépendant d'un paramètre. Liège, Belgium.
- [23] European committee for standardization. EN 1991-1-3 : Eurocode 1 : Actions on structures - Part 1-3 : General actions - Snow loads. Brussels, Belgium, 2003.
- [24] European committee for standardization. EN 1991-1-4 : Eurocode 1 : Actions on structures - Part 1-4 : General actions - Wind actions. Brussels, Belgium, 2010.
- [25] Jaspart J.-P. Partie "Métallique" du cours de CMBBM - 1 Ma CO - Formation à l'Eurocode 3, course given at Liège University. Liège, Belgium.
- [26] Infosteel. Eurocode 3 EN 1993 - Exemples d'application au calcul des structures en acier.

List of Figures

I.1	The Ronan Point failure in 1968 [2]	4
I.2	Failure mode of the Ronan Point in 1968 [2]	4
I.3	The Murrah building failure in 1995 [2]	5
I.4	The Murrah building failure in 1995 [2]	5
I.5	Strategies for Accidental Design Situations [4]	7
I.6	Behaviour of a frame submitted to a column loss [9]	11
I.7	Phase 1	11
I.8	Phase 2	12
I.9	Catenary actions (Phase 3)	12
I.10	Substructure of Hai [7]	13
I.11	Key elements to be verified during Phase 2, Muller [14]	14
I.12	Generalized substructure model [9]	15
I.13	Substructure model [9]	16
I.14	Calculation of the coefficients s_{ij} [9]	17
I.15	Damaged level (Hai [7])	18
I.16	Elements of the damaged level (Hai [7])	18
I.17	Evolution of the internal forces in the columns of the damaged level in the IAP during all the three phases (Hai [7])	18
I.18	Deflection of the columns under uniformly distributed loads [1]	19
I.19	Deflection of the columns under an horizontal applied load [1]	19
I.20	Supplement compressive forces in the beside columns (Hai [7])	20
I.21	From the hypothetical first hinges in the IAP to the hypothetical full plastic mechanism in the IAP	21
II.1	3D reference structure [11]	24
II.2	2D reference frame	25
III.1	Classical 2D element [18]	28
III.2	Discretization of the elements	28
III.3	Illustration of the beams' discretization	29
III.4	Illustration of the cross-sections' discretization	30
III.5	Linear elastic law (infinite elastic behaviour)	30
III.6	Bilinear law - elastic perfectly plastic law (with infinite ductility)	30
III.7	Loading of the reference structure	32
III.8	Modelization of the central column of the frame at ground level	33
III.9	Modelization of the sequences followed in FINELG to model the progressive loss of the column	34
IV.1	Scenarios considered regarding the analysis of the global response of the reference structure	38
IV.2	DAP and IAP of the reference structure under the loss of its central column	39
IV.3	DAP elastic-perfectly plastic - IAP elastic	39

IV.4	Beam plastic mechanism in the DAP	40
IV.5	Catenary actions and arch effect	40
IV.6	Evolution of the normal forces into beams' cross-sections of the DAP	41
IV.7	Schema of the frame's deformation (End Phase 2)	41
IV.8	Illustration of the normal forces into the beams of the DAP (End Phase 3)	42
IV.9	Evolution of the bending moments into beams' cross-sections of the DAP	42
IV.10	Bending moment diagram at the end of Phase 1	43
IV.11	Bending moment diagram at the end of Phase 2	43
IV.12	Bending moment diagram under a downwards vertical load applied at the top of the lost column	43
IV.13	Bending moment diagram at the end of Phase 3	44
IV.14	Evolution of the normal forces into columns' cross-sections of the IAP	44
IV.15	Effect of an horizontal load	45
IV.16	Evolution of the bending moments into columns' cross-sections of the IAP	46
IV.17	Evolution of the normal force into bottom beam's cross-section of the IAP	46
IV.18	Evolution of the bending moment into bottom beam's cross-section of the IAP	47
IV.19	Shape of the bending moment diagram in the bottom beam of the IAP	47
IV.20	DAP elastic-perfectly plastic - IAP elastic-perfectly plastic	49
IV.21	M-N curves	51
IV.22	Order of formation of plastic hinges in the IAP	52
IV.23	Evolution of the normal forces into beams' cross-sections of the DAP	53
IV.24	Evolution of the normal forces into columns' cross-sections of the IAP	54
IV.25	Evolution of the bending moments into columns' cross-sections of the IAP	55
IV.26	Evolution of the axial force into bottom beam's section of the IAP	55
IV.27	Evolution of the bending moment into bottom beam's cross-section of the IAP	56
IV.28	Identified failure modes and elements needed to be verified	57
IV.29	Progressive collapse of the DAP	58
IV.30	DAP and IAP of the reference structure under the loss of an intermediate column	60
IV.31	DAP elastic-perfectly plastic - IAP elastic	60
IV.32	Beam plastic mechanism in the DAP	61
IV.33	Evolution of the normal forces into beams' cross-sections of the DAP	61
IV.34	Schema of the frame's deformation (End Phase 2)	62
IV.35	Evolution of the normal forces into columns' cross-sections of the IAP	62
IV.36	DAP elastic-perfectly plastic - IAP elastic-perfectly plastic	64
IV.37	Plastic mechanism	64
IV.38	Bending moment diagram in the structure when the beam plastic mechanism is fully developed	65
IV.39	M-N curves	65
IV.40	Evolution of the normal forces into beams' cross-sections of the IAP	66
IV.41	Evolution of the normal forces into columns' cross-sections of the IAP	66
IV.42	Identified failure modes and elements needed to be verified	67
IV.43	DAP and IAP of the reference structure under the loss of an exterior column	68
IV.44	DAP elastic-perfectly plastic - IAP elastic & elastic-perfectly plastic	68
IV.45	Evolution of the normal forces into columns' cross-sections of the IAP	69
IV.46	Identified failure modes and elements needed to be verified	70
V.1	Lost columns' designations	75
V.2	$(u_i; N_{AB})$ curves for an IAP elastic and an IAP elastic-perfectly plastic	75
V.3	Evolution of the normal forces into beams' cross-sections of the DAP	76
V.4	Sum of the normal forces into beams' cross-sections of the DAP	77

V.5	Evolution of the normal forces into columns' cross-sections of the IAP	77
V.6	$(u;N_{AB})$ curves for an IAP elastic and an IAP elastic-perfectly plastic	78
V.7	Evolution of the axial forces into columns' cross-sections of the IAP	79
V.8	Lost columns' designations	81
V.9	$(u;N_{AB})$ curves for an IAP elastic and an IAP elastic-perfectly plastic	81
V.10	Evolution of the normal forces into columns' cross-sections of the IAP	82
V.11	Comparison of the $(u;N_{AB})$ curves between the three structures for an IAP elastic	85
V.12	Comparison of the $(u;N_{AB})$ curves between the three structures for an IAP elastic-perfectly plastic	85
V.13	Comparison of the $(u;N_{AB})$ curves between the three structures for an IAP elastic-perfectly plastic	86
V.14	Comparison of the $(u;N_{AB})$ curves between the 6 and 8 spans structures for an IAP elastic-perfectly plastic	87
V.15	Loss of intermediate column	88
V.16	Loss of intermediate column	88
V.17	Loss of intermediate column	88
VI.1	Panel plastic mechanism point on the $(u;N_{AB})$ curve	93
VI.2	Studied substructure	93
VI.3	Panel plastic mechanism	94
VI.4	$(u;\lambda)$ curves for the loss of the central column in the reference structure	95
VI.5	$(u;\lambda)$ curves for the loss of the central column in the reference structure and the second order rigid plastic curve	96
VI.6	Cut in the reference structure in the case of the loss of its central column	97
VI.7	Identified breakpoint (4 spans structure)	98
VI.8	Identified breakpoint (6 spans structure)	99
VI.9	Identified breakpoint (8 spans structure)	99
VI.10	Identified breakpoint (6 spans structure)	101
1	Wind actions	113
2	Equivalent horizontal loads [25]	114
3	Design of the 2D reference frame	114
4	First lateral instability mode of the structure for a considered combination	115
5	Evaluation of the buckling length of the beam	117
6	Design of the 2D 6 spans frame	119
7	Design of the 2D 8 spans frame	119

List of Tables

III.1 Input data for material laws 31

V.1 Comparison of the values of N_{lost} between the three structures 86

VI.1 Lambda for the three structures and the associated errors 95

VI.2 Errors made on N_{lost} 100